TECHNISCHE UNIVERSITÄT MÜNCHEN

Fakultät für Medizin

Institut für Virologie

Hepatitis C virus control: viral resistance, new therapeutic targets and host defense.

Hanaa M. Gaber Moawad

Vollständiger Abdruck der von der Fakultät für Medizin der Technischen Universität München zur Erlangung des akademischen Grades eines

Doctor of Philosophy (Ph.D.)

genehmigten Dissertation.

Vorsitzende: Univ.-Prof. Dr. Agnes Görlach

Betreuerin: Univ.-Prof. Dr. Ulrike Protzer

Prüfer der Dissertation:

1. Priv.-Doz. Dr. Andreas Umgelter

2. Priv.-Doz. Dr. Fabian Geisler

Die Dissertation wurde am 03.08.2016 bei der Fakultät für Medizin der Technischen Universität München eingereicht und durch die Fakultät für Medizin am 12.09.2016 angenommen.

A dissertation entitled

Hepatitis C virus control: viral resistance, new therapeutic targets and host defense.

By

Hanaa Mohamed Gaber Moawad

Submitted to the Faculty of Medicine, Technical University of Munich as partial fulfillment of the requirements for the

Doctor of Philosophy Degree

Supervisor Prof. Dr. Ulrike Protzer

2016

Dedication

I would like to dedicate my thesis to my beloved parents Mrs. Nawal Fayek and Mr. Mohamed Gaber and my family their support and keeping me up whenever I am down.

To the memory of my Grandfather Salah Fayek (1934-2014). For his support and inspiration and to believe that everything is possible.

To the memory of my Uncle Ashraf Fayek (1960-2013). For his encouragement and support for my career.

I dedicate my Ph.D. to you.

Hanaa Gaber 2016

Acknowledgements

I would like to thank a lot of people for their support along one of my important goals in my life, and it is hard to find words to express my gratitude and my deep thanks to them.

First of all, I would like to thank my supervisor Prof. Dr. Ulrike Protzer for the opportunity to join the lab and for her mentorship and guidance. I thank her for giving me the opportunity and freedom to think and grow to become an independent scientist.

Then I would like to thank my thesis supervisory committee Dr. Med. Fabian Geisler and Dr. Andreas Umgelter for the advice and suggestions that I gained in our meetings which helped me guiding my project.

Next, I would like to thank the former lab members, Dr. Christian Bach and Dr. Ke Zhang, for all the technical support and scientific discussions, which helped me a lot in my first project in the lab.

I would like to thank all people in the diagnostic lab especially Dr. Dieter Hoffman, Dr. Barbara Bauer and all assistance, for all viral RNA extractions and the clinical information.

And I would like to thank a wonderful group of people including Stefanie Graf, Xiaoming Cheng, Lili Cho, Cam Tu Ho, Theresa Asen for being always around, and the great person Julia Graf for being kind, supportive, open minded and being open for all discussions and questions. You are a wonderful group of people to work with and I consider you my friends as well as labmates.

Special thanks also goes to Katrin Singethan, I don’t know how to start, thanks a lot you made me feel welcome from the first day we started working together, for being the first to support and introduce me to the S3 lab and to the HCV techniques, more than this to make my life in Munich much easier and for your support in moments when everything seemed to go wrong. Even in your busy time, you could always make a time for problem solving and discussions.

I would like to thank all participants in my Ph.D. projects, especially Akram Amin for working together on what sounds first crazy and impossible idea, for all the discussions, the cooperation which made the outer space environment a possible lab for our project. Then I would like to thank Prof. Dr. Dierk Niessing and Dr. Robert Janowski, for joining the Crystallization project

and offering the platform, the expertise and their effort which succeeded in achieving the project goal.

I would like to thank all people work in the Medical Life Science and Technology Ph.D. program; special thanks go to Desislava Zlatanova, for her positive attitude, for being supportive, patient and helpful in solving all problems and for her guidance along the program requirements and the graduation steps.

Thanks for all the collaborative labs that opened the door to get more insights during my Ph.D., in Germany, Prof. Dr. Ralf Bartenschlager and in the USA Dr. Jake Liang, for giving me the chance for training in their labs.

I would like to thank DAAD (GERLS) program for funding my Ph.D. studies in Germany, for all the before and during and after study guidance and support, I am proud of being an Alumni of this institution.

My deep thanks to NASA and Space X for funding the ``Space part`` of the second project in my thesis and to introduce us to a different research discipline.

List of publications

1- Amany S. Maghraby, Kamel H. Shaker, and **Hanaa M. Gaber.** (2009). **Cross-Reactivity of *Schistosoma mansoni-Fasciola gigantica* Influenced by Saponins.** Z. Naturforsch. **64 c**, 288 – 296.

2- Mahmoud M. Bahgat, **Hanaa M. Gaber,** Amany S. Maghraby. (2009). ***Escherichia coli* shares T- and B-lymphocyte epitopes with *Schistosoma mansoni.*** J Infect Developing Countries. 3(3):206-217.

3- Hanaa M. Gaber, Amany S. Maghraby, Mohamed B. Ahmed, Ruppel A, Mahmoud M Bahgat. (2010). **Immune responses in mice after immunization with antigens from different stages of the parasite *Schistosoma mansoni*.** Z. Naturforsch **(3-4): 289-302.**

4- Xiaoming Cheng , Matthias Broxtermann , Knud Esser , Anna Kosinska , Jan-Hendrik Bockmann1 , Julia Graf , Hanaa Gaber , Yuchen Xia, Wolfgang E. Thasler , Winfried Barchet , Matthias Heikenwälder, Percy Knolle , Norbert Hüser , Ralf Bartenschlager , Bernhard Holzmann , Daniel Hartmann , Jane A McKeating, Ulrike Protzer. **Liver sinusoidal endothelial cells and Kupffer cells define early 2 innate immune response against hepatitis C virus via TLR3. CELL-REPORTS-D-16-02227. (Submitted).**

Posters

- Arevir meeting, 2012.
- Arevir meeting, 2013.
- PhD program poster symposium 2013, **poster presentation.**
- Interact 2014 - Munich PhD Symposium, **poster presentation.**
- TTU hepatitis-DZIF 2014, **poster presentation.**
- American Society for Gravitational and Space Research (ASGSR) 2015, **poster presentation.**
- "Viral Hepatitis - From Bench to Bedside" FALK workshop 2015, **poster presentation.**

Abberviations

aa	Amino acid
Boceprevir	BOC
bp	Base pare
DC-SIGN	Dendritic Cell-Specific Intercellular adhesion molecule-3-Grabbing Non-integrin
DMSO	Dimethylsulfoxide
dsRNA	Double strand RNA
EC50	Half maximal effective concentration
ER	Endoplasmic Reticulum
HCV	Hepatitis C Virus
HCVcc	Hepatitis C virus derived cell culture
HCVpp	HCV Pseudoparticles
HCVTCP	HCV Trans-Complemented Particles
IC50	Half maximal inhibitory concentration
IFN	Interferon
IFNAR	Interferon α/β receptor
IRES	Internal Ribosomal Entry Site
IRF	Interferon regulatory factor
ISG	Interferon-stimulated gene
LDL	Low-density lipoprotein
LDL-R	Low-density lipoprotein receptor
L-SIGN	Liver/lymph node-Specific Intercellular adhesion molecule-3-Grabbing Non-integrin
MAVs	Mitochondrial antiviral-signaling protein
MDA-5	Melanoma differentiation-associated gene 5
MOI	Multiplicity of infection
NF-κb	Nuclear factor 'kappa-light-chain-enhancer' of activated B-cells
NIs	Nucleoside analog inhibitors
NNIs	Non-nucleoside inhibitors

NS	Non-structural protein
NTRs	Non-translated regions
PHH	Primary Human Hepatocyte
PIs	Protease inhibitors
PRR	Pattern Recognition Receptor
qRT-PCR	Quantitative real-time PCR
RdRp	RNA-dependent RNA polymerase
RIG-1	Retinoic Acid-Inducible Gene 1
RNA	Ribonucleic acid
RT-PCR	reverse transcription-PCR
SNP	Single Nucleotide Polymorphism
SR-BI	Scavenger receptor B type I
ssRNA	Single strand RNA
SVR	Sustained virological response
TCID50	50% Tissue Culture Infective Dose
Telaprevir	TLV
TLR	Toll-like receptor
TRIF	TIR-domain-containing adapter-inducing interferon-β
TRIM	Tripartite motif

Abstract

The studies presented in my Ph.D. outline multiple aspects of Hepatitis C research. The first study focused on the establishment of convenient genotypic and phenotypic assays to determine the resistance profile of the protease inhibitors Boceprevir and Telaprevir. The results reveal the association of several mutations within NS3 with the different levels of resistance to protease inhibitors. Moreover, genotyping of IL28b polymorphisms showed that SNP rs12979860 has more predictive values than SNP rs8099917 and that all relapsed patients had a non-CC genotype.

The second study was a part of NASA and the ISS contributions in the space-based research in the biological sciences. The project aimed for determination of the 3D structure of HCV-NS5b of the predominant genotype in Egypt (genotype 4a). During the study, we were able to employ the protein crystallization technology using microgravity environment in the ISS along with the earth crystallography techniques to obtain crystallize of good quality for X-ray diffraction. In the pre-flight procedure, we used the available standardized procedure including protein production, purification and quality check for sample preparation and shipment. During the flight, protein sample was exposed to microgravity for 25 days and the equivalent earth control was exposed to 1 gravity condition. Post flight phase, few crystals grew on the space crystal card and not in the earth one. For technical difficulties, we could not harvest the crystals for further x-ray diffraction experiments. The space experiment followed by further optimization of the crystallization conditions, when we acquired crystals of good quality, crystals were illuminated by the X-ray beam generated by synchrotron sources. The dataset of diffraction images showed that most crystals diffracted to an average of 3.1 Å resolution. The NS5b structural model determined by the Molecular Replacement approach showed that the structure is identical to other HCV-NS5b polymerases, in which the HCV-NS5b of genotype 4a contains six conserved motifs. However, the NS5b protein has different confirmations, the other conformations were not determined because we lack the protein-inhibitor co-crystallization experiment.

In the last study, we aimed to identify the role of TRIM protein family in HCV infection. Here, we could identify several TRIM proteins regulated by interferon and HCV infection, thus we hypnotized a potential association of TRIM proteins with antiviral activities against HCV. In our replicon and infection experiments, we could show that in response to TRIM5, TRIM9, TRIM14

or TRIM25 overexpression, the HCV replication and infection were restricted. Further analysis suggests that TRIM5 positively regulates IFN signaling pathway by upregulating RIG-I, MAVs, TRIF IFN-β expression levels, while TRIM9 could enhance both IFN-b and ISRE promotors' activation.

We could also demonstrate that TRIM14 overexpression decreases HCV replication and infection by triggering the IFN antiviral response, notably, it could augment both IFN-β and NF-κb promoters' activities and increased expression levels of RIG-I, MAVs, TRIF, and IFN-β.

Finally, we could attribute the elimination of HCV infection during the TRIM25 overexpression to the increase of the expression levels of RIG-I, TRIF, MAVs and IFN-β in addition to the enhancement of ISRE, IFN-β, and NF-kb promoters' activities.

List of contents

Chapter I Introduction

1. Hepatitis C virus overview

Before 1989 viral hepatitis C was referred to as NonA NonB hepatitis, which is known now as a leading cause of chronic liver disease, cirrhosis and hepatocellular carcinoma (HCC) (Barth 2015).

The global distribution of HCV varies greatly, while the estimated rate of HCV infection in Europe is around 0.5% of the population, 1.3-1.5 % in the USA and Australia, the highest prevalence has been reported in Egypt with a 15– 20% of the population (Reker and Islam 2014)

The reason for the wide spread of the virus in Egypt is due to the use of contaminated syringes for schistosomiasis treatment during the campaigns to eradicate Schistosoma (Frank C, Mohamed MK et al 2000). Other reasons are the intra-familial transmission, direct blood contact, mother to child, organ transplant, needle-stick injuries, medical dental treatment, drug injection, and sharing contaminated sharp materials like razors and shaving kits (Mohd Hanafiah, Groeger et al. 2013).

Figure 1.1. HCV prevalence and global distribution HCV epidemiology varies enormously between different regions and countries. The map indicates the moderate presence of HCV ranging from 1.5 to 3.5%, with less than 2% in the developed counties, with the highest prevalence (>10%) in Egypt (Mohd Hanafiah, Groeger et al. 2013).

1.1. HCV virology and genome organization

HCV is a single positive-stranded RNA virus belongs to the family of *Flaviridae* (Fournier, Duverlie et al. 2013). The HCV genome contains approximately 9600 base pair (bp) and encodes a long polypeptide protein of 3000 amino acids (aa), which is flanked by non-translated regions (NTRs) at both C- and N- terminals (Bowen and Walker 2005, Lauer 2013)

HCV has high mutation rate owing to the error-prone nature of RNA-dependent RNA polymerase (RdRp). Therefore, HCV divides into 6 genotypes, and each genotype subdivides into subtypes, (e.g.:1a, 1b etc...). The mutations within each subtype are called quasispecies (Halfon and Locarnini 2011) .

1.2. HCV genome organization

The genetic representation is illustrated in figure 1.2.

Flaviviridae family has 3 different genera: *flavivirus*, *pestivirus*, and *hepacivirus*. HCV belongs to *hepacivirus* genera, all viruses belong to *Flaviviridae* is similar in genome organization and viral replication (Katze, He et al. 2002).

HCV genome is flanked by small 5' and 3' NTRs and has one open reading frame that translated into a polyprotein of roughly 3000 aa, followed by polyprotein cleavage by viral and cellular protease into ten gene products. HCV structural proteins are located in the N-terminal region of the polyprotein: the capsid 'core' protein and the glycoproteins, E1 and E2 (Huang, Sineva et al. 2004, Steinmann, Brohm et al. 2008).

While the non-structural (NS) proteins: p7, NS2, NS3, NS4A, NS5A, and NS5B are encoded in the C-terminal of the polyprotein (Halfon and Locarnini 2011).

1.3. Structural proteins

The structural proteins which form the virus particle include Core and the E1-E2 (Sulbaran, Di Lello et al. 2010).

The highly conserved viral core protein is relatively small ~21kDa and consists of 191 aa and located at the N-terminus of the HCV polyprotein. It plays multiple functions such as viral assembly, gene transcriptional regulation, (Zuniga, Macal et al. 2015) apoptosis, alteration of IFN signaling, cell transformation and interference with lipid metabolism (Singaravelu, O'Hara

et al. 2015). Many of the biological functions of the core protein are thought to provide a survival advantage to the virus.

The HCV core protein localizes in the cell cytoplasm and can also localize in the nucleus (Steinmann, Brohm et al. 2008). It circulates in the blood stream and can stimulate cell surface receptors.

The E1, E2 structural proteins are hypervariable glycoproteins and associated with the endoplasmic reticulum (ER). The envelope proteins are of great interest because of their potential use in the development of HCV vaccine (Khan, Whidby et al. 2014). The variability of the E1-E2 region is challenging in the generation of effective neutralizing antibodies (Khan, Whidby et al. 2014) .

Previous studies have demonstrated that E1-E2 proteins can form pseudo-viral particles and these particles capable of eliciting antibody responses (Suzuki, Saito et al. 2012).

1.2.2. Non-structural proteins

The non-structural proteins (NS): p7, NS2, NS3, NS4A, NS5A, and NS5B are associated with viral replication and immune evasion (Lassmann, Arumugaswami et al. 2013).

The non-structural 2 (NS2) is a serine protease responsible for the cleavage of NS2/3 when NS2 expresses alone it localizes to the ER membrane. NS2 dimerizes and yields a cysteine protease with two active sites which cleave between NS2 and NS3 (Shiryaev, Cheltsov et al. 2012). Due to the dimerization, it is believed that NS2 might be involved in viral assembly and release. It can also bind host pro-apoptotic protein, CIDE-B, which subsequently inhibits apoptosis (Guglietta, Garbuglia et al. 2009).

HCV Non-structural protein3/4A (NS3/4A) protein complex localizes to the ER membrane. The complex formation protects the NS3 and it is responsible for multiple biological functions including the viral replication and polyprotein processing. Both N3 protease and helicase activity are enhanced after localization to the ER (Heim and Thimme 2014).

HCV NS3 mediates apoptosis via caspase-8 indicating that it is implicated in the modulation of host cellular functions. It was reported that NS3/4 plays also an important role in HCV immune evasion (Gokhale, Vazquez et al. 2014).

The Non-structural protein 4B (NS4B) is a transmembrane protein that contributes to the formation of HCV replication complexes. The exact function is not known, but mutations in this protein affect the replication efficiency (Gokhale, Vazquez et al. 2014, Heim and Thimme 2014, Tamori, Enomoto et al. 2016).

The Non-structural protein5a (NS5a), is phosphorylated by cellular serine kinases, including MEK1, MKK6, AKT, p70S6K, and cAMP-dependent protein kinase A-a.42-46 and is associated with the ER membrane (Hamamoto, Nishimura et al. 2005). NS5a has two forms, hypo- and hyperphosphorylated form (Huang, Sineva et al. 2004). The hypophosphorylated form is required for efficient HCV replication in cell culture. Therefore, modifications such as point mutation (S2240I) in the NS5a are necessary for permissibility (Hardy, Marcotrigiano et al. 2003) Blight KJ, 2002). Moreover, NS5a can interact with a number of viral and host proteins to promote RNA replication and suppress the IFN-induced antiviral efficacy (Macdonald and Harris 2004, Huang, Hwang et al. 2005).

Non-structural protein 5b **(**NS5b) is RNA-dependent RNA polymerase required for HCV RNA replication (Wang, Ng et al. 2003, Wang, Johnson et al. 2004). It interacts with viral and host proteins, the interaction with NS3 and NS5a plays an important role in the HCV replication complex formation. Interestingly, NS5b interacts with cyclophilin B, a cellular peptidyl-prolyl cis-trans isomerase that regulates HCV replication through modulation of the RNA binding capacity of NS5b (Huang, Hwang et al. 2005).

The initial 21 residues of C-terminal region form a α-helical transmembrane domain responsible for post-translational targeting to the cytosolic side of the ER (Moradpour and Blum 2004). The RdRp is an important target for development of anti-HCV drugs (Afdhal, Reddy et al. 2014)

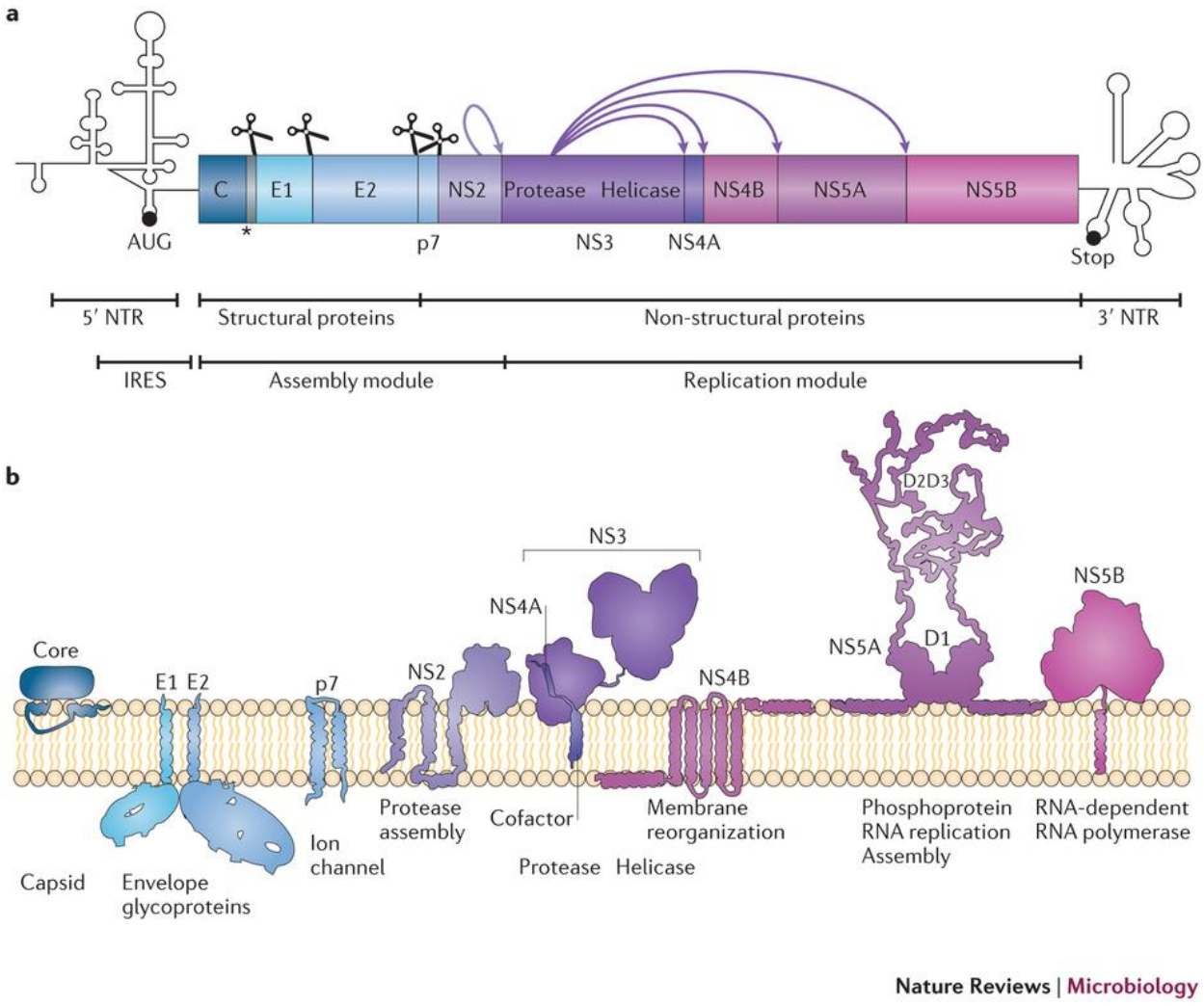

Figure 1.2. HCV genome organization (a) Represents the HCV 3′ non-translated region followed by ORF containing polyprotein, and the 5′ and 3′ non-translated region. The 5′ NTR contains an IRES. Arrows indicate the polyprotein cleavage by the viral proteases and scissors refer to ORF cleavage by cellular proteases. (b) Indicates the polyprotein processing products and the function of the of the cleavage products (Bartenschlager, Lohmann et al. 2013).

1.3. HCV receptors

HCV binding and internalization are mediated by several cell surface molecules.

CD81

CD81 receptor consists of four hydrophobic transmembrane domains (TM1- TM4) and two extracellular domains. Both intracellular and transmembrane domains are highly conserved among different species. Human CD81 mediates binding of HCV envelope glycoprotein E2 (Bartosch, Vitelli et al. 2003), and expression of human CD81 in a CD81-deficient human hepatoma cell line restored HCV pseudoparticles, but an expression of human CD81 does not restore the infection in murine fibroblast cell line (Cormier, Tsamis et al. 2004).

SR-BI

The HCV receptor Scavenger receptor B type I (SR-BI) consists of a 509 aa glycoprotein (Krieger, 2001). It is expressed at high levels in hepatocytes and steroidogenic cells (Krieger 2001, Nakamuta, Fujino et al. 2011). Interestingly, it has been shown that HCV E2 glycoproteins of genotypes 1a and 1b bind to HepG2 cells (a human hepatoma cell line that does not express CD81 (Bartosch, Vitelli et al. 2003).

The SR-BI-HCV E2 protein binding is highly specific: whereas E2 can bind to rodent cells transfected either with human or Tupaia (88 % aa identity with human SR-BI), neither mouse SR-BI (80 % aa identity with human SR-BI) nor CD36 (60 % aa identity with human SR-BI can bind E2. The SR-BI LEL appeared to be responsible for HCV binding via interacting with the HVR1 region (Bartosch, Vitelli et al. 2003).

DC-SIGN AND L-SIGN

Both dendritic cell-specific intercellular adhesion molecule-3-grabbing non-integrin (DC-SIGN or CD209) and liver/lymph node-specific intercellular adhesion molecule-3 (ICAM-3)-grabbing integrin (L-SIGN or CD209L) are HCV tissue-specific receptors, they are expressed in different cell types and play important role in viral pathogenesis and tissue tropism (Cormier, Tsamis et al. 2004). DC-SIGN is expressed at high level in myeloid-lineage dendritic cells, whereas L-SIGN is expressed at the surface of the liver endothelial cells, the interaction between both proteins activates the T cells (Falkowska, Durso et al. 2006, Pichlmair and Reis e Sousa 2007).

LDL-R

The low-density lipoprotein (LDL) receptor (LDL-R) is an endocytic receptor consists of 839 amino acids, mainly the cholesterol-rich LDLs, into cells through receptor-mediated endocytosis (Chung, Gale et al. 2008). The majority of human plasma cholesterol is in LDL form. It was reported that LDLR is involved in the HCV infection, the HCV infection was inhibited when cells were treated LDL peptide inhibitor (Bartenschlager, Penin et al. 2011).

Occludin

Occludin (OCLN) has been identified as an important receptor for HCV (Nakamuta, Fujino et al. 2011, Zeisel, Fofana et al. 2011, Dorner, Horwitz et al. 2013). It is 65 kDa and consists of a four-transmembrane domain protein located in the tight junctions of polarized cells. Human hepatoma cell lines such as Huh7 or cell lines that lack other entry factors (i.e. HepG2 and 293T cells) express detectable levels of OCLN. Although, OCLN overexpression did not enhance infection susceptibility of HCVpp. OCLN knockout led to inhibition of HCVpp infection in Hep3B cells and both HCVpp and HCVcc in Huh-7.5 cells. Taken together, OCLN is an essential receptor for HCV infection in permissive cell lines. Whereas in HCV non-permissive cells, which express other cell entry receptors, OCLN overexpression enhances HCV entry (Nakamuta, Fujino et al. 2011, Dorner, Horwitz et al. 2013)To date, human OCLN has been reported to be a species specific entry factor responsible for HCV infection. Expression of OCLN along with human CD81 may confer HCV permissibility to mouse cell lines (Zeisel, Fofana et al. 2011).

1.4. HCV replication cycle

HCV replication cycle consists of 5 stages: viral entry, protein translation, RNA replication, virion assembly, and release. The entry starts by binding to E2 protein to CD81 (Rajesh, Sridhar et al. 2012), SRB1 (Nakamuta, Fujino et al. 2011), glycosaminoglycans, LDLR (Nakamuta, Fujino et al. 2011), and claudin-1 (Nakamuta, Fujino et al. 2011, Zeisel, Fofana et al. 2011).

The endosome is characterized by the acidic environment which introduces the HCV genome entry into the cytoplasm, where HCV negative sense strand RNA production occurs (Friebe and Bartenschlager 2009, Pham, Coffin et al. 2010). HCV polyprotein translation is driven by the internal ribosome entry site (IRES), initiation of translation occurs via HCV IRES and the 40S ribosomal subunit complex formation. The translation process is followed by viral and cellular proteases processing to form the structural and non-structural proteins. HCV protein expression results in the replication complexes formation in the cytosol. The viral proteins are then arranged

to form the membranous web. Viral assembly occurs after expression and replication of the HCV genome, followed by virions budding into the ER and secretion (Moradpour and Blum 2004, Steinmann, Brohm et al. 2008, Fournier, Duverlie et al. 2013).

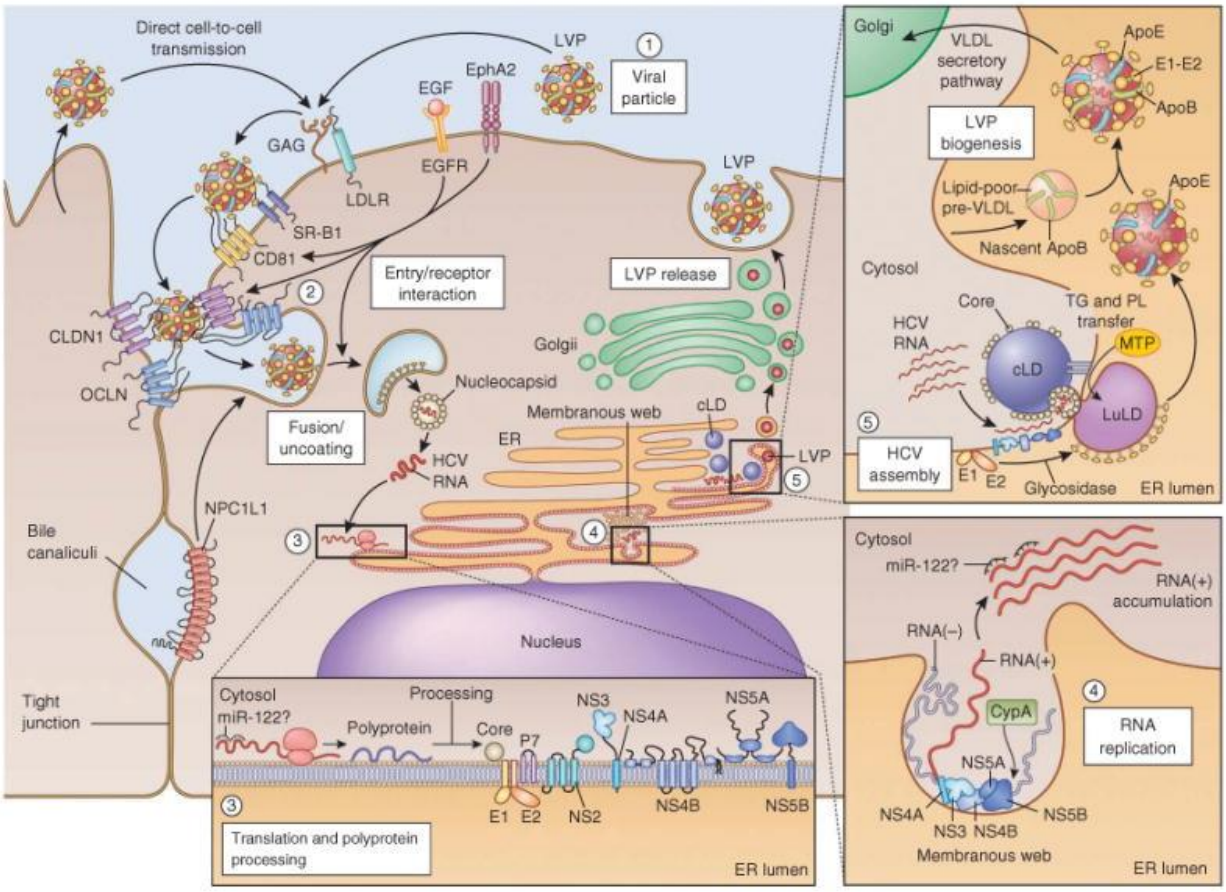

Points of intervention in the HCV life cycle
① The viral particle (neutralizing antibodies, virocidal peptides)
② Entry and receptor interaction (antibodies and small molecules targeting receptors, kinase inhibitors)
③ Translation and polyprotein processing (NS3-NS4A protease inhibitors)
④ HCV RNA replication (NS5B polymerase and NS5A inhibitors, miR-122 antagonists, cyclophilin inhibitors, statins, PI4KIIIα inhibitors)
⑤ Assembly and virion morphogenesis (NS5A inhibitors, DGAT1 inhibitors, glycosidase inhibitors, MTP inhibitors)

Figure 1.3. The HCV replication cycle (1) Extracellular virions bind to cell surface receptors. (2) Uncoating and endocytosis take place, then genome translation. (3 and 4)) Replication occurs in the ER results in conformational change and consequently forms a membranous web. (5) Formation of nucleocapsids and virus assembly followed by release of newly formed virions. (Scheel and Rice 2013)

1.5. HCV cell culture systems

Human hepatocytes are the primary host for HCV (Rajesh, Sridhar et al. 2012). There are some evidence that HCV found in peripheral blood mononuclear cells and the brain, but replication in these tissues has not been confirmed (Zhu, Liu et al. 2016). Some of the early challenges to studying HCV were the inefficient replication of different HCV isolates and the limitations of permissive cell culture systems that support HCV replication.

1.5.1. HCV replicon system

One of the major breakthroughs to study HCV was the development of subgenomic replicons. A replicon is a nucleic acid which is capable of self-replication. Con1 is the first HCV replicon system used to study HCV. It is a full HCV genome which was cloned from genotype 1b isolate (Moriishi and Matsuura 2007, Wakita 2007). In this model the structural proteins are replaced by, a selection neomycin phosphotransferase (neo) gene which allows selecting for G418 resistance, and an IRES from a picornavirus (Jiang, Guo et al. 2008, Pichlmair, Schulz et al. 2009).This results in a bicistronic construct, the first cistron drives the neo gene and the second drives the HCV replicas genes (NS3–NS5B). Then, HCV RNA was reversely transcribed *in vitro* and transfected in human hepatoma cell line Huh-7, afterward, HCV replicon colonies that support replication efficiently replicate in cells (1000–5000 positive-strand RNA molecules per cell) (Friebe and Bartenschlager 2009). Replicon cells can be maintained for years by continuously passaging under selective pressure (Gaudieri, Rauch et al. 2009, Lassmann, Arumugaswami et al. 2013).

After the introduction of the first replicon system in 1999 by Ralf Bartenschlager lab (Bartenschlager, Kaul et al. 2003, Woerz, Lohmann et al. 2009), a number of replicons covering genotypes (1a-4a), and with various reporter genes such as luciferases and fluorescent proteins were constructed to cover the researcher needs to study the HCV RNA replication mechanisms.

Improvements of the replicon system

There are two factors which determine the efficiency of HCV replicons replication: the cell culture adaptive mutations and the permissiveness of the cell line for HCV RNA replication (Hwang, Huang et al. 2010). Mutations enhancing replications were found at the N-terminus of the NS3 helicase, NS4B and in NS5A. Insertion of these mutations into replicons resulted in an

increase in the replication capacity, and the enhancement is depending on the mutations combination (Le Pogam, Yan et al. 2012, Mayhoub 2012, Nakamoto, Kanda et al. 2014). The second step to improve the efficiency of the RNA replication is to select for highly permissive cells. Huh7.5 and Huh7-Lunet are Huh7 cell clones that highly support HCV RNA replication (Robinson, Yang et al. 2010).

Establishment of cell lines stably expresses reporter replicons was an additional step forward for high-throughput screening purposes. Interestingly, con1 containing adaptive mutations replicon cannot produce viral particles in the supernatant of cultured cells (Pietschmann, Kaul et al. 2006). Theses adaptive mutations do not exist in natural viral isolates, and some studies show that they might interfere with viral production and spread.

1.5.2. HCV pseudoparticles (HCVpp)

One of the important models to study HCV early steps of infection is HCVpp. This model is established by transfection of 293T cells with three vectors, first, is HCV E1 and E2, second is the retroviral gag-pol and third is a reporter gene vector (Bartosch, Vitelli et al. 2003). Afterward, HCVpps are secreted by the cultured transfected cells, which can be used to infect Huh 7 cells. Therefore, this system proved important in discovering viral host receptors such as glycosaminoglycans, LDL-R, DC-SIGN, Occludin, and recently Niemann-Pick C1-like cholesterol absorption receptor (NPC1L1) (Ploss and Dubuisson 2012).

1.5.3. HCV cell culture infectious virus (HCVcc)

Another important breakthrough is the HCVcc system when an HCV genotype 2a full-length replicon (JFH-1) isolate was isolated from a Japanese fulminant hepatitis patient (Sung, Shin et al. 2015). HCVcc enables the study of the full viral life cycle in vitro. Infection of hepatoma cells with JFH-1 resulted in the release of infectious viruses which are capable of infecting naive cells (Wakita 2007). Interferon-alpha and DAAs inhibit HCVcc replication, so this system is a useful tool to study antiviral drugs and vaccines. Although HCVcc is an important tool to study HCV, it is limited by the fact that only replicating isolate is restricted to genotype 2 (Gaudieri, Rauch et al. 2009, Caillet-Saguy, Simister et al. 2011).

To improve the system, inter and intragenic chimeras were created, the chimeras are generated from (NS3–NS5b) of JFH-1isolate fused to the core to NS2 region of other HCV isolates. This

created a broad range of virus chimeras to the isolates Con1 (gt 1b), H77 (gt1a), 452 (gt 3a) and J6 (gt 2a), these chimeras are designated Jc1 (Tu, Ziemann et al. 2010, Verbinnen, Jacobs et al. 2012).

1.5.4. HCV trans-complemented particles (HCVTCP)

Recently, HCVTCP system was established, this is a useful system to study HCV early and late stages of infection. The HCVTCP are able of one round of infection but are unable to spread. Different strategies are used to produce HCVTCP, for example, co-transfection with constructs carrying viral glycoprotein genes (Luc-_E1/E2 or (Luc-NS3-5b) (Pai, Prabhu et al. 2005) along with the JFH1 genome as a helper virus into Huh7-Lunet cells (Steinmann, Brohm et al. 2008).

It was reported that HCV RNA subgenomes with different deleterious mutations naturally exist in patients and could be trans-complemented in vitro (Steinmann, Brohm et al. 2008, Suzuki, Saito et al. 2012) and these subgenomes can circulate in vivo and modulate the disease progression.

1.6. Immune responses to HCV infection

1.6.1. Innate immune responses to HCV

Various studies have shown that HCV triggers innate and adaptive immune response and the virus has developed mechanisms to escape the immune response.

Although, HCV persists in high viral loads in patients, but the viral proteins expressed at low amounts to be detected by immunohistochemistry. In HCV chronically infected patients, it is estimated that 30%–50% of hepatocytes are infected (Park and Rehermann 2014).

Despite the fact that HCV establish persistent chronic infection in 80% of the patients, 20% of patients in the acute phase can eliminate the virus, and the elimination is associated with innate immune response mainly IFN-α and β response.

HCV is first recognized by pattern recognition receptors (PRRs) members such as retinoic acid-inducible gene I (RIG-I) and melanoma differentiation-associated gene 5 (MDA-5), RIG-I plays a pivotal role in recognition of positive and negative ssRNA viral genomes (Pichlmair, Schulz et al. 2006), both RIG-I and MDA-5 are interferon stimulated genes that share conserved features and functions. Early during infection, RIG-I recognizes short stretches of the RNA which are rich in poly-U/UC ribonucleotides (Rajsbaum, Stoye et al. 2008), this activates the downstream

signaling pathway. Later, longer RNA intermediates sense TLR3 and PKRs. Therefore, PKRs activation signaling cascades lead to IFN-β and κkβ activation (Liu, Su et al. 2007, Jiang, Guo et al. 2008). TLR3 works as another innate immune molecule helping in surveillance of infected dead cells and in the establishment of antiviral state during the infection. Activation of non-canonical NF-kβ can result in and CXCL10 pro
-inflammatory cytokines production.

Kupffer cells (KC) are macrophages that abundantly localize in the liver and they could produce IFN-β in vitro (Boltjes, Movita et al. 2014). Although HCV is unlikely to replicate in KCs, some studies have shown that HCV RNAs and protein can activate KCs. This may be attributed to the phagocytosis of infected cells and exposure to viral RNA, but this hypothesis has not yet been proven.

Interestingly, KCs increased in the liver of chronically infected patients with high expression level of the activation markers such as CD163 and CD33. Although the contribution of KC on HCV infection is unclear, it was reported that HCV can induce cytokines such as IL-6, IL-1β, and IFN-β (Li, Liu et al. 2009, Pichlmair, Schulz et al. 2009, Pagliaccetti and Robek 2010) and consequently inhibit HCV replication in HCV replicon models. Furthermore, KC cytokines recruit infiltrating leukocytes in the liver and promote virus-specific T cell responses (Meylan, Curran et al. 2005, Simister, Schmitt et al. 2009, Pichlmair, Kandasamy et al. 2012).

1.6.2. Adaptive immune responses during HCV infection

In order to evade host immune system, HCV has developed different escape mechanisms. Moreover, it interferes with the IFN system and the potential for DC function. Although the adaptive immune response is detectable after 6–8 weeks of HCV infection,(Chen and Yu 2010, Mishima, Sakamoto et al. 2010), it plays an important role in viral clearance during the acute phase of infection. During acute HCV infection, patients produce antibodies against structural as well as non-structural protein epitopes. In particular, antibodies fraction called ‘neutralizing antibodies’ can inhibit virus binding, entry, or uncoating. This was demonstrated in a group of women infected by an HCV-contaminated anti-D immunoglobulin. In this homogenous group, in contrast to patients who developed chronic infection, patients who resolved HCV infection early during acute infection are characterized by the early production of neutralizing antibodies (Khan, Whidby et al. 2014). Although this study associates virus clearance with an early neutralizing antibody, virus control has also been noticed in hyperglobulinaemia patients. Another

mechanism of HCV clearance in acute infection is the strong and sustained CD4+ and CD8+T cell responses that target various HCV polyprotein epitopes (Schmidt, Blum et al. 2013, Heim and Thimme 2014).

Several pieces of evidence suggest an important role of both CD4+ and CD8+T cells in HCV spontaneous virus elimination, mainly the association between class I (e.g., HLA-B27) and II (e.g., DRB1⁄1101) alleles (Miki, Ochi et al. 2013).

The importance of T cell responses in virus clearance has been suggested by a study where protected chimpanzees CD8+T cells were depleted. This led to HCV persistence until the recovery of CD8+T cell response. Moreover, CD4+T cells depletion in protected chimpanzees resulted in HCV persistence and emergence of CD8+ escape mutations (Heim and Thimme 2014). Another recent study has shown that the IL-17 and 21 cytokines production of CD161+CCR6+CD26+CD4+ T expanded cells led to virus clearance. Using MHC class I, allele HLA-A2 gene transuded replicon cells showed that HCV-specific CD8+T cells possessed a dominant IFN-gamma production (Pichlmair, Kandasamy et al. 2012, Miki, Ochi et al. 2013) . Taken together, CD4+T cells are central regulators, while virus-specific CD8+T cells primarily function as the key effectors.

1.6.3. Immune escape

In order to evade host immune system, HCV has developed different escape mechanisms. Moreover, it interferes with the IFN system and the DC function. One of the escape mechanism is the cleavage of MAVS (Gale and Foy 2005)) and TRIF (Heim and Thimme 2014) by NS3-4A serine protease. This resulted in inhibition of IFN-β and Interferon-stimulated gene (ISG) induction in infected hepatoma cells (Liu, Su et al. 2007, Chen, Wang et al. 2014). This is supported by some studies which detected cleaved MAVS in HCV-infected livers (Gokhale, Vazquez et al. 2014, Heim and Thimme 2014) and the presence of an inactive form of IRF-3 (Lau, Tam et al. 2002, Meylan, Curran et al. 2005).

HCV core protein plays a role in immune escape mechanisms by inactivation and degradation of the STAT-1 and -2 which is required for the expression of ISGs such as PKR, 2'-5' OAS, ISG-p56, IRF-7 (Kanda, Steele et al. 2007, Gaudieri, Rauch et al. 2009, Heim 2012). Moreover, IFN activity can be blocked by NS5A protein blocking IRF-1 production and induction of IL-8 chemokine (Meylan, Curran et al. 2005, Seth, Sun et al. 2005) and subsequently inhibits IFN activity (Helbig, Lau et al. 2005).

1.7. Genotyping and phenotyping of HCV protease inhibitors resistant mutations

1.7.1. HCV therapy

Approximately 75% HCV patients develop chronic infection and this might lead to severe illness, including cirrhosis and hepatocellular carcinoma (HCC) (Wakita 2007, Pham, Coffin et al. 2010).

In 1991 interferon was approved by FDA as the first treatment for hepatitis C (Donaldson, Harrington et al. 2015) . A few years later, a combination of pegylated interferon-α (PEG–IFNα) and ribavirin was approved, this leads to cure of 20-80% of infection depending on the genotype, age and genetic host factors such as interleukin-28B polymorphisms (Ansaldi, Orsi et al. 2014, Rupp and Bartenschlager 2014, Qian, Zhu et al. 2016). Overall sustained virological response (SVR) in patients infected with genotype 2 and 3 is up to ~85% of treated patients, while it is successful only in ~45% of genotype 1 and 4 treated patients (Ferenci 2004). Later in 2011 the first direct-acting antiviral agents (DAAs) protease inhibitors BOC (Victrelis) and TLV (Incivek) were approved (Schiering, D'Arcy et al. 2011, Manns and von Hahn 2013). The new standard of care therapy consists of BOC or TLV in combination with PEG–IFNα and ribavirin raised the cure rates of HCV genotype 1 patients up to 70%, with treatment duration of 24 to 48 weeks (Hofmann and Zeuzem 2011, Rupp and Bartenschlager 2014). However, the SVR has improved with the new combination therapy. The emergence of resistant mutations is a main considerable drawback for the first generation of HCV protease inhibitors. The second wave of HCV protease inhibitors includes Simeprevir and Faldaprevir (Izquierdo, Helle et al. 2014). They improved the pharmacokinetics and have a higher genetic barrier. Daclatasvir is the first NS5A inhibitor with potent antiviral activity and broad genotype coverage (Pawlotsky 2013). Sofosbuvir is a nucleotide NS5B inhibitor. Combined with Daclatasvir, it was the first approved IFN free therapy (Degasperi and Aghemo 2014).

1.7.1.1. A decade of interferon- ribavirin standard of care therapy

Ribavirin is a (1--D-ribofuranosyl-1, 2, 4-triazole-3-carboxamide), guanosine analog a, that has been approved for other viruses treatment before HCV discovery. When ribavirin administrated alone for HCV treatment, it resulted in a decrease of HCV viral load and improved the liver enzymes in 40% of patients (Crotty, Cameron et al. 2001, Lau, Tam et al. 2002).

The ribavirin proposed antiviral mechanisms are: activation of virus mutagenesis resulting in accumulation of lethal virus forms, immunomodulatory effect, and induction of TH1 cytokines.

Another antiviral mechanism of ribavirin is its function as inosine-5-monophosphate dehydrogenase (IMPDH) inhibitor. Thus, it inhibits guanosine triphosphate, resulting in abnormal viral RNA form (Zhou, Liu et al. 2003).

Interferon-alpha (IFN-α) in HCV treatment

The interferons are naturally secreted cytokines produced by the cell. They have diverse functions including, antiviral activities, cell growth and regulation of immune response. Interferons antiviral activity was first discovered over half a century. It was reported that influenza infected cells secreted a protein which was able to control infection in vitro. Due to the interesting antiviral activity reported for interferons, researchers paid attention in using them for virus treatment (Katze, He et al. 2002) .

IFN-α, proved useful in the treatment of chronic hepatitis c infection as it decreases serum levels of HCV RNA and normalizes ALT levels. In 1998 the interferon- α and ribavirin combination therapy were approved for HCV treatment. Three years later, the PEGylated interferon- α along with ribavirin were approved for HCV treatment and improved the overall SVR of 75-80% in genotype 2 and 3 and limited to 40% in genotype 1 and 4 treated patients (Ferenci 2004, Manns, Wedemeyer et al. 2006). The issue of the differences SVR rates is attributed to the association of different factors with the response, among those (HCV genotype, co-infections and viral load) and host factors such as (age, sex, race and the recently identified genetic factor IL28b polymorphisms) (Balagopal, Thomas et al. 2010). One of the IFN-α antiviral mechanisms is the activation of PKR, the essential innate immunity regulator. The PKR mediates the phosphorylation of eukaryotic initiation factor-2 (eIF2a) and consequently blocks the HCV viral protein synthesis (Jiang, Guo et al. 2008).

1.7.2. Direct-acting antivirals (DAAs)

In spite of the increase of the SVR rates using the PEGylated interferon-α -ribavirin therapy, it has side-effects such as anemia, depression and limited efficacy for genotype 1 and 4 treatment. Thus, the need for more efficient anti-HCV therapies arouses. The better understanding of HCV life cycle and proteins function led to the development of multiple DAAs. These drugs target different steps in the virus replication and infection steps. There are three classes of DAAs: NS3/4A protease inhibitors (PIs), NS5A inhibitors and NS5B nucleoside and non-nucleoside polymerase inhibitors (NPIs&NNPIs) (Wang, Ng et al. 2003, Biswal, Cherney et al. 2005, Marascio, Torti et al. 2014, Bunchorntavakul and Reddy 2015).

1.7.2.1. Protease inhibitors

In 2003 (Lamarre, Anderson et al. 2003) have reported the first proof of concept that NS3/4A protease inhibitor BILN 2061 was able to decrease the viral load within 48 hours. However, the inhibitor has been withdrawn from further development due to the potential for cardiac toxicity.

The first generation of protease inhibitors (Telaprevir and Boceprevir)

In 2011, the FDA approved the linear compounds TLV (VX-950) and BOC (SCH 503034) for HCV genotype 1 therapy, both are administrated in combination with PEG–IFNα and ribavirin (Hofmann and Zeuzem 2011, Shiryaev, Cheltsov et al. 2012, Elbaz, El-Kassas et al. 2015). The triple therapy increased the SVR rates in genotype 1 treated patients up to 75%. The in vitro and in vivo studies showed that linear ketoamide has a low genetic barrier, meaning that a single substitution in one aa can confer resistance (Halfon and Locarnini 2011). The single aa substitutions confer low to high resistance for both TLV and BOC and the existence of two or more substitutions synergize the resistance effect (Hofmann and Zeuzem 2011, Rupp and Bartenschlager 2014, Welzel, Dultz et al. 2014, Elbaz, El-Kassas et al. 2015). Therefore, further studies including ours have evaluated the clinical resistance associated with treatment failure. The R155K and A156T substitutions are class-specific mutations (Nakamoto, Kanda et al. 2014, Welzel, Dultz et al. 2014, Elbaz, El-Kassas et al. 2015). Moreover, they are predominant in the patient quasispecies as both cause strong steric hindrance and modify the inhibitory interactions in a way which cannot be compensated. Other mutations such asV36, T54, V55 and V/I170 are also associated with PIs resistance (Lassmann, Arumugaswami et al. 2013). Typically, the drug resistance is determined in vitro and the degree of resistance measured as the fold increase in the 50% and 90% inhibitory concentrations (IC50 and IC90, respectively). Additionally, the variant must be able to propagate in vitro, notably, in the presence of drug highly resistant variants are less fit and vice versa (Chayama and Hayes 2015).

Although the analysis of PIs resistance is important for the further protease inhibitors development, the drug resistance testing was not recommended for patients before DAA therapy (Halfon and Locarnini 2011).

Second wave of PIs, Simeprevir

Simeprevir belongs to the second-wave of protease inhibitors and it has some advantages over the first wave inhibitors. These include higher genetic barriers to resistance and better pharmacokinetic profiles (Nakamoto, Kanda et al. 2014, Qian, Zhu et al. 2016). This drug was approved for treatment of genotype 1 patients in combination with peg-IFNα/RBV and administrated once daily, the triple therapy increased the SVR rates up to 80-85% in naïve treated patients (Bunchorntavakul and Reddy 2015). In genotype 1a patients, Q80K polymorphism is prevalent in about 30% of American patients and in 19% of European patients (Izquierdo, Helle et al. 2014, Sarrazin, Lathouwers et al. 2015). This led to the failure of the therapy with simeprevir+PEG/RBV. Therefore, screening for the presence of a Q80K polymorphism at baseline is recommended, and alternative treatment should be considered (Izquierdo, Helle et al. 2014). In November 2014 the FDA has approved Simeprevir+Sofosbuvir therapy for HCV genotype 1 patients, this combination was the first oral IFN-free therapy (Asselah and Marcellin 2015).

HCV PIs resistance tools

Similar to other RNA viruses, HCV replication is characterized by a high replication rate (1×10^{12}) particles per day) (Crotty, Cameron et al. 2001, Katze, He et al. 2002). In addition, HCV replication is characterized by the genetically error prone because of the low fidelity of RdRp. The error rate reaches 10^{-4} for one single mutation (Crotty, Cameron et al. 2001) which results in one mutation every genome. This inaccurate replication machinery besides the high replication rate leads to HCV with high sequence diversity. As a result, in chronic HCV infection, the virus exists as a multitude of genetically distinct but closely related viral variants called quasispecies. Mutations can be introduced in HCV during both negative-strand RNA intermediate, and the synthesis of the new positive strand RNA genome from the negative one (Habjan, Andersson et al. 2008). With the availability of HCV DAAs, the SVR increased up to 75% (Bunchorntavakul and Reddy 2015)for patients infected with HCV genotype 1, but DAAs capability is hampered by the presence of resistance variants that generate amino-acid substitutions within the targeted protein, which in turn influence the viral sensitivity to these DAAs. Variants with reduced susceptibility to DAAs can exist naturally before treatment starts, but usually at low levels and under DAAs treatment the drug may select for pre-existing

resistance variants and decrease the virus susceptibility to the drug (Halfon and Locarnini 2011, Le Pogam, Yan et al. 2012, Issur and Gotte 2014). Thus, patients should be monitored for resistance selection over the course of treatment. Two integral techniques are used to characterize viral resistance: genotypic and phenotypic assays

Genotypic assay for HCV PIs resistant analysis

A genotypic assay is the detection of the sequence mutations in the viral genome that cause drug resistance. HCV resistance examination during drug treatment is important for understanding the impact of resistant mutations on the clinical outcome and improving the strategies for new drug design (Ferenci 2004, Thibeault, Bousquet et al. 2004, Moriishi and Matsuura 2007, Halfon and Locarnini 2011).

The utilization of genotypic-resistance tool is important for therapeutic decision- making in patients. Patients monitoring should be done in three phases: baseline (pre-treatment) samples, during and post-treatment samples (Le Pogam, Yan et al. 2012).

For baseline samples, viral sequences are analyzed to detect any known resistant variants or possible novel ones. On treatment samples, patient samples are monitored for sequence changes which likely decrease the sensitivity to the drug.

Post-treatment samples, existence or absence of resistant variants give a hint on the virus fitness and the resistance profile compared to the wild type.

PCR (population sequencing) is the most common method for genotypic analysis, but as mutation detection is assay sensitivity dependent (Verbinnen, Jacobs et al. 2012), so the population sequencing is suitable for single mutation pattern and for mutations that exist in less than 10%. While clonal sequencing, ultra-deep sequencing or the TaqMan mismatch amplification mutation assay, are sensitive enough to detect minor resistant variants at 0.01% level (Curry, Qiu et al. 2008).

The phenotypic analysis should be performed on concurrent samples to assess the level of decreased susceptibility related to specific mutations and to the baseline sample. Interpretation of data from samples at viral suppression needs to take into account the fact that different genotypes, subtypes, or specific regions differ in the minimum viral load required for

amplification (Qi, Bae et al. 2009, Imhof and Simmonds 2010). Low template numbers negatively impact assay performance in two ways: (1) the relative proportion of each variant detected increases as a result of reduced amplification of co-existing minority variants, potentially yielding larger discrete changes in frequency estimates; and (2) the chances of re-sampling increases.

Phenotypic assay for HCV PIs resistant analysis

Phenotypic assays are methods used to characterize the susceptibility of the resistant variants to the drugs, the phenotyping is conducted either by cell based: including replicon-based and viral enzymatic assay, or by the biochemical-based enzymatic assay. In the cell-based phenotypic assay, the subgenomic viral RNA model is generally used for anti-HCV research. For insertion of patients fragment, shuttle vector constructs are used. Therefore, clinical isolates are collected and either amplified and cloned into the shuttle vector with a combination of quasispecies, or by insertion of the individual clone in the shuttle vector (Qi, Bae et al. 2009, Imhof and Simmonds 2010, Halfon and Locarnini 2011, Verbinnen, Jacobs et al. 2012). Several shuttle vectors were developed covering the 1a, 1b and 2a subtypes.

Numerous studies examined the utility of the shuttling vector for insertion of different lengths of the HCV genome, they showed that (NS5a-NS5b), (NS3-4A) up to (NS3-NS5b) could be successfully inserted. The shuttle vector used to test for PIs, enables the insertion of NS3 protease or the NS3 protease-helicase domain (Qi, Bae et al. 2009). Investigation of the insertion of the genome from clinical isolates showed that the replication decreased significantly. This could be attributed to the incompatibility between replicon lab strain and the viral genome derived from the patient in addition to insertion of clinical isolates from different subtype than the shuttle vector (Qi, Bae et al. 2009, Binder, Tetangco et al. 2011).

Analysis of the phenotypic results explained by measuring EC50 (the effective concentration of drug needed to inhibit virus replication by 50% in vitro) of clinically derived isolates and compare it to the EC50 of baseline samples, in case baseline samples are unavailable, the EC50 can be compared to the EC50 of the reference replicon (Huang, Hwang et al. 2005, Hwang, Huang et al. 2010).

Interpretation of phenotypic results

Analysis results should be related to a reference (replicon/virus/reporter) control that is run in each assay and can be reported as the fold change EC50. Understanding the significance of a given fold change value is a major challenge. Different cut-off values include technical (accounting for assay variability), biological (accounting for natural variation in drug susceptibility), and clinical (relating drug susceptibility to clinical responses) (Binder, Tetangco et al. 2011, Shiryaev, Cheltsov et al. 2012, Lassmann, Arumugaswami et al. 2013).

1.7.3. NS5a inhibitors

The non-structural NS5A is a zinc-binding phosphoprotein and consists of approximately 447 amino acids and localizes to the ER-derived membrane (Macdonald and Harris 2004, Huang, Hwang et al. 2005, Pai, Prabhu et al. 2005). Along with NS5b protein, it plays an important role in HCV replication and assembly. In addition, it is implicated in the interactions with host cellular function. Therefore, NS5A has been identified as an interesting target for HCV inhibitors development. One possible mechanism of NS5A inhibitors is the inhibition of hyperphosphorylation. Thus, the regulation of phosphorylation is required for efficient viral replication. However, other mechanisms might be involved, for example, NS5a inhibitors mislocalize the NS5a in the ER, which causes errors in the viral assembly (Ranjith-Kumar, Wen et al. 2011, Wang, Wu et al. 2012, Issur and Gotte 2014).

Ledipasvir and Daclatasvir

Ledipasvir is an oral NS5a inhibitor with a broad activity against genotypes 1a, 1b, 4a, and 5a in vitro, but has lower activity against genotypes 2a and 3a. The combination therapy Sofosbuvir+Ledipasvir (Harvoni) at first has been approved for treatment of genotype1, and later it has been extended for genotype4, 5 and 6 treatment (Nakamoto, Kanda et al. 2014, Asselah and Marcellin 2015).

Daclatasvir is another oral NS5a inhibitor. It has a broad coverage of HCV genotypes. Clinical trials have shown that Daclatasvir is more active than Ledipasvir in genotype 3 patients (Bunchorntavakul and Reddy 2015). At first, Daclatasvir in combination with Sofosbuvir has been approved to treat genotype 3. Very recently, FDA has extended the approval of Daclatasvir+Sofosbuvir with or without ribavirin for genotype 1 and 3 (Asselah and Marcellin 2015, Bunchorntavakul and Reddy 2015).

Resistance to NS5a inhibitors

NS5a resistant variants pre-exist within HCV quasispecies without any previous exposure to these drugs. A study has reported that half of the relapsed patients after ledipasvir and sofosbuvir combination therapy were associated with NS5a-resistant variants that pre-exist before therapy (Le Pogam, Yan et al. 2012, Nakamoto, Kanda et al. 2014, Chayama and Hayes 2015). The baseline Ledipasvir resistant variants are, M28T, Q30R/H, L31M, Y93C/H for genotype 1a, and Y93H in genotype 1b which exists in 100 % of patients. These mutations led to lower SVR in patients harboring mutation (Bunchorntavakul and Reddy 2015, Chayama and Hayes 2015). Thus, DAAs from other classes should be used to avoid the cross-resistance.

1.7.4. NS5b polymerase inhibitors

The HCV NS5b polymerase is an important viral protein mediating RNA viral replication, it is composed 591 aa. The enzyme catalytic domain can be structured in hand like structure and it consists of 'fingers', 'palm' and 'thumb' subdomains and the active site is conserved among genotypes, and located in the palm, and 'fingers and thumb' domains are in close interactions. The structural studies have shown that the NS5b has enclosed conformation, with fingertips at one side and b-hairpin linker on the other side. As a result, the closed conformation forms a single-stranded RNA space, which initiates the replication process (Wang, Ng et al. 2003, Powdrill, Bernatchez et al. 2010).

In addition to its role in the virus replication, NS5b plays several roles in pathology by interaction with cellular proteins such as lipid kinase phosphatidylinositol 4-kinase III alpha (PI4KIIIa), and Caprin 1, a cell-cycle associated phosphoprotein, forms a complex with Ras-GTPase-activating protein-binding protein 1 (G3BP1) which has been shown to interact with both HCV NS5b and the 5' end of the HCV minus-strand RNA indicating that it is part of HCV replication complex (Elhefnawi, ElGamacy et al. 2012, Mosley, Edwards et al. 2012, Karam, Powdrill et al. 2014, Asselah and Marcellin 2015). Therefore, the NS5b attracted the attention as a therapeutic target for HCV.

Sofosbuvir

NS5b RNA polymerase inhibitors are classified into two different classes, nucleoside analog inhibitors (NIs) and non-nucleoside inhibitors (NNIs). NIs are ribonucleosides or ribonucleotides analogs that compete with natural ribonucleotide for binding polymerase active site. The first NI investigated in patients is Valopicitabine. Studies reported only low to moderate antiviral activity

(Afdhal, Reddy et al. 2014). Further clinical developments of valopicitabine have been stopped due to toxicity issues.

NIs like sofosbuvir (GS-7977) has broad activity against all HCV genotypes. It terminates the viral synthesis as a false substrate by interacting with the growing RNA chain which results in termination of chain formation. In addition to the pan-genotypic activity, one main advantage over other inhibitors is the high genetic barrier (Janardhan and Reau 2015). The approval of Sofosbuvir along with other DAAs, as the first IFN free all oral combination therapies is an important breakthrough in HCV treatment. Ledipasvir and sofosbuvir (Harvoni) were first approved for HCV genotype 1 chronic patients. The clinical trials have shown impressive results, with SVR rates reached 100% in naïve patients. For other genotypes, sofosbuvir is approved in combination with IFN for therapy (Welzel, Dultz et al. 2014, Nakamura, Kanda et al. 2016). Recently, FDA has extended the approval for patients with genotype 4, 5, and 6 chronic hepatitis C virus (HCV) infection and for patients co-infected with HIV (Ploss and Dubuisson 2012).

Unlike NIs class of inhibitors, the NNIs inhibitors achieve its activity by binding to one of allosteric enzyme sites and this causes a conformational change in the active site and stops the replication complex.

Resistance to polymerase inhibitors

Sofosbuvir is favored for its high genetic barrier, in vitro studies have identified S282T mutation to confer resistance to Sofosbuvir (Mosley, Edwards et al. 2012). Nevertheless, in phase III trials this mutation was not detected, whereas in phase II trials (LONESTAR), only one patient was relapsed under Sofosbuvir monotherapy and this was associated with S282T mutation (Le Pogam, Yan et al. 2012). Despite what was observed in other trials of SOF co-administration with other DAAs like DCV, SMV, or LDV, S282T was not detected in any relapsed patients. Even though this mutation occurred much more commonly in approximately 20% of patients and almost all of patients accomplished SVR. So contrary to PIs, the Sofosbuvir S282T mutation did not affect the treatment outcome (Nakamura, Kanda et al. 2016).

NNIs are associated with three main resistant variants (414T, 419S, and 422K), these mutations occur among the six HCV genotypes. However, NNIs in development have shown that they are possibly effective in combination with other DAAs classes with no cross-resistance (Kayali and Schmidt 2014, Bunchorntavakul and Reddy 2015, Donaldson, Harrington et al. 2015).

1.7.5. Host genetic predictor of treatment response

IL28b polymorphisms

Interferon lamba3 belongs to type III interferons, it is encoded by IL28B, and it is induced by antigens binding to the toll-like receptors (Balagopal, Thomas et al. 2010, Barreiro, Pineda et al. 2011, Asselah, De Muynck et al. 2012). Subsequent to the production of type III interferons, several cellular pathways are triggered, converging with the type I IFN signal transduction and follow by transcription of ISGs (Lange and Zeuzem 2011).

Single nucleotide polymorphism (SNP) is one form of genetic variation, it occurs at a specific location in the genome and they have a frequency of 1% of the population. Overall, SNPs occur more frequently in non-coding regions of the genome than in coding regions.

Genome-wide association study (GWAS) conducted the association of the IL28 rs12979860 and rs8099917 single nucleotide polymorphisms (SNPs) with the SVR in HCV infection. The rs12979860 SNP is positioned upstream the *IL28B* gene and exists either as C or T allele. Numerous studies have shown that rs12979860 SNP is the strongest predictor of HCV treatment response. Thus, the IL28 rs12979860 C/C genotype is strongly associated with HCV spontaneous clearance and with obtaining the SVR in patients treated with interferon-based therapy. Whereas, IL28 rs12979860 C/T genotype, and IL28 rs12979860 T/T genotype associated with virus persistence and poor response to IFN based therapy. C allele has been linked to lower baseline levels of ISGs in liver tissue as well as a sharper drop in HCV RNA on interferon therapy (Thomas, Thio et al. 2009, Lindh, Lagging et al. 2011, Tillmann, Patel et al. 2011, Asselah, De Muynck et al. 2012)This In the line with the association of low baseline levels of ISGs are associated with a better response to treatment.

rs8099917 is another IL28B polymorphism which located between the IL28A and IL28B genes. It is a strong genetic predictor of the HCV treatment response, it has either homozygous G/G, homozygous T/T and heterozygous G/T allele. Individuals with rs8099917 G/G minor allele were found to have low IFN-λ3 expression levels in patients PBMCs (Ito, Higami et al. 2011) Moreover, the rs8099917 G/G minor allele is more frequent in African-American populations compared to European populations, that consistent with the poor response rates in African-Americans to IFN treatment (Thomas, Thio et al. 2009, Barreiro, Pineda et al. 2011, Lindh, Lagging et al. 2011, Tillmann, Patel et al. 2011).

1.8. Crystallization of HCV NS5b polymerase and structure determination

1.8.1. Protein function and structural analysis

Proteins are biological macromolecules, which are related to almost all functions in living cells (Giege 2013). The human body contains more than 100,000 proteins and there are 10 billion ones in the whole universe. Proteins consist of amino acids which are linked together by covalent bonds to make peptides (Raymond, Lovell et al. 2009) . Peptides consist of approximately 100 aa, while polypeptides consist of long chains of hundreds up to thousands of aa. Proteins are formed of one or more polypeptides. Protein function is coupled to its conformation. Considering that protein are large macromolecules, the structure is divided into primary, secondary, tertiary and quaternary (Neamati 2001, Williams, Kuyper et al. 2005).

Protein interaction and function occur via tertiary structure. Consequently, protein structure determines its function. Therefore, researchers seek to determine the protein structure and its relation to the function. The determination of the structure has proven important in many aspects including the structure-guided drug design (M S Smyth 2000).

1.8.2. Protein crystals characteristics

Crystal is a highly symmetric structure which occurs naturally for organic and non-organic substances. In 1985, Kendrew et al have identified the myoglobin three-dimensional structure by x-ray analysis. Protein crystals have different forms and sizes. Thus, the growth conditions affect the diffraction quality which determines the quality of crystal structure modeling. Protein crystals are characterized by size ranging from 0.1 to 0.3 mm, with the largest does not exceed one millimeter dimension. Protein crystals are fragile because of their weak non-covalent bonds and the high water content in them. Therefore, protein crystals should be handled carefully (M S Smyth 2000).

1.8.3. Principles of protein crystallization

In the process of protein structure determination, obtaining a high purified protein in large quantities (few milligrams) is a crucial step for successful crystallization. Once the protein has been obtained in a pure form finding the best protein crystallization condition is a very important step, this includes the right combination of pH, ionic strength, temperature, protein concentration, the concentration of various salts and additives.

There are different approaches for protein crystallization. The most popular ones are the vapor diffusion and the hanging drop method. In solution, crystal growth consists of crystal nucleation followed by growth. The initial screens usually led to small crystals formation then followed by further improvements to obtain larger crystals. Once crystals obtained, they are further exposed to diffraction.

1.8.4. X-ray diffraction and data collection

The X-ray diffraction is delivered by synchrotrons, and then crystals resulting in the diffraction process are a combination of two steps: scattering and interference. The scattering occurs by the interaction between the X-rays and the protein crystal. Subsequently, the scattered waves interact with one another and form the diffraction pattern. Therefore, crystal quality is an important determinant for the resolution (the higher, the better), and the mosaicity (the lower, the better) which determine the degree of lattice perfection. The diffracted X-ray data are collected by X-ray detector and used to solve the protein structure (Chayen 2004, Wakayama, Yin et al. 2006, Newby, O'Connell et al. 2009) .

1.8.5. Protein crystallization in microgravity

Microgravity

Gravity is a natural phenomenon that brings objects with matters together by gravitational force. Therefore, earth acts as a magnet which attracts objects with a force that is commonly described as one g or one earth gravity (Snell and Helliwell 2005, Wakayama, Yin et al. 2006, McPherson and DeLucas 2015). Microgravity or reduced gravity can be created by obtaining a free fall state. This can be exemplified in the drop fall provided by NASA and other facilities, which results in reduced gravity for 4-5 seconds, in aircraft results in 15 seconds of reduced gravity, whereas rockets create several minutes of reduced gravity (Wakayama, Yin et al. 2006).

However, microgravity environment can be conducted by previously mentioned facilities. Therefore, orbiting space crafts provide a solution to establish microgravity conditions for a longer time.

Microgravity provides an opportunity for different areas of research such as biotechnology, fluid physics, fundamental physics and materials science(Snell and Helliwell 2005, DiFrancesco and Olson 2015). Of interest is biotechnology where researchers can benefit from microgravity to study protein crystal growth, mammalian cell tissue cultures, and fundamental biotechnology.

1.8.6. Gravity vs. microgravity for protein crystallization

Researchers have shown that almost 30% of protein crystals grown in space return better X-ray diffraction data than the equivalent ones grown on Earth(Wakayama, Yin et al. 2006, Tanaka, Umehara et al. 2007, Takahashi, Ohta et al. 2013). The reasons behind this can be generally stated in "Factors that claimed to prevent or disturb protein crystal growth are eliminated under microgravity environment." These factors include sedimentation, mass transfer, concentration gradients and convective currents (Carruthers, Gerdts et al. 2013).

Sedimentation in crystallography is the tendency of crystals to precipitate in fluids, considering that gravity acts as a magnetic force which influences sedimentation. Microgravity environment has very less sedimentation rate; therefore formed crystals have little effect on each other in the fluid. On gravity, nucleation of protein crystals occurs in supersaturated fluids and the crystallization process starts when a small aggregates form the nucleus. In contrary to gravity, microgravity crystals nucleate and grow in a depletion zone, where there is less convection, thus crystals grow by stable diffusion of molecules to the depletion zone and this leads to large crystals formation (Leng and Salmon 2009, Giege 2013, Kim, Siesser et al. 2015).

Proof of concept and success stories of crystallization in microgravity

As mentioned earlier, crystals grown in microgravity may exhibit better properties than the ones grown on earth, therefore microgravity aroused as an attractive option for crystallization of proteins with enhanced qualities (Snell and Helliwell 2005, Takahashi, Ohta et al. 2013).

Crystallization in microgravity started three decades ago, but early protein crystallization trials either were poorly documented or described and noted only in space agencies reports mainly because of the failure or partial success. The results of protein crystals of lysozyme, canavalin, and serum albumin grew in microgravity showed that crystals grown in space were more homogeneous, of a higher quality and generally of larger size. In consequence, these proteins showed better X-ray diffraction compared to the earth formed crystals.

A series of crystallized proteins in space showed superior resolution of values less than 1.5 Å including, human insulin, fungus Proteinase K and hen Lysozyme. The results accumulated from microgravity crystallization trials revealed that about 20% of crystallized proteins have better characteristics compared to earth-grown ones. In terms of benefits, high-quality crystals would

fulfill pharmaceutical industry needs and help in the drug design research. In addition, it will provide better understanding and improvements in the microgravity environment research.

However, first space crystallization trials lack the proper control because of the uncontrolled temperature. The collected results formed a base for improvement of the Vapor Diffusion Apparatus (VDA) which was used for previous crystallizations in space and a better understanding of the effect of gravity on crystallization.

Focus on microgravity crystallization results of viruses and viral protein

In the US Shuttle mission IML-1, impressive crystallization results were obtained for Satellite tobacco mosaic virus (STMV). The STMV crystals were of remarkable size ranging from 1 to 1.5 mm, while some other crystals were small in size and were of incomplete and irregular shape, this could be explained by the interruption of the crystallization process (Lorber 2002).

In the United States Microgravity Laboratory- 1 mission (USML-1), HIV-reverse transcriptase protein has been flown to space; the crystallization results showed improvements in both resolution values and crystals order of the space-grown crystals compared to the earth-grown control (Stanley Koszelak 1995).

1.8.7. Crystal structure of viral proteins and drug research

There are several methods to study viruses including, serology, spectrophotometry, electron microscopy and X-ray crystallography.

The structure-based drug design and structural determination using several techniques including X-ray crystallography are interactive processes. In 1935, Wendell Meredith Stanley determined the first virus crystal structure of Tobacco mosaic virus crystal and in 1946 he was awarded Nobel Prize in Chemistry for his work (Wlodawer, Minor et al. 2008).

Over the last half century, virus structures accumulated providing a basis to understand virus capsid assembly, which makes a portal for antiviral drug design. One of the best examples of the structure-based drug design is the HIV protease inhibitors. The presence of several crystal structures of HIV-1 PR –inhibitor complex prompted the drug design against the protease domain. In contrast, the absence of structural information of HIV-1 integrase limited the integrase inhibitors design (Neamati 2001).

Another successful story for structural based antiviral design is Influenza virus neuraminidase inhibitor (Zanamivir).The crystal structure of neuraminidase led to the recognition of the specific enzyme inhibitor (Anderson 2003, Malito, Carfi et al. 2015).

1.8.8. HCV protein crystallization

It took a century from the recognition of viruses as microorganisms till the determination of virus structure on the atomic level. The structural determination of viruses on the atomic level illustrates the virus shape and arrangement of the active site. This consequently led to the interpretation of the virus life cycle. Several methods are utilized for structure determination including X-ray crystallography, electron microscopy and NMR (DiMattia, Govindasamy et al. 2005).

HCV genome varies between different genotypes and subtypes. Thus, sequencing studies collected more than 20000 sequences for HCV. The nucleotide and amino acid sequence analysis of HCV could predict the protein structure, with several 3D structures of HCV proteins are available and this covers structural and structural proteins of different genotypes. The 3D structure of HCV NS5b reveals that it has six conserved motifs, furthermore, it folds in fingers, palm and thumb subdomains. It has also shown that finger and thumb subdomains interact with each other. A unique characteristic of HCV NS5b is the presence of a β-hairpin loop pouch into the active site of the palm subdomain, this suggested to be an important feature for initiation of the virus replication (Wang, Ng et al. 2003, Biswal, Cherney et al. 2005, Hamamoto, Nishimura et al. 2005, Karam, Powdrill et al. 2014). Overall, the NS5b structure determination could explain the virus replication, initiation, and elongation mechanisms and this is targeted for anti-HCV inhibitors design (Ma, Leveque et al. 2005, Powdrill, Bernatchez et al. 2010, Talele, Arora et al. 2010).

1.9. The role of tripartite motif family members (TRIM) in mediating susceptibility to HCV infection

1.9.1. Cellular response to viral infection

Intracellular pathogens such as viruses can lead to chronic infection. Viruses including hepatitis C and B, HIV or Epstein–Barr virus establishes chronic infection by evading the host immune

system and by functional T-cell exhaustion (Vigano, Perreau et al. 2012, Ye, Liu et al. 2015, Beltra and Decaluwe 2016).

However, the elimination of HCV virus is associated with expression of high levels of IFN-γ and low levels of CD38 activation marker at the CD8+CTLs. Contrary to the elimination of HCV infection, the liver injury is associated with CTLs secreting high levels of CD38 and low levels of IFN-γ. In HCV resolved patients, epitopes presented by MHCII CD4+T-cell responses are associated with high levels of IL-2 and IFN-γ (Guglietta, Garbuglia et al. 2009, Sun, Rajsbaum et al. 2015), while chronicity is associated with upregulation of CD4+regulatory T cells that suppress HCV-specific CTL in patients. Moreover, CD4+and CD8+T cells express high amounts of the PD-1 receptor which associated with T cell exhaustion (Ye, Liu et al. 2015).

Toll-like receptors (TLRs) and retinoic acid inducible gene-I like RNA helicases are two important families of PRRs, receptors which can recognize pathogen-associated molecular patterns (PAMPs) at different stages of the virus lifecycle. Consequently, binding results in IFN synthesis and IFN pathway activation (Takeda and Akira 2004, Thompson and Locarnini 2007, Firdaus, Biswas et al. 2014).

TLRs play an important role virus infection, they are classified into two groups depends on the subcellular localization of intra-and extracellular receptors. Therefore, extracellular TLRs can interact with virions on the cell surface, while and intracellular TLRs can recognize viral nucleic acids. Each TLR recognizes a specific PAMP (Heim and Thimme 2014).

Anti-viral TLRs includes TLR3, TLR7 and TLR9 are localized in the ER, following viral infection they translocate to the endosome (Takeda and Akira 2004, Thompson and Locarnini 2007) .

TLR3 sense the viral double-stranded (dsRNA) during the replication of single-stranded RNA viruses (ssRNA), while TLR7 detects the ssRNA and TLR9 recognize DNA PAMP with CpG dinucleotides. Most of the TLRs such as TLR7 and TLR9 are associated with Myeloid differentiation factor 88 (MyD88) adaptor molecule, while TLR3 is dependent on TRIF adaptor molecule (Katze, He et al. 2002, Heim and Thimme 2014).

Activation of MyD88 dependent pathway by TLRs, recruits protein kinases such as IL-1 receptor-associated kinase (IRAK), resulting in activation of Transforming growth factor B-

activated kinase (TAK1), TAK1-binding protein1 and 2. This activation, as a result, activates IkB complex which leads to activation of NF-κB (Meylan, Curran et al. 2005).

Unlike TLR7 and 9, TLR3 associated with TIR domain-containing adaptor (TRIF/TICAM-1), this is mediated by the interaction of TRIF with non-canonical IKk kinases such as TANK-Binding kinase (TBK1) (Firdaus, Biswas et al. 2014). Activation of TBK1 induces IRF3 and IRF7 resulting in the production of IFN-β and ISGs (Suzuki, Saito et al. 2012) .

HCV can invade the immune system at different levels, some groups have shown that NS34A cleaves TRIF molecule, this leads to interruption of IRF3 and NF-κB activation pathway (Heim and Thimme 2014). In addition, HCV NS5a binds to MyD88 molecule and interrupts the further interactions, this leads to inhibition of cytokines production (Shiryaev, Cheltsov et al. 2012, Heim and Thimme 2014). Furthermore, IRF7 plays an important role in controlling HCV infection and it has been observed that HCV decreases IRF7 production; this effect can be rescued by stimulation of TLR7, this leads to IRF7 stimulation and reduction of HCV replication (Meylan, Curran et al. 2005, Kanda, Steele et al. 2007, Majumdar, Chattopadhyay et al. 2015).

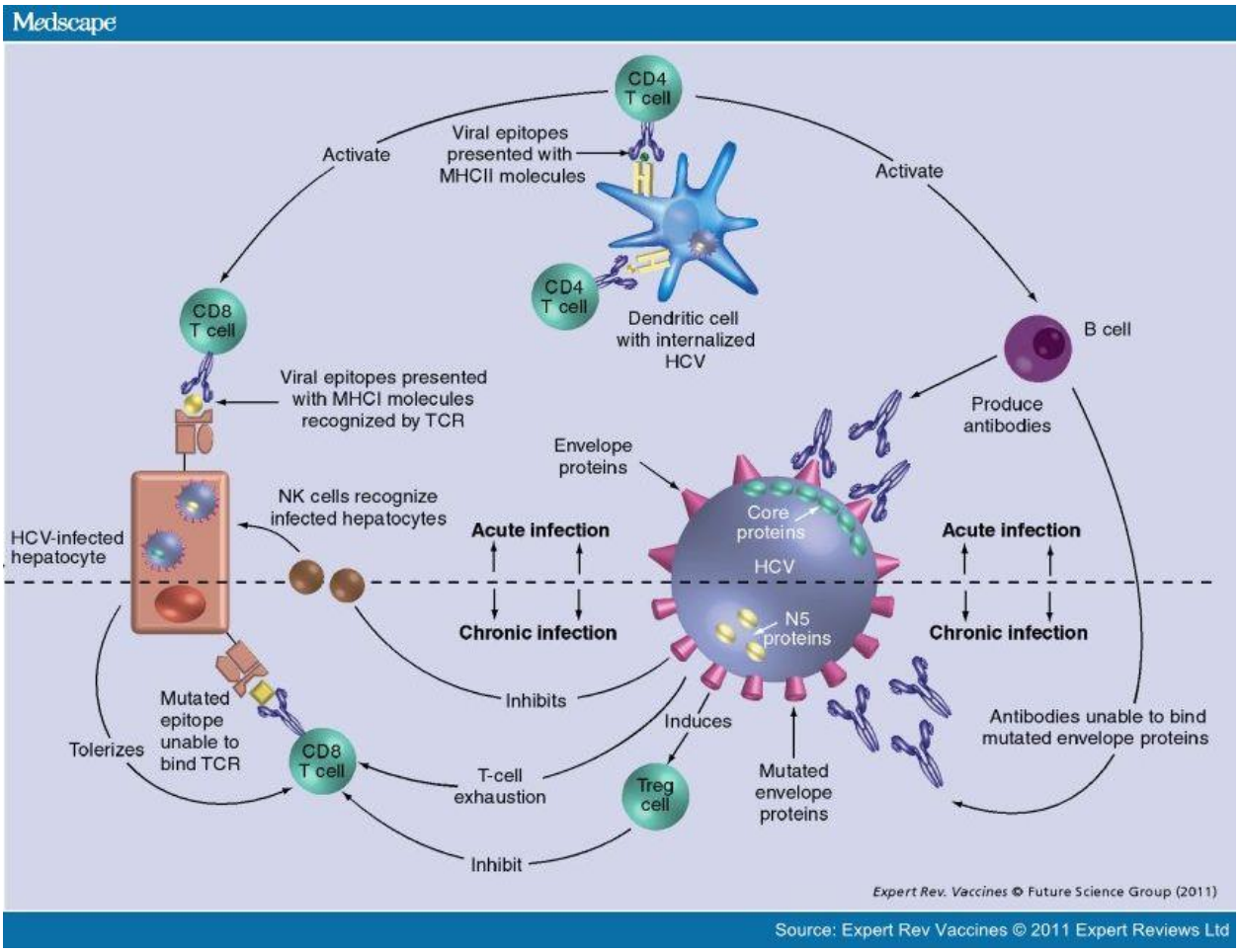

Figure 1.4. Some aspects of the cellular response to HCV infection Multiple elements in the immune system are crucial in resolving the infection: During acute infection (Upper part), a wide range of adaptive immune responses are observed, while during the chronic infection (lower part), the T cells are exhausted and the antibodies are not able to recognize the viral proteins.

1.9.1.1. Interferons and their role in HCV infection

Interferons activation during HCV infection

Interferons (IFNs) belong to cytokines and have anti-viral activity. IFNs are divided into three classes: type I IFNs consist of IFN-α, IFN-β, IFN-ε, IFN-κ and IFN-ω; type II consists of IFN-γ; and type III IFNs include 3 IFN-λ (-1, -2 and -3)(Zhou, Michal et al. 2013, Gokhale, Vazquez et al. 2014).

Type I IFN receptors and signaling

All IFN-α subtypes bind to the same receptor IFN-α receptor (IFNAR), which consists of two subunits (IFNAR1 and IFNAR2). Upon binding, receptors are activated by dimerization and phosphorylation. Following receptors activation, IFNAR1 subunit binds to Tyrosine Kinase (TYK2) and IFNAR2 binds to Janus kinase (JAK). Upon binding, JAK and TYK2 trans-activate each other, results in activation of signal transducer and activator of transcription (STAT) 1, STAT2 and STAT3 (Rajsbaum, Stoye et al. 2008, Metz, Reuter et al. 2013, Majumdar, Chattopadhyay et al. 2015).

Thus, activated STATs interacts with IRF9 and translocates into the nucleus to form interferon-stimulated gene factor 3 (ISGF3), this complex subsequently binds to ISRE of the IFN stimulated genes promoters. Therefore, this binding results in the induction of antiviral state (Spiegel, Pichlmair et al. 2005, Kanda, Steele et al. 2007, Schoggins, Wilson et al. 2011).

Type II IFN: Consists of IFN-γ, it is produced by certain cells such as (NK) cells, CD4+ T helper cells and CD8+ cytotoxic T cells (Ye, Liu et al. 2015)65. IFN-γ binds to IFNGR which consists of two subunits IFNGR1 and IFNGR2 (Zhou, Michal et al. 2013, Jilg, Lin et al. 2014).

Type III IFN: Is recently identified, it consists of IFN-λ family (IFN-λ1, -2 and 3) which also known as (IL29, IL28A, and IL28B) respectively (Eksteen 2011). Upon viral infection, they sense by binding to IFN-λ receptor chain which consists of IL28RA and IL28RB (Li, Liu et al. 2009).

Type I and III IFN are produced in response to viral infections. In viral infection, IFN signaling occurs via PRRs, in the case of HCV, RNA is detected by TLRs and by retinoic acid-inducible gene (RIG)-I-like receptors (RLRs).

RIG-I (also known as s DDX58) and MDA-5 (also known as IFIH1) (Meylan, Curran et al. 2005, Pichlmair, Schulz et al. 2006, Takeuchi and Akira 2008) belong to RLRs, they contain 2 N-terminal caspase recruitment domain (CARDs), DExD/H-box helicase domain . Upon recognition of HCV dsRNA, RIG-I and MDA-5 undergo conformational changes; this allows their binding to MAVS (also known as VISA, CARDIF or IFN-β promoter stimulator 1(IPS-I) (Meylan, Curran et al. 2005). The formed complex then activates downstream proteins TBK1 and IKKε kinases, which in turn activates IRF3 and NF-κB (Majumdar, Chattopadhyay et al. 2015).

In HCV-infected cells, IFN type I and III are induced via two independent pathways, TLR3 and RIG-I and subsequently stimulation of hundreds of ISGs. In acute HCV-infected patients, the expression of ISGs in hepatocytes was shown to be upregulated (Jilg, Lin et al. 2014, Ignatius Irudayam, Contreras et al. 2015).

1.9.2. The role of ISGs in controlling HCV infection

IFNs can upregulate hundreds of ISGs, and several of ISGs have broad antiviral activity, some of those ISGs are protein kinase R (PKR), 2'-5' oligoadenylate synthetase (OAS), MxA and ISG15 (Sadler and Williams 2008). Many ISGs antiviral mechanisms are unknown, it has been noted that HCV-infected cells produce ISGs pattern which overlaps with the ISGs induced by IFN. Surprisingly, high levels of ISGs at the infection baseline are associated with the poor response to IFN based treatment. In chimpanzees and CHC patients, the ISGs levels increase upon HCV infection (Simister, Schmitt et al. 2009, Wilson and Stamataki 2012).

In order to determine ISGs with anti-viral activity, several studies have been done in Huh7 and Huh7.5 hepatoma cell lines. Basically, two approaches were used the overexpression by the introduction of the individual ISGs in the cells using lentivirus followed by infection with HCV. In these experiments, a number of introduced ISGs were associated with the suppression of HCV replication, with the robust antiviral effect observed for RIG-I, MDA-5, IRF1, IRF 2, IRF 7 and Viperin (Helbig, Lau et al. 2005, Seo, Yaneva et al. 2011, Wang, Wu et al. 2012).

Viperin stands for (virus-inhibitory protein, ER-associated, interferon-inducible), it is type I IFN inducible gene, and it is evolutionary conserved. It belongs to radical S-adenosyl methionine domain containing enzymes and consists of 361 aa with 42kDa. Viperin can be induced by different stimulus such as type I, II and III IFNs, the dsRNA analog poly I:C, lipopolysaccharide (LPS), and by several viruses (Seo, Yaneva et al. 2011, Wang, Wu et al. 2012). It has been reported that Viperin inhibits wide range of viruses, including an alphavirus (Sindbis virus), an orthomyxovirus (Influenza A virus), a paramyxovirus (Sendai virus), a rhabdovirus (VSV), and a retrovirus (HIV-1) (Jiang, Guo et al. 2008), and flaviviruses (HCV, West Nile virus, and Dengue virus).

The overexpression of Viperin resulted in suppression of HCV replication, it´s localization in lipid droplets and ER proposes that the anti-HCV mechanism depends on lipid droplets cooperation. Whereas HCV replication complex take place in ER-lipid droplets, and the N-terminal alpha-helix Viperin is associated with ER and lipid droplets. Of note, HCV NS5a and

Viperin have similar N-terminal alpha-helix, therefore Viperin could interact with NS5a on the ER-lipid droplets (Wang, Wu et al. 2012). Another proposed viperin's anti-HCV activity is its binding to vesicle-associated membrane protein-associated protein subtype A (VAP-A), which is known as a host factor essential for HCV replication by interaction with both NS5a and NS5b (Helbig, Lau et al. 2005, Wang, Wu et al. 2012).

Another class of ISGs named Interferon-inducible transmembrane proteins (IFITMs), with the exception of IFITM5, IFITM1,-2 and -3 are induced by IFNs. It has been reported that IFTIMs proteins play an active role against a wide variety of viruses. IFITM1 was found to interfere with HCV on the entry level; this occurs through binding of IFITM1 to the HCV co-receptors CD81 and occludin, consequently this inhibits the virus entry (Schoggins, Wilson et al. 2011).

IFITM3 has been reported to interfere with HCV replication; this is supposed to function via interruption of HCV IRES-mediated translation. Another proposed mechanism overlaps with Viperin mechanism, is the negative regulation of VAP-A, which in turn suppress the virus entry(Jiang, Guo et al. 2008, Seo, Yaneva et al. 2011, Wang, Wu et al. 2012) .

ISG15, identified as an ubiquitin-like molecule (UBL), it conjugates with hundreds of proteins which are involved in several pathways. The protein modification (ISGylation) occurs through activation of E1, E2, and E3 enzymatic subsequent events (Randall, Chen et al. 2006). ISG15 has antiviral activity against different viruses, including HIV and SINV. ISG15 has antiviral activity against different viruses including, HIV and Sendai Virus (Sadler and Williams 2008). Overexpression of ISG15 in IFN-alpha/beta knockout mice resulted in a reduction in the Sendai Virus infection.

The effect of ISG15 on HCV is controversial; in one report they showed that ISG15 overexpression resulted in an increase in HCV replication, the ISG15 pro-viral role is supported by another report whereas silencing of ISG15 inhibits the HCV replication. Moreover, knockdown of the ISGylation negative regulator USP18 results in suppression of HCV via the IFN-alpha-mediated mechanism. In line with this, knockdown of USP18 enhances the antiviral activity against viruses including, such as SINV, hepatitis B virus and VSV (Randall, Chen et al. 2006). The knockdown of USP18 is associated with general enhancement of the ISGs expression, an increase in the cellular protein ISGylation and sustained activation of JAK-STAT pathway. It was observed that liver biopsies from chronically HCV-infected patients, there is a

high increase in UPS18 and ISG15 expression levels, and this could partially explain the poor response to IFN based treatment (Sadler and Williams 2008, Nenasheva, Kovaleva et al. 2015).

1.9.3. The TRIM protein family

TRIM (tripartite motif) proteins (also known as RBCC) are a Ring domain–containing proteins, in human, there are ~70 members of TRIM proteins (Meroni and Diez-Roux 2005, Boudinot, van der Aa et al. 2011, Marin 2012). They are involved in many biological functions including cell proliferation, apoptosis, cell signaling pathways and antiviral defense mechanisms. Many TRIM proteins are ISGs and induced by IFNs (Napolitano and Meroni 2012).

The evolution analysis of TRIM genes revealed that, they are divided into two groups: one group is conserved and present in vertebrates, a second group, evolves more rapidly and present only in vertebrates (Sardiello, Cairo et al. 2008).

TRIM members consist of an N-terminal RING, one or two B-boxes, and coiled-coil (CC) domains (RBCC). The RING domain confers Ubiquitin E3 ligase activity by binding to (UBE2 or E2), which conducts protein modification (Ye and Rape 2009, Napolitano, Jaffray et al. 2011). The B-box domains (B1 and B2) are zinc-binding motifs, they have a different spacing of the conserved Cys and His residues, B-boxes exist only in TRIM family proteins, and the exact function is still unclear(Marin 2012), some studies showed that intact B-boxes are necessary for TRIMs biological functions. Following the B-box domains is the CC domains, is a helical structure which mediates protein-protein interactions in particular homo and hetero-oligomerization, this supports the formation of high molecular weight complexes, which can be useful for the TRIMs function. Based on the C-Terminal domain of TRIM proteins, they are divided into eleven subgroups. The C-terminal domain contains (PRY or SPRY alone or merge of both domains (known asB30.2 domain), recently in TRIM evolution this domain showed a broad expansion which is important for selection, this could explain the importance of this domain in the innate immune recognition of retroviruses (Meroni and Diez-Roux 2005, Rhodes, de Bono et al. 2005, Ozato, Shin et al. 2008, Du Pasquier 2009). TRIMs have different expression patterns depending on the tissue, and their localizations are in both cytoplasm and in the nucleus (Rajsbaum, Stoye et al. 2008, Versteeg, Rajsbaum et al. 2013).

TRIMs modify proteins by ubiquitination

Ubiquitination is a protein post-translational modification that conjugates the Ubiquitin (Ub), a highly conserved cytoplasmic protein (76 aa) to the target protein. This process involves Ub-activating (E1) enzyme, Ub-conjugating (E2) enzyme and Ub ligase (E3) (Choo and Zhang 2009). At first, Ub is activated by E1 enzyme, forming thioester bond, followed by transmission of activated Ub to the cysteine residues of the E2 enzyme, and finally, the E3 mediates the ligation of the Ub to the target protein (Choo and Zhang 2009, Calistri, Munegato et al. 2014). There is one E1 enzyme, around 30 E2 enzymes, and hundreds of E3 enzymes, the high diversity of E3 group define the substrate specificity during ubiquitination. Based on the catalytic core domain there are three groups of the E3 ligases, HECT, RING and U-box protein groups (Sardiello, Cairo et al. 2008). The ubiquitination process can be mono or poly-ubiquitination, the protein monoubiquitination results in a regulatory role in protein trafficking and transportation. Poly-ubiquitination process occurs via several rounds of ubiquitination resulting in a long chain of Ub (Ye and Rape 2009).

Ub contains lysine residues at different positions (Lys6, Lys11, Lys27, Lys29, Lys33, Lys48 and Lys63). Two residues are proven to be associated with Ubiquitination, the (Lys48 and Lys63). While, Lys48-poly-Ub linkage results in 26S proteasome degradation, Lys63 Ub linkage recruits functions associated with non-proteolytic functions such as NF-kβ signaling, DNA repair and protein endocytosis (Napolitano, Jaffray et al. 2011, Versteeg, Rajsbaum et al. 2013). The Ubiquitination can be reversed by a group of enzymes called Deubiquitinating enzymes (DUBs), these enzymes can cleave the Ub from the target protein (Choo and Zhang 2009).

1.9.3.1. TRIM proteins immunological functions

TRIM family members have been implicated in several functions such as cell differentiation, apoptosis, neurogenesis, muscular physiology and innate immune responses. A recent study has shown that TRIM69 plays an important role in zebrafish brain development, the study shows that TRIM69 is expressed in early stages of the embryos brain development, this occurs through regulation of AP-1 pathway (AP-1 functions in a variety of cellular processes, including proliferation, differentiation, and apoptosis), and knockdown of TRIM69 resulted in deformed brain formation, this effect could be reversed when human TRIM69 mRNA was injected into deformed phenotype mice (Han, Wang et al. 2016, Han, Zhao et al. 2016).

The integrity of the cellular membrane is important for the cellular function, several genes have been implicated in the cell membrane repair such as dysferlin4. Other genes such as TRIM72 (mitsugumin 53 (MG53), a muscle-enriched member of TRIMs, has been shown to be an important factor in the cellular membrane repair at the site of injury (Cai, Masumiya et al. 2009, Alloush and Weisleder 2013). In addition, it was observed that muscular membrane damage in TRIM72−/− mice cannot be properly repaired and myopathy phenotype was observed in mice. In vivo experiments showed that injection of recombinant human MG53 (rhMG53) protein can prevent myocyte death. As TRIM72 exist in the blood of mice and other animals, it provides one more advantage for their potential future therapeutic applications. If future researchers prove benefits rendering neuronal cell death, this would be beneficial for potential therapy in neurodegenerative diseases (Alloush and Weisleder 2013).

TRIM proteins involvement in cancers and other diseases

TRIM proteins such as TRIM19, TRIM24, and TRIM25 have been associated with the breast and prostate tumorigenesis development and leukemia progression, this due to their ability to regulate the activation of nuclear and hormone receptors (Nisole, Stoye et al. 2005, Rhodes, de Bono et al. 2005, Rajsbaum, Garcia-Sastre et al. 2014, Masroori, Merindol et al. 2016).

TRIM19 (PML) molecule manages different cell functions such as apoptosis and DNA damage. It has been reported that PML function as a tumor suppressor, its fusion with retinoic acid receptor alpha (RARα) prevents the proper functions of PML and RAR, this complex formation is involved in the acute promyelocytic leukemia. In addition, Pml–/– cells are associated with nuclear bodies mislocalization (Mandell, Jain et al. 2014).

TRIM24 is regulated the activation of several nuclear receptors, including estrogen and retinoic acid, its role in tumorigenesis is variable, however it acts as a tumor suppressor in liver cancers through interfering with RARα-mediated transcription in mice, its overexpression in human breast cancers associated with poor prognosis (Hatakeyama 2011, Elabd, Meroni et al. 2016).

1.9.3.2. TRIM5

TRIM5 belongs to class-IV TRIM family; it contains three zinc-binding domains, a RING, a B-box type 1 and a B-box type 2, and a coiled-coil region, and composed of 493 amino acids, it is expressed in different tissues either intra or extracellularly, in case of liver it is expressed

intracellularly, TRIM5 mainly localizes in the cytoplasmic bodies (Nisole, Stoye et al. 2005, Rhodes, de Bono et al. 2005, Wu, Kirmaier et al. 2013).

TRIM5 alpha is best known as a retroviruses restriction factor, (de Silva and Wu 2011, Pertel, Hausmann et al. 2011, Wu, Kirmaier et al. 2013). Rhesus Monkey TRIM5 alpha has been identified as a restriction factor for HIV-1 and N-tropic murine leukemia virus, in contrast, human TRIM5 does not restrict HIV-1 and shows mild restriction of HIV-2, this indicates the species-specific nature of TRIM5. It inhibits HIV early during infection entry and this can be contributed to the absence of reverse transcripts. TRIM5 different domains contribute to the restriction of viral infection, the Ring domain is responsible for its E3 ligase activity, the B-box domain is associated with the high-order assembly, the coiled-coil domain functions in the TRM5 dimerization which is required for capsid binding, the variation in the B30.2/SPRY domain is responsible for the recognition specificity. It was hypnotized that TRIM5 alpha interacts directly with the core protein. Therefore, upon virus entry the B30.2 domain recognizes the core, presence of viral core enhances the formation of TRIM5 hexamers, and formation of hexamer lattice allows efficient binding and coverage of the core protein, this results in rapid capsid uncoating and blocking of viral infection. (Pertel, Hausmann *et al.* 2011), studied the TRIM5 role in the innate immune signaling to retroviruses. Consequently, they have found that TRIM5 mediates the innate immune response, which in turn establishes an antiviral state, thus can reduce the spread of viruses (de Silva and Wu 2011).

Moreover, several TRIM family proteins including TRIM5 are playing a role in autophagy via participating in the formation of the ULK1-BECN1 active complex. In addition, overexpression of TRIM5 led to autophagy activation, while TRIM5 knockdown resulted in the inhibition of autophagy. Another role of TRIM5 in the autophagy mechanism is its role as an autophagy receptor via its interaction with LC3 (Mandell, Jain et al. 2014). Moreover, it was observed that TRIM5 co-localizes with autophagosome, this observation was tested to check if TRIM5 mediates HIV degradation via autophagosome degradation, the study showed that rhTRIN5 recognizes and interacts with HIV-1capsid consists of the p24 viral protein, which act as a lysosomal substrate (Mandell, Kimura et al. 2014, Lascano, Uchil et al. 2016). The study also found that HIV-1 but not SIV was reduced, thus proposed that TRIM5 specific interaction with HIV-1 capsid protein mediates the HIV degradation.

In a study of the etiology of Multiple Sclerosis (MS) and retroviruses, a link between MS and TRIM5 has been observed, the investigation of 12 SNPs located in the TRIM5 intron 1, whereas TRIM5 RING is encoded by exon 2 showed that SNP rs3802981 is associated with MS development (Nexo, Christensen et al. 2011).

1.9.3.3. TRIM9

TRIM9 protein is also known as (RNF91and SPRING), it is consists of three zinc-binding domains, a RING, a B-box type 1 and a B-box type 2, and a coiled-coil domain, it localizes to the cytoplasmic bodies (Tanji, Kamitani et al. 2010).

The mRNA expression analysis in mice, revealed that TRIM9 mRNA is mainly expressed in the central nervous system during the embryo development, the study also investigated the arrangement of the protein in the nervous system, they supposed that TRIM9 is brain specific and is highly expressed in the cerebral cortex and hippocampus (Caterina Berti 2002, Yang, Li et al. 2014). Moreover, alterations in the Parkinson's disease (PD) and dementia with Lewy bodies (DLB) were detected, whereas brain affected areas have less TRIM9 expression, this finding represent the first prove of TRIM9 involvement in the neurodegenerative diseases (Winkle, Olsen et al. 2016) .

As several members in the TRIM family proteins act as E3 ligase and have, TRIM9 was tested for its E3 activity, in vitro assay showed that TRIM9 act as a self-ubiquitination molecule, furthermore proteasomal inhibitor treatment led to increase in TRIM9 protein, that suppose that TRIM9 undergoes the proteasomal degradation. Moreover, the reduction of TRIM9 protein was observed in mice infected with rabies virus which resulted in down-regulation of several proteins including TRIM9 and as a consequence, accumulation of synaptic vesicles (Yang, Li et al. 2014).

Another role TRIM9 in the nervous system is, its role in the regulation of neurotransmission, the tightly regulated process involves the formation of SNARE complex formation which is important in the neurotransmission, it was reported that TRIM9 specifically interacts with SNAP-25 and adjusts the SNARE complex formation (Tanji, Kamitani et al. 2010).

Since several TRMs involved in the innate immune signaling, TRIM9 was investigated for its role in the immune system. The study showed that, C-I TRIM subfamily including, TRIM9 is highly expressed in CD4+ T cells, while very low or hardly detectable in the macrophages and dendritic cells (Rajsbaum, Stoye et al. 2008, Chan, Towers et al. 2014).

Notably, TRIM C-1 members are highly expressed in T cells and it is the only subgroup contains the COS-FN3 motif, this suggests it role in the T cell regulation (Rajsbaum, Stoye et al. 2008).

An interesting study has revealed that TRIM9 act as a negative regulator of KF-kb in the brain cells. NF-κB has two signaling pathways, canonical and non-canonical pathways, and misregulation of these pathways are associated with cancers, inflammation, and autoimmune disseises. Activation of NF-κB canonical response is dependent on IkB kinase (IKK) complex (IKKa, IKKb, and IKK-g), the inactive form of NF-κB is controlled by IkB inhibitory protein, activation of IKK complex led to phosphorylation of IkBa and b-TrCP, this followed by the release of NF-κB active form. The negative regulation of TRIM9 occurs through its interaction and stabilization of b-TrCP, and this consequently inhibits activation of NF-κB and cytokines (Shi, Cho et al. 2014).

TRIM9 has two isoforms, long (TRIM91) and short (TRIM9s), the long form acts as a negative regulator of the NF-κB , and a recent study has investigated the role of TRIM9 in viral infections, a recent study has found that the short form of TRIM9 acts as a positive regulator of IFN signaling against RNA and DNA viruses. Following viral infection, TRIM9s undergoes self-ubiquitination and enhances the recruitment of GSK3β to TBK1 which results in stimulation of IRF3 signaling cascade. The study analyzed the role of TRIM9 isoforms in VSV infection, when 293T cells transfected with TRIM9s showed a reduction in the VSV infection, while TRIM91 only has modest effect when transfected at high concentration (Qin, Liu et al. 2016).

Interestingly, TRIM9s has antiviral activity against both RNA and DNA viruses, when TRIM9s-overexpressing cell line infected with VSV and Herpes simplex virus HSV-1, low levels of viral RNA was detected compared to wild-type cells (Qin, Liu et al. 2016).

1.9.3.4. TRIM14

The trim14 protein consists of a B-box, a coiled-coil, and a C-terminal PRY-SPRY domain but misses the RING domain; it is localized in the mitochondria and expressed in different tissues (Rajsbaum, Stoye et al. 2008, Uchil, Hinz et al. 2013, Nenasheva, Kovaleva et al. 2015).

Several studies have investigated TRIM14 function in viral infections and innate immunity, for instance in HIV-1-infected patients TRIM14 is upregulated compared to uninfected donors, moreover, TRIM14 was highly expressed PBMCs of influenza A-infected patients and in hepatocytes of HCV-infected patients. Along these lines, the effect of TRIM14 on the SINV was investigated in HEK–trim14 cell lines, the study showed that overexpression of TRIM14 led

to reduction of SINV replication and this reduction is associated with increase in the expression of several genes such as IFN-α, IL6 (IFNb2), ISG15, RAF-1, NF-κB (Nenasheva, Kovaleva et al. 2014).

TRIM14 is an IFN stimulated gene and the investigation of its role in the innate immune signaling revealed that TRIM14 advocate the immune response against viral infections. Upon viral infections, TRIM14 undergoes polyubiquitination and recruits the NF-κB to the MAVS, resulting in stimulation of both IRF3 and NF-κB pathways. Furthermore, TRIM14 knockdown resulted in interruption of NF-κB association with the MAVS which consequently attenuates the antiviral response. This reveals that TRIM14 is a part of the mitochondrial antiviral immunity.

TRIM14 facilitates the type I IFN response via activation of ISRE, NF-κB, and IFN-β promoter activity. Thus, when TRIM14 overexpressed cells infected with VSV, virus replication was inhibited correlating with the transfection dose (Nenasheva, Kovaleva et al. 2014, Zhou, Jia et al. 2014, Nenasheva, Kovaleva et al. 2015).

Some data have suggested the association of TRIM14 expression with tumorigenesis; in tongue squamous cells carcinoma (TSCC) one of the lethal cancers, the aggressiveness of the disease is correlated with the NF-κB pathway activation, in a microarray study TSCC cell survival and resistance to therapy was correlated with the activation of NF-κB pathway. TRIM14 acts as a regulator of several genes which are involved in the NF-κB pathway activation, and when TRIM14 investigated in TSCC patient tissues, data showed that TRIM14 upregulation is associated with the disease stage and with the survival duration. The in vitro analysis of TRIM14 function in TSCC, when Cal127 and SCC9 cells stably transfected with TRIM14, cells showed remarkable growth and resistance to apoptosis induced by chemotherapy (Xuan Su1 2016).

1.9.3.5. TRIM25

TRIM25 also known as Estrogen-responsive finger protein and RING finger protein 147, it consists of N-terminal RING domain, B-box type 1 domain, B-box type 2 domain, coiled-coil domain and C-terminal SPRY domain and localizes to the cytoplasm (Gack, Shin et al. 2007).

TRIM25 is involved in several functions. Its role in the regulation of the RNA expression has been determined, whereas the E3 ligase acts as a specific Lin28a/TuT4 cofactor for uridylation pathway, Lin28a is an RNA binding protein which controls miRNA) maturation (Choudhury, Nowak et al. 2014) mRNA translation and splicing.

Furthermore, TRIM25 expression is involved in several cancers such as ovarian, breast and gastric cancers. It was reported that TRIM25 overexpression is associated with ovarian and breast cancers, while its downregulation was observed in endometrial carcinoma. The analysis of gene expression in gastric cancers revealed that TRIM25 is upregulated in gastric cancer tissues compared to normal ones. Moreover, TRIM25 high expression was associated with low survival of GC patients. Further analysis showed that knockdown of the TRIM25 in GC cell lines (MGC-803 and AGS), hampered the cells invasion compared to the control ones. Interestingly, the study showed that TRIM25 enhances cells migration and invasion by activating TGF-β pathway. Which makes it an interesting target for future therapy perspectives (Zhu, Wang et al. 2016).

Due to the role of many TRIMs in the innate immunity, TRIM25 was investigated for its role in the regulation of innate immunity. RIG-I is an important receptor recognizes viral RNA and undergoes activation process results in the induction of IFN.

TRIM25 acts as an activator for RIG-I, it mediates the RIG-I ubiquitination via interaction of TRIM25 SPRY domain with RIG-I CARD domain which undergoes Lys 63 ubiquitination results in activation of RIG-I downstream signaling (Gack, Shin et al. 2007, Castanier, Zemirli et al. 2012, Choudhury, Nowak et al. 2014).

Given its role in RIG-I ubiquitination, TRIM25 has been proposed to be implicated in the IFN-β production, this was proved when TIRM25WT, TRIM25+/-, and TRIM25-/- MEF cells were transiently transfected with IFN-β promoter plasmid, IFN-β promoter was activated in TRIM25 WT MEF cells with early undetectable activation in TRIM25-/- MEF cells. Moreover, TRIM25 expression in MEF cells decreases the VSV infection, in contrast, high levels of the VSV were detected in TRIM25-/- cells (Choudhury, Nowak et al. 2014, Zhang, Elabd et al. 2015).

Aims of the Thesis

This dissertation is divided into three sections, each one describes a study on HCV.

The aim of study 1: Genotypic and phenotypic analysis of HCV-NS3 variants under protease inhibitors treatment.

The overall aim of the first part of the thesis was to characterize the resistance to HCV protease inhibitors drugs by genotyping and phenotyping. Furthermore, as IL28b is an important host factor associated with the clinical outcome, we wanted to determine the association of the IL28b polymorphisms with SVR in our cohort.

This was accomplished by the following objectives:

1- Establishment and optimization of the genotypic assay of HCV resistance variants (Pre-exist and/or acquired under protease inhibitors treatment).
2- Establishment of phenotyping resistance assay for the analysis of viral fitness and characterization of the resistance profile of the protease inhibitors drugs.
3- Establishment of TaqMan assay for genotyping of IL28b polymorphisms and determination of the relationship between different SNPs and the clinical outcome.

Aim of study 2: Crystallization of HCV-NS5b protein of genotype4a under Microgravity conditions and structure determination:

One aim of NASA missions is to use the advances of the microgravity conditions in the International Space Station (ISS) for scientific research. Thus, throughout the second part of the thesis, we used the microgravity environment of the ISS to crystallize the HCV-NS5b protein of genotype 4a and compare it to the crystallization in 1 g control conditions. Followed by determination of the 3D structure of the HCV-NS5b protein.

These aims were determined as follows:

1- HCV-NS5b protein expression and purification.
2- Protein crystallization under microgravity conditions.
3- Protein crystallization optimization.
4- X-ray diffraction and structure determination.

Aim of study 3: Identification and characterization of TRIM proteins role in HCV infection

Since several TRIMs are interferon-inducible genes and have antiviral activities, we hypothesized that they could have antiviral activities against HCV. We, therefore, sought to investigate whether TRIM proteins could modulate HCV infection and the involvement in type I IFN signaling.

These aims were achieved by:

1- Investigation of the TRIM genes differential regulations during HCV infection and upon IFN treatment.
2- Assessment of whether TRIM5, 9, 14 and 25 have an antiviral activities against HCV infection.
3- Investigation of whether TRIM5, 9, 14 and 25-mediate the regulation of IFN I signaling pathway, in particular, HCV cell receptors and adaptor molecules.

2. Chapter II Materials and Methods

2.1. Materials

2.1.1. Patient samples

For genotypic and phenotypic analysis, blood samples were obtained from patients enrolled in the PEPSI project. All patients with established chronic hepatitis C infection of genotype1, who were clinically resistant or partial responders to protease inhibitors.

2.1.2. Chemicals and reagents

Agarose	Invitrogen
Ampicillin	Roth
BOC	SeqChem Ltd., Pangbourne, UK
Bovine Serum Albumin, BSA BSA-	Sigma-Aldrich
Collagen R	Serva
Dithiothreitol	Sigma-Aldrich
DMSO	Sigma-Aldrich
EDTA	Roch
EGTA	Roth
Ethanol	Roth
Fatty Acid-Free	Sigma-Aldrich
FCS	Gibco
Geneticin	Gibco
Glycine	Roth
HCl 37% (w/w)	Roth
Isopropanol	Roth
PBS	Invitrogen
Penicillin/Streptomycin	Gibco
Polyethylene Glycol (PEG) 8000	Promega
Potassium chloride	Sigma-Aldrich
RNA loading buffer	Sigma-Aldrich
Sodium pyruvate	Gibco

TLV	SeqChem Ltd., Pangbourne, UK
Tris	Roth
Triton-X- 100	Sigma-Aldrich
Tritonx100	Roth
Trypsin- EDTA	Gibco
Tween 20	Roth
Yeast Extract	Gibco
6 x DNA loading dye	Thermo Fisher
Roti®-GelStain	Roth
Pierce ECL Western Blotting Substrate	
OptiMEM	Life Technologies
DMEM	Invitrogen

2.1.3. Kits

Cell Proliferation Kit II (XTT)	Promega
CellTiter-Blue® Cell Viability Assay	Promega
High Pure PCR Product Purification Kit	Roche
LightCycler 480 SYBR Green I Master	Roche
Lipofecatmine2000,Transfection Reagent	Life Technologies
Ni-NTA Spin Columns	Qiagen
NucleoBond Xtra Maxi Kit	Macherey & Nagel
NucleoSpin®RNAII kit	Macherey & Nagel
PJET Plasmid Miniprep Kit	Promega
SuperScript III First-Strand Synthesis SuperMix for qRT-PCR	Life Technologies
SuperScript® III One-Step RT-PCR System with Platinum ® Taq DNA Polymerase	Life Technologies
Luciferase Assay System	Qiagen
T7 Megascript RNA synthesis kit	Life Technologies
Wizard® Genomic DNA Purification Kit	Promega

2.1.4. Enzymes

Fast Digest Pvu1	Thermo Scientific
FastDigest AscI	Thermo Scientific
FastDigest ClaI	Thermo Scientific
FastDigest XbaI	Thermo Scientific
FastDigest XhoI	Thermo Scientific
Shrimp alkaline phosphatase	Roche
T4 DNA Ligase	Thermo Scientific

2.1.5. Plasmids and bacterial strains

Plasmid/Bacteria	Description	Source
HCV plasmids		
pFKi341piLucNS3-3`_ET_Cla1xAsc	Con-1 genotype 1b based control vector, harboring only one AscI restriction site without a deletion	Ralf Bartenschlager, Heidelberg
pFKi341piLucNS3-3`_ET Cla2xAsc	Con-1 genotype 1b based shuttle vector, harboring two AscI restriction sites	Ralf Bartenschlager, Heidelberg
pFKi341PILuc3-3'H77S_NTRscorrected	Con-1/H77s genotype 1b-1a chimeric based control vector	Ralf Bartenschlager, Heildelberg
Jc1=pFK-JFH1J6C-846_dg	HCVcc is J6-JFH1 chimera, highly infective strain and produces high virus titer after infection	Ralf Bartenschlager, Heidelberg
pET-30b(+) plasmid	Bacterial expression vector with an N-terminal His•Tag, thrombin/T7•Tag, configuration plus	Novagen

Escherichia coli-Stbl3		Invitrogen
Escherichia coli-BL21		Novagen
TRIM and IFN pathway plasmids		
TRIM5	Myc-tagged EGFP- pCDNA3+ vector containing full length TRIM5	Kindly provided by Andrea Ballabio lab
TRIM9	Myc-tagged EGFP pCDNA3+ vector containing full length TRIM9	Kindly provided by Andrea Ballabio lab
TRIM14	Myc-tagged EGFP- pCDNA3+ vector containing full length TRIM14	Kindly provided by Andrea Ballabio lab
TRIM25	Myc-tagged EGFP- pCDNA3+ vector containing full length TRIM25	Kindly provided by Andrea Ballabio lab
pGL3-IFNβ-Luc		Kindly provided by Simon Ruthenfüsser lab.
pISRE-Luc		Kindly provided by Simon Ruthenfüsser lab.
pGL3-NF-κB-Luc		Kindly provided by Simon Ruthenfüsser lab.

2.1.6. Primers

Primer ID	Sequence
Genotyping and phenotyping	
NS3 NM 1a	Cgcgtgcggtgacatcatcaa
NS3 NM 1a	Gtggagtacgtgatggggctgc
NS3 NM 1b	Cgggcctacgagaccttgcg
NS3 NM 1b	Caggactgtgccgatgcccaa

NS3 nest 1a	Cgtaggggccaggagatact
NS3 nest 1a	Attgttctcaccccggtcct
NS3 nest 1b	Cccgtcgtcttctctgacat
1a PCR NS3–4A F2	Attagtcaatcgataccatggcgcccatcacggcgtacgc Ccagcagac
1a PCR Prot R2 (E1202G)	AtatgctcaggcgcgccgttgtccgtgaacaccggggacCtcatggttgtccctagg
1b PCR NS3–4A F2	AttagtcaatcgataccatggcgccyatcacggcctactcCcaacagacgcg
1b PCR Prot R2 (E1202G)	AtatgctcaggcgcgccgttgtcygtgaagaccggrgacCgcatrgtrgttcccat
HCV genotype 4a cloning primers	
HCV GT4a, NS5b- XbaI+ RBS (Fw)	Ccg Tctaga Gaaggag Atatac Atgtca Atg Tca Tat Tca Tgg Act Ggg
HCV GT4a, NS5b- XhoI (Rv)	Aat Ctcgag tcgggcatgagacatgctgtgataaatgtc
SNPs primers and probes	
SNP rs12979860 Fw	Tgtactgaaccagggagctc
SNP rs12979860 Rv	Gcgcggagtgcaattcaac

TRIM primers for RT-qPCR

Primer ID	FW	RV	Primer bank ID
TRIM1	Ccagcctccgtggttcttaat	Acaggtcaattcagactccagt	223890256c1
TRIM5	Aagtccatgctagacaaaggaga	Gttggctacatgccgattagg	283046695c1
TRIM6	Actgggttgacgtgaccct	Tcccacaaacctcacttgtct	310772219c1
TRIM9	Gtgtgcggctccttctatcg	Gctgtataggctcatcttgtcca	190341103c1
TRIM11	Gagaacgtgaacaggaaggag	Ccatcggtggcactgtagaa	24497621c1
TRIM13	Gttttgccttgctcccacaac	Tccttacggcatgtaggacac	55953111c1
TRIM14	Tgaaggggaaattcactgaactc	Agcctctggacaggatcgg	15208664c1
TRIM15	Tccctgaaggtggtccatgag	Caggatcttgcccgaggatt	149193330c1
TRIM16	Gtcctgtctaacctgcatggt	Ggcagtatcgccagttgtg	48255912c1
TRIM21	Tcagcagcacgcttgacaat	Ggccacactcgatgctcac	56549143c1
TRIM22	Ctgtcctgtgtgtcagaccag	Tgtgggctcatcttgacctct	313760627c1
TRIM25	Aatcggctgcgggaatttttc	Tctcacatcatccagtgctct	68160936c1

TRIM29	Ctgttcgcgggcaatgagt	Tgccttccatagagtccatgc	109826574c1
TRIM31	Aacctgtcaccatcgactgtg	Tgattgcgttcttccttacgg	62865603c1
TRIM32	Ccgggaagtgctagaatgcc	Cagcggacaccattgatgct	153791513c1
TRIM33	Atgtggagagtggctatgtaaga	Gggcgttgaccagatgctc	74027248c1
TRIM35	Tgaaggaggacgacgtttctt	Gcccaggtacttgcagacatc	94536781c1
TRIM37	Tatggagaaattgcgggatgc	Gtcagccagcgcctaatacag	189458900c1
TRIM40	Acatctcttctgtcgagtgtgc	Ggcagatatagcctgtcccta	156523274c1
TRIM41	Ctgccgagtttgtgtaaccca	Ctcctccatgtcaccctcgta	350276165c1
TRIM52	Atggctggttatgccactact	Ctcgtcctccttactccacag	34147443c1
TRIM54	Atcgtgcaggcatgaggttg	Cctcgcacatgaggtgctg	301897807c1
TRIM55	Ttgtcagcacaacctgtgtag	Cccatgtctatccaaaaccactt	34878835c1
TRIM58	Taccaggtaaagctccagatgg	Gaaagccacgatgcttctcaa	112421126c1
TRIM60	Ctccaagaggagtctagctgt	Tccttccaggatacactgagg	37622897c1
TRIM61	Tctgtcagaaagacctagagctt	Cacggtgcattgtattcctcc	224451016c1
TRIM62	Cgagcagcatcaggtcacc	Ccagttgtcgcttgagcag	217035094c1
TRIM67	Cgtgtcccgagcatgaaatg	Cctgagatagttgtgccttgtg	134288905c1
TRIM7	Cacgcccttaagatccagag	Gggagagctggagaaagagg	
TRIM71	Gtacccatctgtcgtgagtgc	Cggctttgacctccgactg	84993741c1
RIG-I	Gatgccctagaccatgcagg	Gccatcatccccttagtagagc	
MAVS	Ggacgaagtggcctctgtcta	Catggggtaacttggctcctt	
TRIF	Gccaccttctgcgaggatttc	Gttcacctggtgcaggctc	
IFNB1	Atgaccaacaagtgtctcctcc	Gctcatggaaagagctgtagtg	

2.1.7. Cell lines

Huh7 - human hepatoma cell line.

Huh7.5- Hepatoma cell line; Subclone of Huh7; highly permissive for HCVcc infection.

HepG2-HFL- Hepatoma cell line; expresses liver-specific miR-122 besides entry factor CD81.

Con1- Hepatoma cell line, containing genotype 1b (con1) replicon.

Huh7-Lunet- Hepatoma cell line, subclone of Huh7 cells, which was infected with HCV and then treated with IFN-α or a selective HCV inhibitor, permissive Huh-7-descendant.

ED43/SG-Feo(VYG)- Hepatoma cell line, containing genotype 4a (ED43) replicon.

2.1.8. Cell culture media

Cell culture growing media	
Cell line	**Medium composition**
Huh7, Huh7.5, Huh7-Lunet	DMEM, 10% FCS,1% L-Glu, 1%P/S, 1%NEAA, 1%Pen/Strep
HepG2-HFL	DMEM, 10% FCS,1% L-Glu, 1%P/S, 1%NEAA, 1%Pen/Strep, 1 mg/mL of puromycin
Con1, ED43	DMEM, 10% FCS, 1% L-Glu, 1%P/S, 1%NEAA, 1%Pen/Strep, 500 µg/mL Geniticine
PHHs	William's E Medium 10% FCS (FetalconeII), 1%Pen/Strep 1% L-Glu, Insulin, (40 IU / ml), (4.4 mg / ml) Hydrocortisone, (40 mg / ml) Gentamincin, 10 ml DMSO

2.1.9. Devices and equipment

Name	Supplier
Beckmann Avanti	Beckmann
Biosafety cabinet	Heraeus
Co2 incubator	Heraeus
DNA/RNA electrophoresis systems	Peqlab
Electrophoresis gel imaging system	Peqlab
Eppendorf 5417C/R centrifuge	Eppendorf
Incubator	Heraeus
LightCycler® 480II	Roche
Microplate reader Infinite 200 PRO	Tecan
Protein Gel Electrophoresis Equipment	Biometra
Spectrophotometer NanoVue	GE Healthcare

Thermomixer	Eppendorf
Thermocycler T300	Biometra
Gene Pulser II	Bio-Rad Laboratories

2.1.10. Software

Name	Supplier
Windows7, Microsoft Office	Microsoft
Graphpad Prism 5	GraphPad Software,
Light Cycler 480 Software	Roche
Magellan 6	Stüber Systems
TCID50 calculator	Molecular virology, Heidelberg
Fusion	Vilber Lourmat
i-control	Tecan diagnostic
Pymole	https://www.pymol.org/
Endnote	

2.2. Experimental Methods: Part I

2.2.1. Viral RNA extraction

Viral RNA was isolated from all patient serum samples using the QIAamp Virus BioRobot MDx kit (Qiagen, Belgium). RNA extraction was performed using the high throughput M1000 robot extractor (Abbott Diagnostics).

2.2.2. HCV-NS3 RT- PCR amplification and sequencing

Samples were transcribed and amplified in one-step, in which both cDNA synthesis and PCR amplification in a single tube using gene-specific primers was used to amplify a 1 kb fragment. The RT-PCR thermal cycler protocol was as following; one cycle at 55°C for 30 min followed by PCR cycles, 94 ◦C for 2min, 35 cycles of (94 ◦C for 30 s, 55 ◦C for 30 s, 72 ◦C for 3min) and one cycle at 72 ◦C for 7 min.

Amplification products were analyzed by 1% agarose gel electrophoresis, in 1 x TAE buffer. Samples were mixed with 6 x DNA loading dye (Thermo Fisher) and circa 6 µl were loaded per lane on the agarose gel. Electrophoresis reactions were run at 80 - 100 V. The DNA was stained with Roti®-GelStain (Roth) (0.5 µg/ml) and viewed under a UV light with a wavelength between 280 and 320 nm, with the Electrophoresis gel imaging system (Peqlab).

DNA concentration determination

The Spectrophotometer NanoVue (GE Healthcare) was used to determine the DNA concentration using a 3 µl sample. DNA measurements are read at a wavelength of 260 nm, while purity is determined by dividing the absorbance at 260 nm with the absorbance at 280 nm. Pure DNA has a value between 1.7 and 1.9. Lower values are revealing protein contamination, while higher values designate the presence of RNA in the sample.

2.1.3. DNA sequencing and genotypic analysis

Direct and clone sequencing

DNA sequencing used to determine the exact base pair sequence of a DNA fragment. The PCR-based sequencing reaction is based on the enzymatic method. The reaction includes both dNTPs as well as dideoxyribonucleoside triphosphates (ddNTPs), where the addition of ddNTPs to the DNA strand primers chains the reaction termination. As the dNTPs are fluorescently labeled with different dyes they can be recited on an automated DNA sequencer. For direct sequencing,

amplified PCR products were purified by agarose gel extraction using High Pure PCR Product Purification Kit (Roche) following the manufacturer's instructions. For clonal sequencing, amplified PCR products were ligated into a cloning vector using CloneJET PCR Cloning Kit (Thermo Fischer), followed by plasmid purification using GeneJET Plasmid Miniprep Kit (Thermo Fischer). Purified PCR products and selected clones were submitted for sequencing.

Genotypic analysis

Sequence data produced from PCR sequence analysis was submitted to (http://hcv.geno2pheno.org/) HCV drug resistance database to generate an HCV drug resistance profile. Based on the HCV drug resistance profiles, resistant samples were selected for the subsequent phenotypic drug resistance analysis.

2.1.4. *In vitro* phenotypic analysis of HCV drug resistance

Cloning and plasmid purification

Using cloning primers, RT- PCR amplification was done as previously described. PCR products and the shuttle vector DNA were digested with Fast digest AscI and ClaI (Thermo Scientific). Vector DNA fragment and PCR products were purified. The shuttle vector was later treated with shrimp alkaline phosphatase (Roche). In order to ligate DNA insert with DNA vector, the following protocol was used: insert DNA was ligated to vector DNA in a ratio of 1:3, with indicated reaction buffer and 2 U of T4 DNA ligase enzyme in a total reaction volume of 20 µl. The reaction was incubated for approximately 16 hours at 16°C. The ligated DNA vectors were transformed into *E.coli* STBL3 competent cells as follows. Competent cells, formerly stored at -80°C were permitted to thaw for 10 minutes on ice. About 5 to 10 µl of ligated DNA were mixed with 100 µl of competent cells and incubated on ice for 30 minutes. The reaction mixture was heat shocked at 42°C for 1 min and incubated on ice for a further 5 min. A volume of 400 µl of 1 x LB medium was added to the cells and the reaction was allowed to shake for 1 hour at 37°C. For direct large scale preparation of bacterial clones, the transformed bacteria were grown in a 250 ml LB-medium containing ampicillin antibiotic with shaking at 200 rpm overnight.

Large scale preparation of plasmid DNA (MaxPreps)

Maxipreps cultures from transformed DNA were grown in 250 ml 1 x LB medium overnight at 37°C and pelleted by centrifugation at 6000 rpm for 15 minutes. The preparations were done

with the NucleoBond Xtra Maxi Kit (Macherey-Nagel) according to the manufacturer's instructions.

RNA *in vitro* transcription

A panel of samples was used in the antiviral experiment to establish the resistance profile of the PIs. Each chimeric replicon was initially used to generate RNA for phenotyping experiments. The plasmid DNA was linearized by digestion with Fast Digest Pvu1 (Thermo Scientific) at 37 ◦C for 1 hour. RNA was synthesized using a T7 Megascript RNA synthesis kit (Invitrogen) following manufacturer's instruction.

In order to study the resistance profile of HCV NS3 variants, in vitro transcribed RNA samples were purified using MEGAclear™ Kit (Ambion) following manufacturer's instruction.

Electroporation and drug titration

In order to determine the resistance profile of chimeric replicons, purified RNA was prepared for electroporation into Huh-7-Lunet cells. Before electroporation Huh-7-Lunet cells were maintained in growth medium indicated previously, cells were harvested by trypsinization. Cells were washed with PBS prior to electroporation. Cells were adjusted to 1×107 cell/ml, 0.4 ml of cells were transferred with 10µg of RNA using 0.2cm width cuvette (Bio-Rad, Laboratories). Cuvettes were pulsed at 960µF and 270V with a Gene Pulser II (Bio-Rad Laboratories). Cells were then transferred to 20ml of complete medium. Cells were seeded in a white 96-well plate with a clear bottom (Costar) at 100µl/well and incubated overnight. For determination of 50% inhibitory concentration (IC50), incubated plates were treated with serially diluted PIs in DMSO (0.5% final DMSO concentration), 72 hours later, cells were harvested for luciferase measurement.

To determine the luciferase activity, plates were washed with once PBS followed Lysis by adding 50µl of lysis buffer (Promega) and rocking for 20 min with, then 50 µl of Luciferase substrate (Promega) was injected into each well using Microplate reader Infinite 200 PRO Injector (Tecan) to the well. Luciferase was measured with a Microplate reader Infinite 200 PRO (Tecan). IC50 values of PIs were calculated and compared to control samples using the GraphPad Prism program (GraphPad Software Inc., La Jolla, CA).

2.2.5. IL28b polymorphism genotyping

DNA extraction

Genomic DNA was extracted from the whole blood using Wizard® Genomic DNA Purification Kit (Promega).

PCR and direct sequencing

PCR was carried out with Platinum® Taq DNA Polymerase (Invitrogen), 10 pmol of each primer, and 10 ng of genomic DNA. The thermal cycler settings: one cycle of, 94°C for 5 min; 35 cycles of , 94°C for 30 s, 60°C for 30 s, 72°C for 30 s, and one cycle of, 72°C for 7 min. For sequencing, PCR products were purified and subjected to sequencing.

TaqMan SNP genotyping assay

To determine the IL28b polymorphisms, TaqMan predesigned SNP genotyping assay was used to genotype rs8099917 polymorphisms, and to genotype rs12979860 polymorphisms, the PCR reaction and conditions as the following: TaqMan genotyping assay specific mixture and TaqMan universal PCR master mix reagent (Applied Biosystems) were used for genotyping. The PCR genotyping conditions were as following: 10 min at 95°C and 40 cycles of 10 s at 95°C, 1 min at 60°C and 10 s at 72°C. The assay was done by Light Cycler 480 II system (Roche). Data were analyzed by endpoint genotyping.

2.3. Experimental Methods: Part II

2.3.1. Expression and purification of HCV-NS5b

To generate pET30b-GT4a HCV-NS5b construct, HCV RNA was isolated from the plasma of a patient infected by HCV-4a, the NS5b sequence was RT-PCR amplified using HCV GT4a NS5b- XbaI- RBS (Fw) and HCV GT4a NS5b- XhoI (Rv) primers. The forward primer added the Ribosomal binding site (RBS) and XbaI sequences to the 5' end of the gene and reverse primer added XhoI sequence to the 3' end of the gene. PCR product and pET30b+ (Novagen) were digested with XbaI and XhoI before ligation. The pure cut DNA were then ligated as follows, DNA was ligated to vector DNA in a ratio of 1:3, with indicated reaction buffer and 2 U of T4 DNA ligase enzyme in a total reaction volume of 20 µl, resulting in pET30b-GT4a HCV-NS5b construct. The ligated DNA vectors were transformed into *E.coli* BL21 (DE3) competent cells as follows. BL21 (DE3) cells were transformed with the pET30b-GT4a HCV-NS5b expression plasmid and plated on an LB agar plate containing 100 µg/mL kanamycin. To check for insertion of HCV-NS5b, a single colony was picked and cultured for mini preparation. The purified plasmid was then subjected to sequencing. After sequence confirmation, the same colony was cultured at 37°C with shaking at 250 rpm till OD600 reached ~0.6. To induce protein expression, isopropyl β–D–1–thiogalactopyranoside (IPTG, 0.5 mM) was added to the culture and the culture cells were cooled to 32°C for 4 hours. Cells were harvested by centrifugation at 10000 x g and 4°C for 30 minutes and the pellet was stored at –80 °C until use. For recombinant protein purification, cell pellets were resuspended in lysis buffer NPI-10 (50 mM NaH2PO4, 300 mM NaCl, 10 mM imidazole) pH 8 and disrupted by sonication on ice (QSonica Misonix 200 (Qsonica), 1-minute pulse 1-minute pause for several rounds). Whole cell lysate was clarified by centrifugation at 14,000 x rpm for 30 minutes at 4°C. Soluble cell lysates were loaded onto 1 mL Ni–NTA agarose beads (Qiagen). The loaded resin was washed with NPI-20 (50 mM NaH2PO4, 300 mM NaCl, 200 mM imidazole), and the product was eluted in NPI-50 (50 mM NaH2PO4, 300 mM NaCl, 500 mM imidazole).

SDS-polyacrylamide gel electrophoresis (SDS-PAGE)

To check for protein expression and purity, an aliquot of each step was run under denaturing conditions in a sodium dodecyl sulfate-polyacrylamide gel. Therefore, gels were made using an acrylamide concentration of 12% for the resolving gel. The acrylamide/bisacrylamide solution

was a 30% stock solution. The polymerization reaction was started when 1/1,000 volume TEMED and 1/1,000 volume saturated ammonium persulphate added to the solution of the separating gel and then was poured into gel casts. Then, 1 ml of isopropanol was applied to remove air bubbles, and the gel was allowed to polymerize for ~20 minutes. The stacking gel containing 5% acrylamide stock solution was applied. After insertion of the comb, the gel left to polymerize. After polymerization, gel cast was assembled into electrophoresis module and the tank filled with 1X running buffer. Protein samples were mixed with a relative volume of 6X Laemmli buffer containing DTT as a reducing agent. Further denaturation was done by incubation for 5 min at 95°C before loading onto the gel. To estimate the molecular weight of the protein sample, a protein standard "Prestained Protein Marker"(Thermo Scientific) was used and gels were run at 35mA per gel.

After electrophoresis, proteins were stained with Coomassie blue solution for overnight at 22-25°C. Thereby proteins were fixed within the gel. For destaining, gels were incubated for 20 min at 22-25°C in a 5% methanol/5% acetic acid solution, the solution was changed when until clear staining obtained.

Western blot

To confirm the expression of His-Tagged HCV NS5b, Proteins were resolved by SDS-PAGE and after electrophoresis transferred to a polyvinylidene difluoride membrane (PVDF) (GE, health) using a Trans-Blot SD Semi-Dry Transfer Cell (Bio-Rad, Munich, Germany). PVDF membrane was activated by soaking into Methanol for I min. Then all components were soaked in 1X transfer buffer () and the blotting sandwich was layered as follows: From bottom to top: sponge layered with filter paper followed by the gel, the PVDF membrane, a piece of filter paper and the second piece of sponge. The assembly was then run at a constant run at 18V for an hour.
The membrane was then blocked for non-specific binding by incubation in blocking buffer (TBS-T containing 5% milk powder). The membrane was then incubated at 4°C in m anti-His primary antibody diluted in (TBS-T containing 5% milk powder) at a dilution of (1:2000). The membrane was then washed 3X 10 min with (TBST), then the membrane was incubated with HRP- secondary antibody at a concentration of 1:10000 for an hour at room temperature. The membrane was then washed three times as described above. Bound antibodies were detected by ECL+- system (Amersham) and protein bands were visualized by Fusion.

2.3.2. Protein Large-scale production and purification

To obtain enough protein for crystallization, the cell culture volume was scaled up and protein was expressed and induced as previously described. The cell cultures were then transferred to 300ml centrifuge tubes and spun at 14,000 g for about 30 minutes to pellet the cells. The cell pellets were frozen in a -80 ˚C freezer for overnight storage. The next day, the cells were thawed and were resuspended in lysis buffer and lysed by sonication. The cell lysate was clarified by centrifugation at 14,000 g for 60min at 4°C. The supernatant was then processed for purification.

His-tag purification of HCV-NS5b protein

To purify the His6-HCV-NS5b protein, two purification steps were performed, First, the Nickel-NTA column method. Briefly, Ni-NTA column was equilibrated with lysis buffer. The cleared supernatant was loaded onto the Ni-NTA column with a suction pump. Impurities that were weakly bound to the column were detached by washing the column with a wash buffer with a low imidazole concentration (50 mM NaH2PO4, 300 mM NaCl, 20 mM imidazole, pH 8.0). To elute the NS5b protein elution buffer with a high concentration of imidazole (50 mM NaH2PO4, 300 mM NaCl, 550 mM imidazole, pH 8.0) was used. Flow-through was collected and the protein concentration and purity were examined by a UV absorption and SDS-PAGE.

Gel filtration chromatography of HCV NS5b protein

The purified protein sample obtained from previous purification step was injected to the ÄKTA system, and AIX was performed with a flow rate of 1 ml/min. For the first half an hour the sample was washed over the column with the low-salt buffer (20 mM Ethanolamine – 50 mM NaCl buffer at pH 9) and the flow-through was collected in 1 ml fractions. After several washes, the buffer passing over the column was changed to 20 mM ethanolamine – 1 M NaCl buffer at pH 9. The protein peak sample was eluted with this high salt buffer and fractions were collected in 2 ml. Wash and peak fractions were analyzed in 12% SDS-PAGE. The purest fractions were then pooled and concentrated with Amicon ultrafiltration system to the final concentration of volume of 16mg/mL. The protein sample was then aliquoted and flash frozen and stored at -80°C for crystallization experiments.

2.3.3. Microgravity crystallization

Filling and Freezing of CrystalCards™

Protein, buffer and precipitant samples were shipped on dry ice to (Protein BioSolutions, Inc., Gaithersburg, Maryland, United States of America,). Samples were kept frozen prior filling onto Crystal cards. The CrystalCards™ were filled using Protein BioSolutions, Inc.'s Plug Maker™ with the parameters. Two cards were filled, one for microgravity and one for 1g control. Next, cards were stored at -80 °C prior to the launch.

Protein crystallization in the ISS

Microgravity card was placed in card frame, implanted into individual zip closure plastic bags and placed into NanoRacks NanoLab module and transported to the SpaceX launch facility at Kennedy Space Center, Florida. NR PCG1 was kept at -80 °C until moved to the -95 °C General Laboratory Active Cryogenic International Space Station (ISS) Experiment Refrigerator (GLACIER) on the SpaceX Dragon capsule ~12 hours before launch. Launch occurred on NR PCG1 was removed from the GLACIER and stored in Expedite the Processing of Experiments for Space Station (EXPRESS) rack 4 on the Japanese Experiment Module of the International Space Station. The experiment was permitted to thaw at 23-24 °C. The control 1g NanoLab module was subjected to the equal alterations in temperature. The ISS card then returned from the ISS after 21 days of exposure to microgravity. Both cards were then surveyed with the microscope for crystals formation.

2.3.4. Optimization of crystallization

Crystallization experiments for NS5b were performed at the X-ray Crystallography Platform at Helmholtz Zentrum München.

The initial crystallization screening of NS5b was set up at 292 K using 4 mg/ml of protein with a nanodrop dispenser in sitting-drop 96-well plates and commercial screens. The conditions were then optimized to obtain monocrystals of sufficient dimensions and quality for the X-ray diffraction experiments. Optimization was performed using the sitting-drop vapor diffusion method at 292 K in 24-well plates. When crystals of potential good quality were obtained, crystals were looped with nylon loop and flash frozen in liquid nitrogen.

2.3.5. X-ray diffraction and data collection

For the X-ray diffraction experiments, the NS5b crystals were mounted in a nylon loop and flash cooled to 100 K in liquid nitrogen. The cryoprotection was performed. Diffraction data for HCV-NS5b crystals was collected Diffraction data was collected on the ID30 beamline (ESRF, Grenoble, France). Data collection was performed at 100 K. The dataset was indexed and integrated using XDS and scaled using SCALA. Intensities were converted to structure-factor amplitudes using the program TRUNCATE.

2.3.6. Structure determination and refinement

The structure of NS5b was solved by molecular replacement using the crystal structure of the RNA-dependent RNA polymerase from hepatitis C virus (PDB code: 1C2P, Lesburg et al., 1999) as a search model. Both proteins share 75% sequence identity. Model building was done in COOT. The refinement was done in REFMAC5 using the maximum likelihood target function including TLS parameters. The current model is characterized by R and Rfree factors of 22.4% and 32.2% (Table 2). The stereochemical analysis of the model was done in PROCHECK and MolProbity.

2.4. Experimental Methods: Part III

2.4.1. Cell Culture

Growth and maintenance of Huh7.5, Huh7

Huh7 and Huh7.5 cells were cultured in complete DMEM (See Materials).

Growth and maintenance of HepG2-HFlL

Huh7 and Huh7.5 cells were cultured in complete DMEM supplemented with 1 mg/mL of puromycin (See Materials).

Growth and maintenance of ED43

Huh7 and Huh7.5 cells were cultured in complete DMEM supplemented with 500 µg/mL Geneticin (See Materials).

Primary human hepatocytes (PHHs)

PHHs were obtained from (Grosshadern Hospital Munich), adhered to 12 well plates coated with collagen, PHHs were 95% pure.

All cells were maintained at 37°C in a Co2 incubator.

2.4.2. HCV virus production

For the production of HCV-JC1 strain, the Jc1=pFK-JFH1J6C-846 plasmid was used. The plasmid was into *E.coli* STBL3 competent cells. The reaction mixture was heat shocked at 42°C for 1 min and incubated on ice for a further 5 min. A volume of 400 µl of 1 x LB medium was added to the cells and the reaction was allowed to shake for 1 hour at 37°C. The transformed bacteria were grown in a 250 ml LB-medium containing ampicillin antibiotic with shaking at 200 rpm overnight. Plasmid DNA was then purified using the NucleoBond Xtra Maxi Kit (Macherey-Nagel) according to the manufacturer's instructions. RNA was synthesized from plasmid DNA using a T7 Megascript RNA synthesis kit (Invitrogen), and then RNA was purified using MEGAclear™ Kit (Ambion) following manufacturer's instruction.

For electroporation with HCV RNA, Huh7.5 cells at 70-90% confluence were trypsinized and resuspended in PBS. Cells were then resuspended at 1.5 x 10^7/mL Cytomix. 10µg RNA was used to electroporate 400 µl cell suspension, cells were pulsed at 975 µF, 270V with a Gene Pulser II (Bio-Rad Laboratories). The cells were immediately transferred into DMEM (1.3

electroporation/150 cm2 flask). Flasks were transferred to the BL3 lab in maximum 4 hours post electroporation). Cell supernatant was collected every day for circa 2 weeks. Cell supernatants were centrifuged at 1000 g, clear supernatants were mixed at (1:5) with 40% PEG 8.000 for at least 24 h at 4°C. Finally, supernatants were centrifuged for 2.5 h at 5.000 g, 4°C, the virus pellet was re-suspended, aliquoted and stored at -80°C.

TCID50 for HCV virus titer determination

Huh7.5 cells were seeded at a density of $1x10^4$/ well in a (96 well plate). Next day, virus stock or supernatants with unknown virus titer were serially diluted and applied to the cells. 72h later, cells were fixed with 4% PFA for 20 min at room temperature. Cells were washed 3X with PBS and were permeabilized with 0.5% TritonX100 in PBS for 10 min. Cells were blocked with 5% BSA in PBS for 30-60 min at room temperature. Cells were incubated with anti HCV-NS3 (1:3000 in 1%BSA) overnight at 4°C, followed by incubation with anti-mouse HRP antibody for 1 hour at room temperature. The substrate was added and positive cells were counted for 50% Tissue Culture Infective Dose (TCID50) calculation.

2.4.3. HCV infection experiments

Huh7, Huh7.5, HepG2-HFL cells were infected with HCV (JC1) at 0.1 Multiplicity of infection (MOI) and the PHHs cells were infected at (5 MOI). Cells were then incubated at 37°C for indicated durations for each experimental setup.

2.4.4. Interferon treatment experiments

For interferon-alpha treatment experiments, cells were treated with IFN (1000IU/ml) and incubated at 37°C for indicated time intervals given for each experiment.

2.4.5. Transient transfections

One day prior transfections, cells were seeded in an appropriate plate format. On the day of transfection, plasmid DNA was diluted serum-free OptiMEM medium and incubated for 5 min at RT. Lipofectamine (Lipofectamine 2000, Invitrogen) was diluted OptiMEM for 5 min at RT. Diluted DNA was added to diluted lipofectamine, and the complex allowed to form by incubation for 20 min at RT. The transfection mix was then added dropwise to the wells. Cell numbers and DNA amounts are indicated in the table below.

Plate format	Cell number	DNA amount	Lipofectamine amount	Transfection volume
6-well plate	$3\text{-}4\times10^5$	0.4-2µg	5µL	400µL
12-well plate	$1\text{-}2\times10^5$	0.2-1µg	2.5µL	200µL

2.4.6. Cell viability assay

The viability of TRIMs transfected cells was determined using CellTiter-Blue® Cell Viability Assay (Promega). Briefly, 12 well plates were transfected with different TRIM5, 9, 14, 25. 72h post-transfection, cells were treated with CellTiter-Blue reagent 100µl diluted in 400 µl media. Cells were incubated at 37°C for 2-4 hours. Fluorescence intensities were measured, the viability was calculated in relation to control cultures.

2.4.7. Reporter gene assay

For pGL3-IFNβ-Luc, pISRE-Luc, pGL3-NF-κB-Luc promoter plasmids encode F- luciferase gene, the promoters' activities were determined using firefly luciferase assay. Cells were seeded and co-transfected with DNA from one of the promoter plasmids along with DNA from TRIM or pCDNA3.1 control plasmid. For some experiments, further HCV infection or IFN treatment were performed. Cells were then incubated at 37°C for the desired durations. Cells were washed with PBS followed by lysis with 50µl of lysis buffer (Promega) and agitation for 20 min. Firefly luciferase was assayed by adding 50 µl oF-Luc substrate (Promega) in each well, and luminescence readings determined using Microplate reader Infinite 200 PRO (Tecan) and normalized to protein contents.

RNA extraction, reverse transcription and q-PCR

RNA was extracted from cells using the NucleoSpin®RNAII kit"(Macherey Nagel) following manufacturer instructions. RNA purities and concentrations were measured using NanoVue. RNA was subsequently reverse transcribed to cDNA using the SuperScript® III First-Strand Synthesis SuperMix kit (Invitrogen) as follows, 5 µl of 2x RT reaction mix were combined with 1 µl of RT enzyme mix and 4 µl of extracted RNA. cDNA was transcribed in a thermocycler with following temperature profile: 25 °C for 5 min, 50 °C for 30 min, 85 °C for 5 min, 4 °C. Then 0.5 µl of RNaseH (5000U/ml) were added to each preparation.

To determine the expression of genes of interest, the qPCR reaction was carried out using the cDNA sample missed with 0.5 µl of reverse primer (20 µM), 0.5 µl of forward specific primers

(20 µM) and 5 µl SYBR® Green Mix (Invitrogen, Karlsruhe, Germany). Relative expressions to GAPDH (housekeeping gene) were determined using Light Cycler 480 Software using.

Chapter III Results and Discussion

3. Part I: Genotyping and phenotyping of HCV protease inhibitors resistance mutations

3.1.1. HCV PIs resistant testing

3.1.1.1. RT-PCR amplification of HCV protease-helicase domain (NS3PH)

For PCR amplification of HCV NS3PH, HCV sequences from HCV database were aligned using Clustal W and two sets of primers were designed to amplify each subtype. A nested PCR was applied for some samples to increase the PCR sensitivity. All RT-PCR were performed using SuperScript™ III One-Step RT-PCR System with Platinum® Taq High Fidelity and PCR conditions described in the materials and methods part.

We then applied the protocol to amplify HCV NS3PH of patients under protease inhibitors therapy. The amplification protocol of HCV NS3PH (≈ 900 bp) was successful for amplification of patient isolates with a virus titer limit ≈ 10^3 IU/mL.

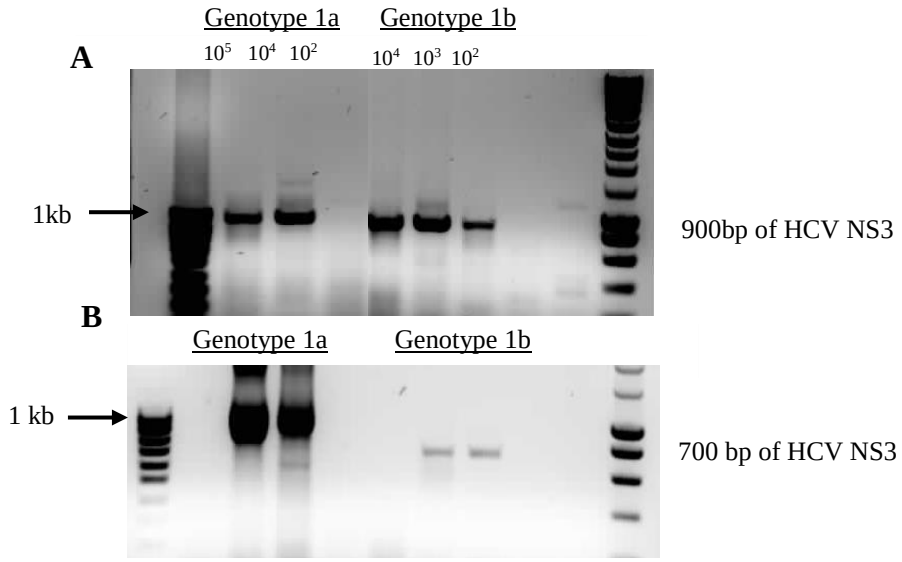

Figure 3.1. RT-PCR amplification of HCV NS3PH of patient serum samples with different viral loads and subtypes HCV 900 bp protease domain (A), 900 bp protease domain using outer primers (B), and 800 bp protease domain subtype1a, 700 bp protease domain of subtype1b were amplified respectively, from genotype 1a and 1b serum virus with viral loads between 10^5 IU/ml and 10^2 IU/mL.

3.1.1.2. Detection of resistant mutations either by direct or clone sequencing analysis

In order to determine the resistant mutations in patient samples, HCV-NS3 isolates were PCR amplified and sequenced either by direct or clonal sequencing. After that, the resultant sequences were screened for nucleotide variants and compared to wild-type sequences using geno2pheno (HCV) the web service analysis tool. Figure 3.2 A, the histogram shows the HCV NS3 sequence results. Figure 3.2.B indicates an amino acid change at position V36M. Figure 3.2.C, geno2pheno report summarizes the variations in the NS3 domain with a prediction of the resistant mutation to the wild-type virus and the cross-resistant to PIs. In the case of novel substitution, the geno2pheno can predict the probability of resistance and the resistance factor to PIs. The method enables the identification of HCV variants within 3 days, and the analysis by geno2pheno HCV can estimate the response to the PI therapy.

A

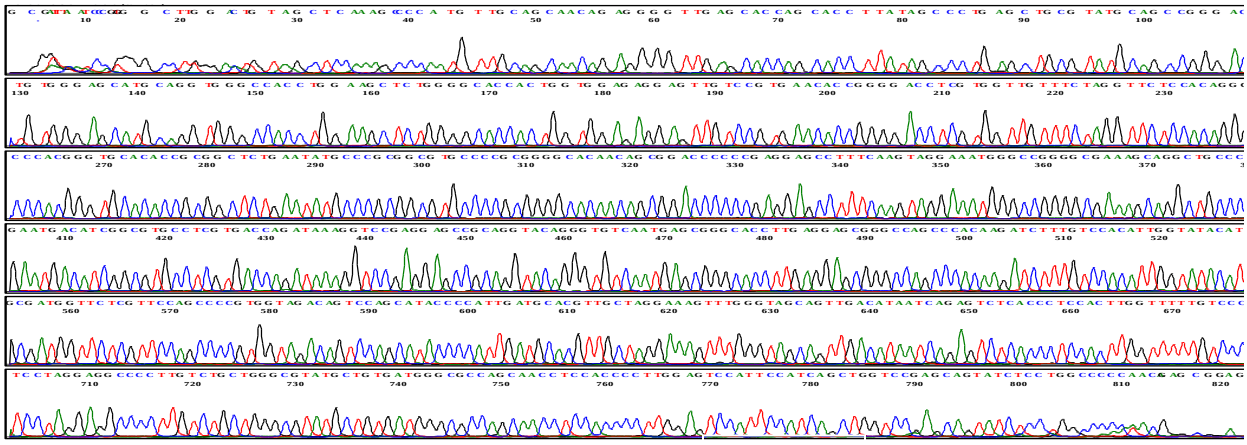

B

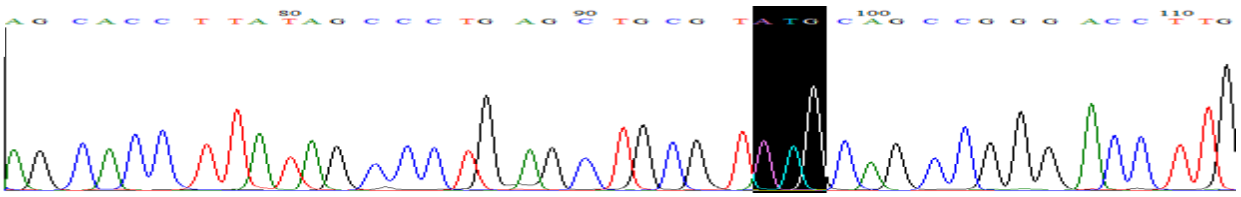

C

geno2pheno®

HCV resistance prediction from genotype (version 1.0)

I. General information

Patient:		Study Id:	
Birth date:		Viral load:	
Sample received:		Sample collected:	
Sample ID:	896581a - 1052837	Predicted genotype:	1
Sample type:		Report date:	
Physician:		Reported by:	

II. Substitutions

NS3 region	V33T, Q34L, V36M, A40T, Q80K, S91A, V151A, M179T

III. Resistance analysis

Drug	Prediction		Scored Mutations
Boceprevir	resistant		36M
Telaprevir	resistant		36M

Figure 3.2. HCV NS3PH resistant variants determination HCV NS3PH domain was RT-PCR amplified from viral RNA samples and then submitted for sequencing, the chromatogram shows (A) whole NS3 domain obtained from sequencing (B) nucleotide sequence substitution (GTG→ATG) leads to amino acid codon change (V36M) (C) resistant mutations were determined using geno2pheno (HCV).

3.1.1.3. Pre-existence and emergence of BOC/TLV-resistant variants in HCV patients

For determination of HCV NS3 mutation pattern, a total of 41 samples were screened, direct or clonal sequencing was used followed by variants analysis with geno2pheno (HCV). Substitutions of residue 36 (V36A/M/L), 54 (T54S), 80 (Q80K), 132 (I132V) 155 (R155K), 156 (A156T) were determined in patient samples exposed to Boceprevir/TLV treatment or preexist in naÏve patient samples before Simeprevir treatment. Novel substitutions at 156 (D156P), 168 (D168I/V) and 174 (N174G/R/S/L) were identified in some patient samples with possible resistance to PIs.

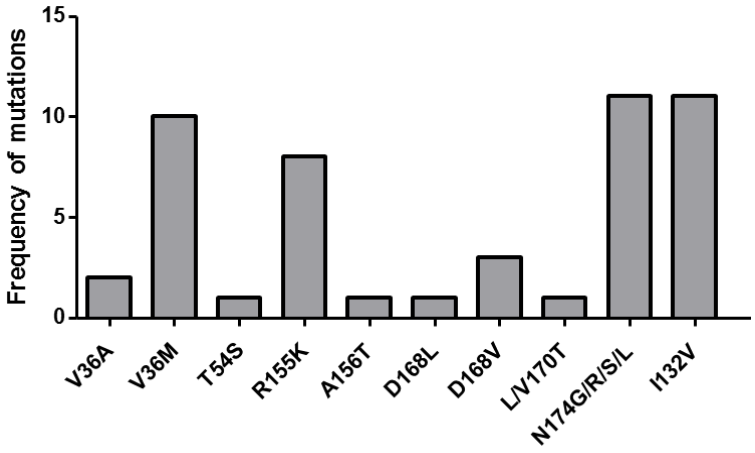

Sequenced patients		
	Subtype 1a	Subtype 1b
Variant	28 patients	13 patients
V36A	2 (7%)	0
R155K	2 (7%)	0
V36M+R155K	9 (32%)	0
Q80K	7 (25%)	0
A156T/P/L	0	5 (38%)
N174 G, R, S, L	5 (18%)	2 (15%)

Figure 3.3. Detection of resistant mutations In total we genotyped 41 samples. We isolated RNA, and then NS3 was RT-PCR amplified and sequenced. Mutation patterns were identified by alignment to geno2pheno (HCV). Out of the 41 either resistant or naÏve samples prior Simeprevir treatment, V36A/M/L, T54S, R155K, A156T, Q80K, I132V have been identified previously to cause resistance to BOC, TLV and/or Simeprevir whereas, D156P, D168I D168V, and N174G, R, S, L are possible novel mutations.

3.1.1.4. Construction of shuttle vector containing patient isolates

For shuttling of HCV-NS3 protease, we used Con1-ET-2xAsc-delta shuttle vector harbors three adaptive mutations (E1202G, T1280I, and K1846T) to enhance the RNA replication (Friebe and Bartenschlager 2009). First HCV-NS3 PCR amplification and insertion of a Cla1 and Asc1 cloning sites and E1202G adaptive mutation, NS3 protease domain from patient samples identified as resistant or possibly resistant in the genotyping analysis were cloned into the shuttle vector. Chimeric replicons carrying the heterogeneous genes from clinical isolates expected to

have less replication capacity.

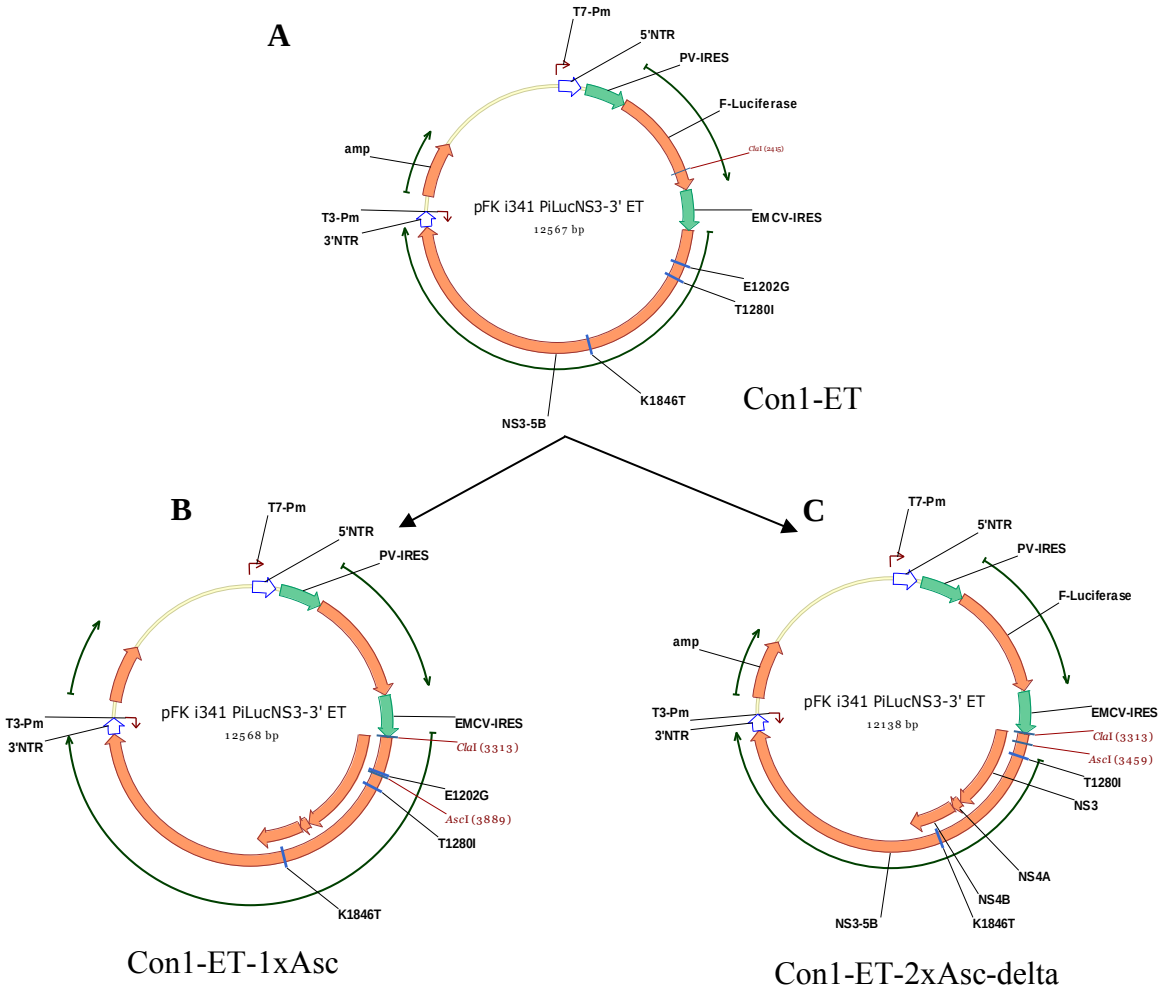

Figure 3.4. Generation of control and shuttle constructs (A) Parental replicon Con1-ET. (B) Introduction of a ClaI-Site at position 3313 and a single AscI-Site at position 3889; deletion of original ClaI-Site at position 2415 insertion of new Cla-11-ET-2xAsc-delta shuttle vector. (C) Con1-ET-2xAsc-delta, introducing a second AscI-site at position 3459 a deletion of base pairs 3459 to 3889 was possible to render this replicon replication-incompetent.

3.1.1.5. Replicative fitness of control and shuttle vectors

To examine the replication fitness of the shuttle vectors (Con-1 ET.1xAsc and Con1/H77), RNA was in vitro-transcribed and electroporated into Lunet cells, and the replicon fitness was measured by F-Luc reporter activity. The results showed 60% reduction in the replication capacity of Con-1 ET.1xAsc replicon compared to Con1-ET. While the replication capacity of Con1/H77 was hindered compared to Con-1 ET.1xAsc. The replication fitness of Con-1 ET.1xAsc makes it suitable for shuttling of NS3 patient samples while the significant reduction in Con1/H77 replication fitness hinders the ability to use it for shuttling of NS3 isolated from patients infected with genotype 1a.

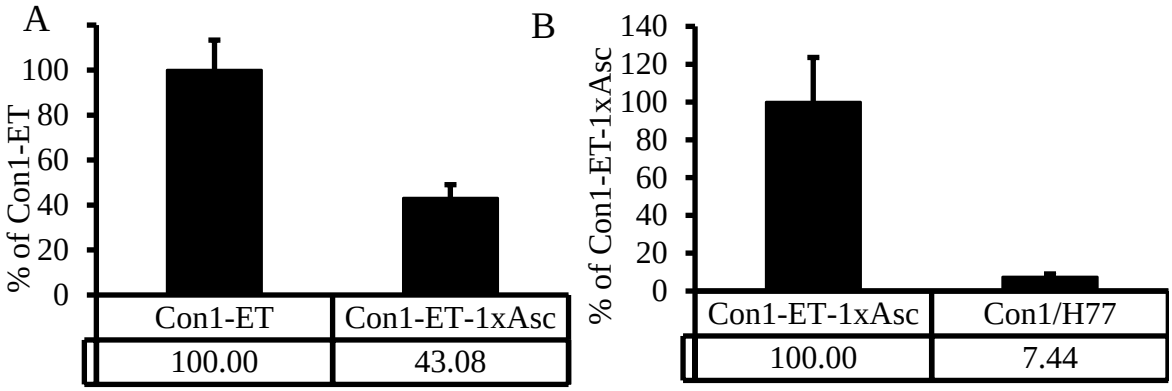

Figure 3.5. Comparative analysis of replication capacity of control replicons (A) Con-1 ET.1xAsc control vector based on genotype1b, the replication capacity normalized to Con1-ET parental vector and. (B) Con1/H77 control vector based on genotype1a, the replication capacity normalized to Con1-ET-1xAsc.

3.1.1.6. Replicative fitness of HCV NS3 resistant variants

In order to determine the relative replication capacity of resistant variants, chimeric replicons containing HCV NS3 variants were constructed and *in vitro* transcribed RNA, and then replicons were transfected into Lunet cells. After 72 hours, F-Luc was measured and compared to Con1-ET or Con1/H77S depends on HCV subtype.

We noted that the replication fitness of cells bearing the Q80K replicons dropped to less than 50% compared to the wild-type replicons. Moreover, replicon cells with single A156P, D168V or

double (A156P and D168V) mutants, showed replication capacity of less than 50% compared to the wild-type replicons.

We also found that, the presence of V36 variants in the chimeric replicons caused a decrease in the replication fitness by 65% in ratio to the wild type, furthermore the replication capacity of chimeric replicon cells containing amino acid substitution R155K was lower than the wild type by 52%, in addition, presence of the double mutants A156P and D168V lead to reduction in the replication capacity by 44%.

In agreement with previous studies, replicon cells containing have less replication capacity compared to the wild type and the most common double mutants are V36A and R155K.

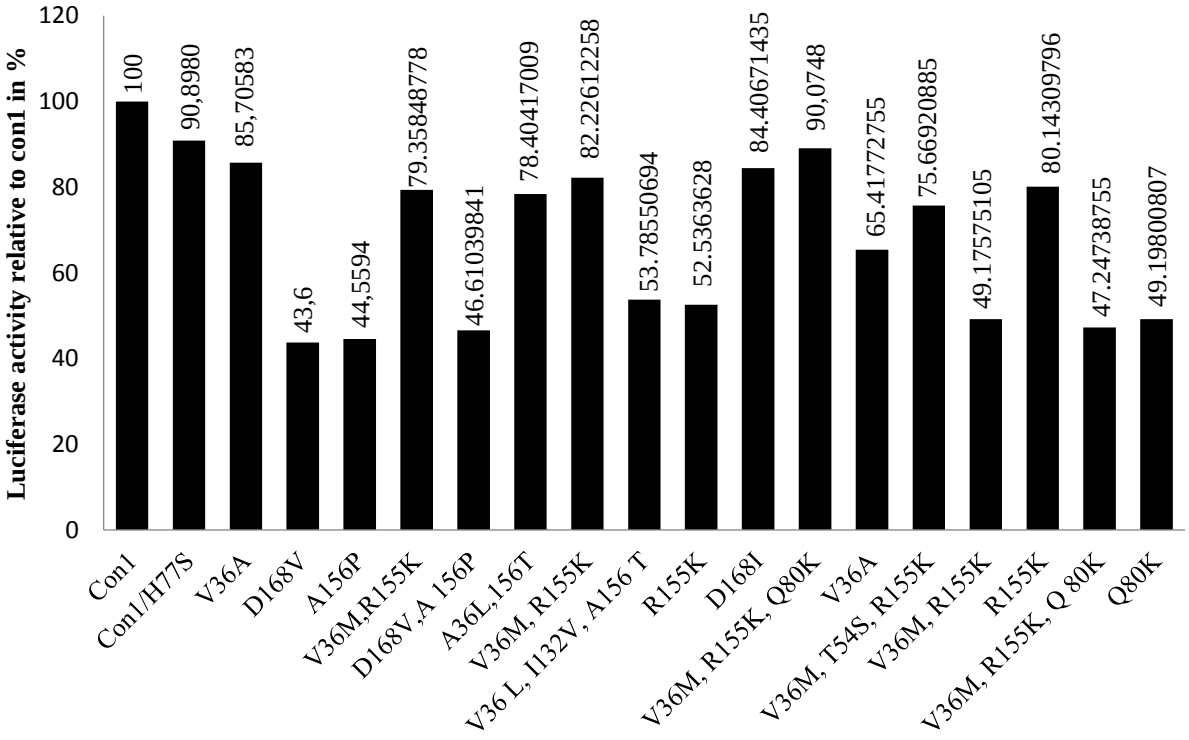

Figure 3.6. The replicative capacity of HCV NS3 variants Relative replication capacity was determined by measuring luciferase activities after 72 h of transfection into Lunet cells.

3.1.1.7. Titration curves of BOC and TLV

In order to determine the drug inhibitory concentration (IC50) of PIs (Boc and TLV). Parental and control plasmids (Con1-ET and Con1-ET-1Asc) were used. We performed a 72 hours assay, first, RNA from each plasmid was prepared, electroporated into Lunet Cells and then (5,000 cells/well) were plated in a 96 well plate. Next day, the medium was removed and replaced with medium containing serial dilutions of (Boc or TLV). Cells were incubated with the PIs for 48 hours, followed by cell lysis and Luc measurement and then IC50 for both drugs was calculated. Incubation with Boc in cells containing Con1-ET, showed IC50 at 0.2141 µM, while cells containing Con1-ET-1Asc replicons had IC50 at 0.1413 µM Boc (Figure 3.7. A) While in the case of incubation with TLV, the drug IC50 for cells containing Con1-ET was 0.2317µM TLV and 0.1787 µM for cells containing Con1-ET-1Asc replicons (Figure 3.7. B).

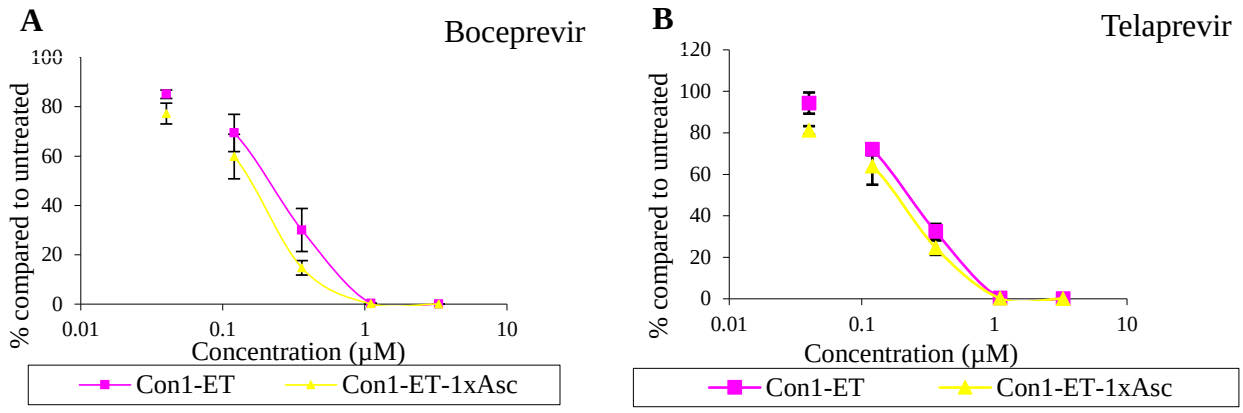

Figure 3.7. Titration curves of BOC and TLV For determination of the IC50, the parental and control plasmids were used, briefly in vitro transcribed RNA of parental Con1-ET and control vector Con1-ET-1Asc. RNA was then transiently transfected to cured Huh-7 cells (Lunet). Cells were incubated with different concentrations of (A) BOC (B) TLV, 72 h later the luciferase activity was measured and IC50 determined.

3.1.1.8. Titration example of chimeric replicon containing NS3 protease variants

To control for the assay sensitivity and variability, we used an additional control by inserting V36A resistance mutation by site-directed mutagenesis in Con1-ET. In Figure 3.8, we represent

an example of HCV patient isolate cloned in the shuttle vector, this isolate contains V36L, I132V, A156T mutations in the NS3 domain, the IC50 value of these variants had 6-fold increase over that of wild type replicon, and 13.4 fold increase over that of wild type replicon of

A

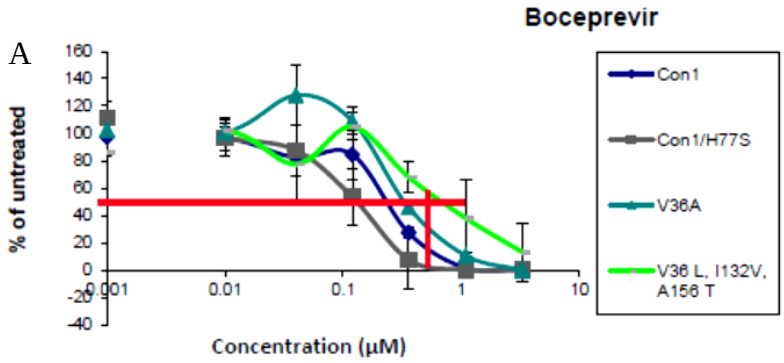

	IC50 (nM)	IC90 (nM)
Con1-ET	113.5	1021.5
Con1/H77S	118.2	1063.8
V36A	319	2871
V36L, I132V, A156T	709.2	6385.5

B

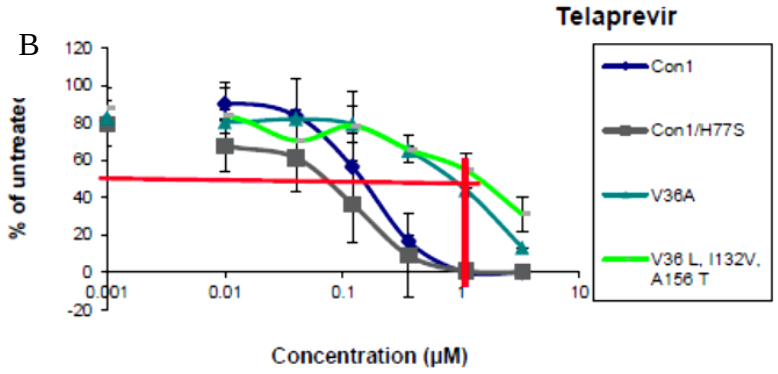

	IC50 (nM)	IC90 (nM)
Con1-ET	136.5	1228.5
Con1/H77S	80	720
V36A	320	2880
V36L, I132V, A156T	1040	9360

Figure 3.8. Determination of IC50 of chimeric replicon containing (V36L, I132V, A156T) to BOC and TLV Lunet cells were transfected with control constructs; Con-1, Con1/H77, V36A and chimeric constructs containing protease variants to be tested V36L, I132V, A156T (A) susceptibility to BOC and (B) TLV. 72 h later luciferase was measured and compared to untreated samples.

3.1.3. Susceptibility of resistant isolates to BOC and TLV and their replication fitness

In total, we performed phenotyping for thirteen patient isolates with either new or previously identified resistant mutations. A panel of the resistance mutations was cloned in Con1-ET-2xAscI shuttle vector, the resistance factor for replicon cells containing mutations was determined by fold change in relation to replicon cells containing Con1-ET plasmid.

To simplify the resistance results, we divided the resistance into low, moderate and high resistant mutations, we considered (>5 fold) as low resistance, while (>10 fold) as intermediate resistance and more than 10 as highly resistant.

Figure 3.9.A, shows the degree of mutation resistance to BOC, mutations with low values including, (V36M, R155K), (A36L, 156T), (Q80K) and (V36M, R155K), whereas (V36L, I132V, A156), (R155K), (D168I), (V36A), (V36M, T54S, R155K) are associated with moderate levels of resistance.

Figure 3.9.B, shows the degree of resistance to TLV, we classified the resistant values into low level (>5 fold), intermediate (5–10 fold) or high-level resistance (>10fold). The following substitutions have low resistance levels: (V36M, R155K), (A36L, 156T), (Q80K) and (V36M, R155K, Q80K). Those with (R155K), (V36L, I132V, A156) and (V36M, T54S, R155K) have an intermediate resistance. And those (Q80K), (R155K), (D168I) and (R155K) have high resistant values. The phenotyping showed that resistant mutations have different levels of resistance. Moreover, BOC and TLV share the same resistance profile.

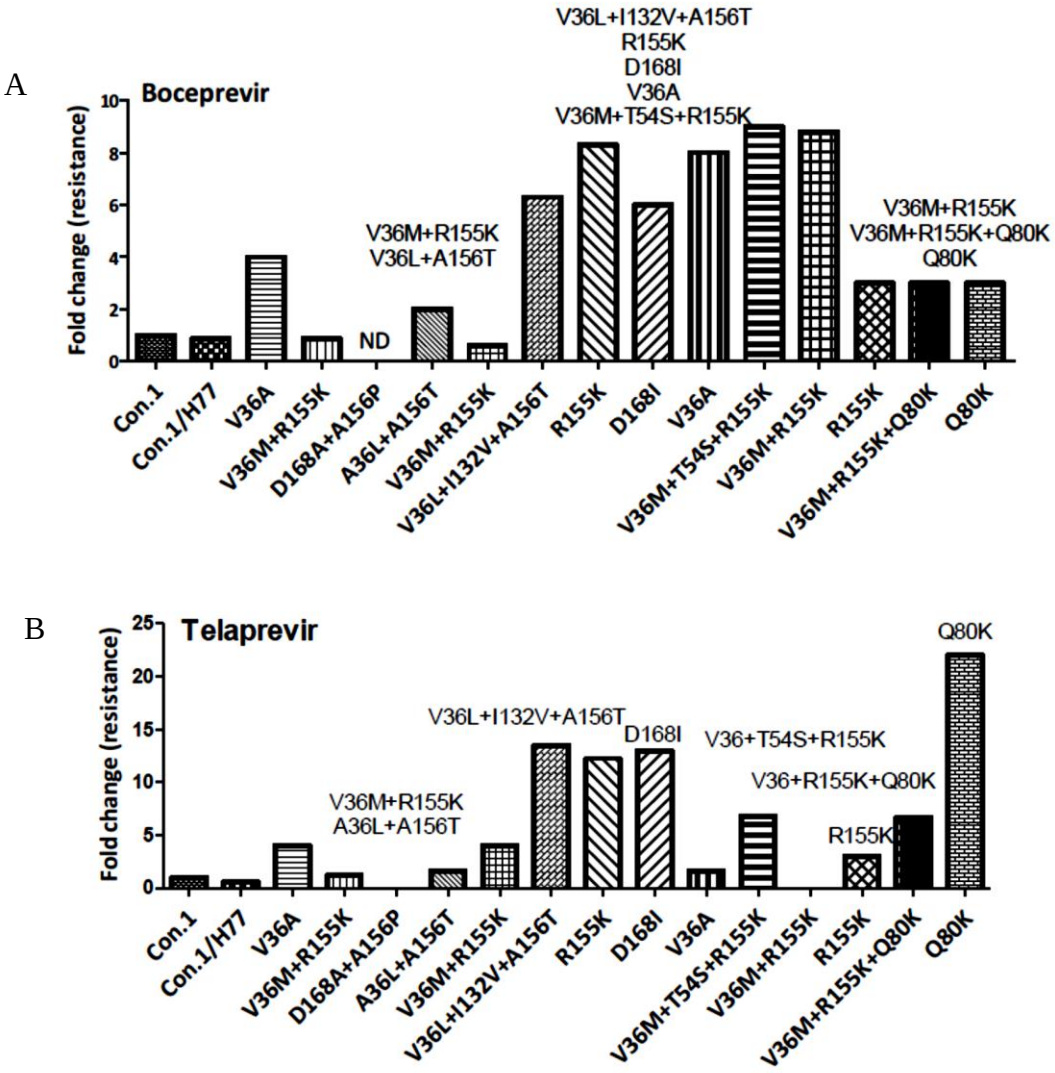

Figure 3.9. In vitro susceptibility of chimeric replicons harbouring NS3 protease variants RNA transcribed from different variants constructs was transfected into Lunet cells, cells were treated with serial dilutions of (A) BOC (B) TLV, 72h later, luciferase was measured and IC50 determines, the FC was determined compared to the control plasmid.

3.2. IL28 polymorphisms in HCV treatment response

3.2.1. IL28b rs8099917T/G, rs12979860C/T polymorphism genotyping

3.2.1.1. Direct DNA sequencing method

The association between IL28b polymorphisms and the HCV SVR has been intensively studied. Therefore, we have established a fast convenient method for rs8099917T/G, rs12979860C/T genotyping and compared it to the gold standard sequencing method. DNA was extracted and PCR amplified (Figure 4.1.A), and then subjected to Pyrosequencing. As shown in (Figure 4.1.B), the homologs rs12979860 SNP with genotype CC or TT has one peak in the chronogram, while heterologous SNP with CT genotype has two peaks. Same is applied for rs8099917 (Figure 4.1.C).

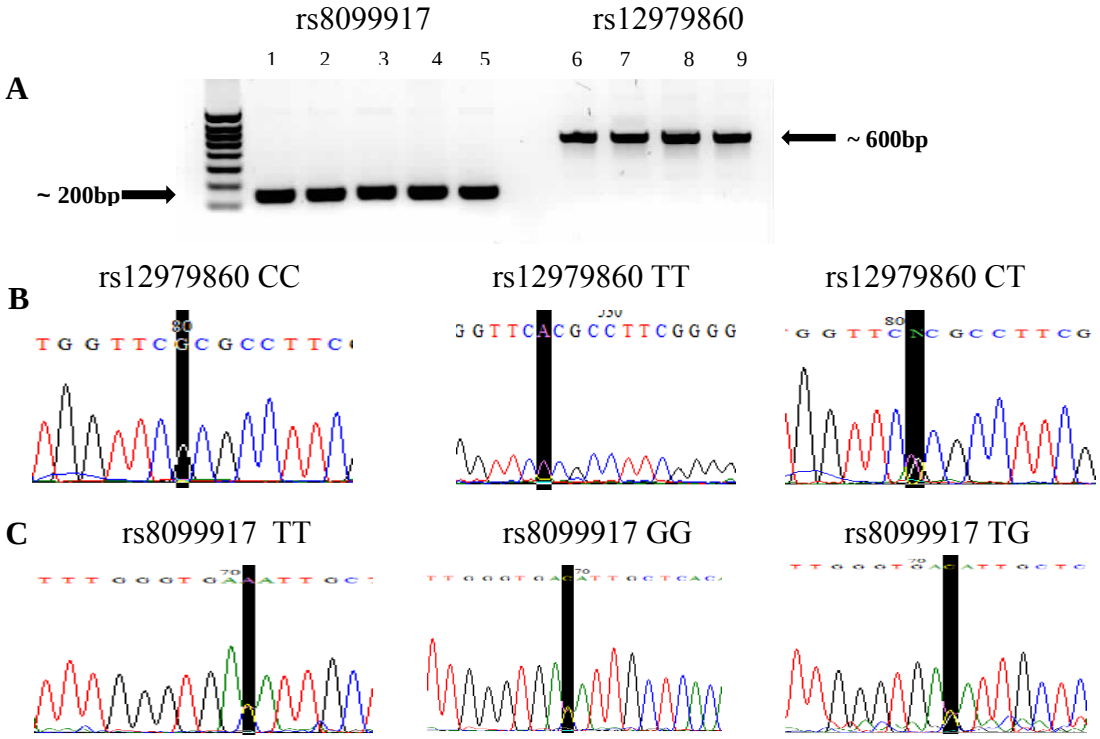

Figure 3.10. Determination of IL28B variants rs8099917T/G, rs12979860C/T by sequencing Genomic DNA was extracted from donor blood samples, (A) amplicons were PCR amplified for SNP rs12979860 (1-5), SNP rs8099917 (6-9). (B) SNP rs12979860 variants. (C) SNP rs8099917 variants.

3.2.1.2. Establishment of TaqMan assay for IL28b allele discrimination

TaqMan SNP Genotyping is a highly flexible technology for polymorphisms determination. Therefore, we have established the TaqMan assay for IL28b rs8099917T/G, rs12979860C/T polymorphisms. TaqMan is a PCR-based assay, in which specific primers and probes are used, one probe is coupled to (FAM) with Ex/Em=495-516, and the other probe is coupled to (VIC) with Ex/Em= 538-554 and both probes contain minor groove binder (MGB). As each probe is allele specific, it will break once it binds its allele releasing the fluorescence signal.

To determine an unknown SNP, purified DNA with unknown SNP allele and reference DNA samples with known SNP allele covering homozygous and heterozygous alleles are included. Figure 3.11.A illustrates that in the case of rs12979860C/C homozygous allele, high fluorescence intensity is detected in one channel (533-580), the left-handed side of the figure, and only background signal on the other channel. Whereas, in the case of rs12979860T/T homozygosity, a high fluorescence intensity is detected in the one channel (465-510), and background signal in the second channel (Figure 3.11.b). In the case of rs12979860C/T heterozygous allele, equal fluorescence intensity is detected in both channels (Figure. 3.11.C).

A scatter plot Figure 3.11.D, the green color indicates the rs12979860C/C homolog allele, blue color indicates rs12979860T/T, and the red is rs12979860C/T heterologous allele. In scattering plot Figure 3.11.E, the green triangles represent the homologous rs8099917T/T, the blue triangle represents the homologous rs8099917G/G, and the red ones represent the heterologous rs8099917T/G.

When we compared the genotyping results obtained by TaqMan assay with the results obtained by direct sequencing, we confirmed the reliability of TaqMan to distinguish between two different SNPs, which make it the assay of choice to genotype HCV patients SNPs in our experiments.

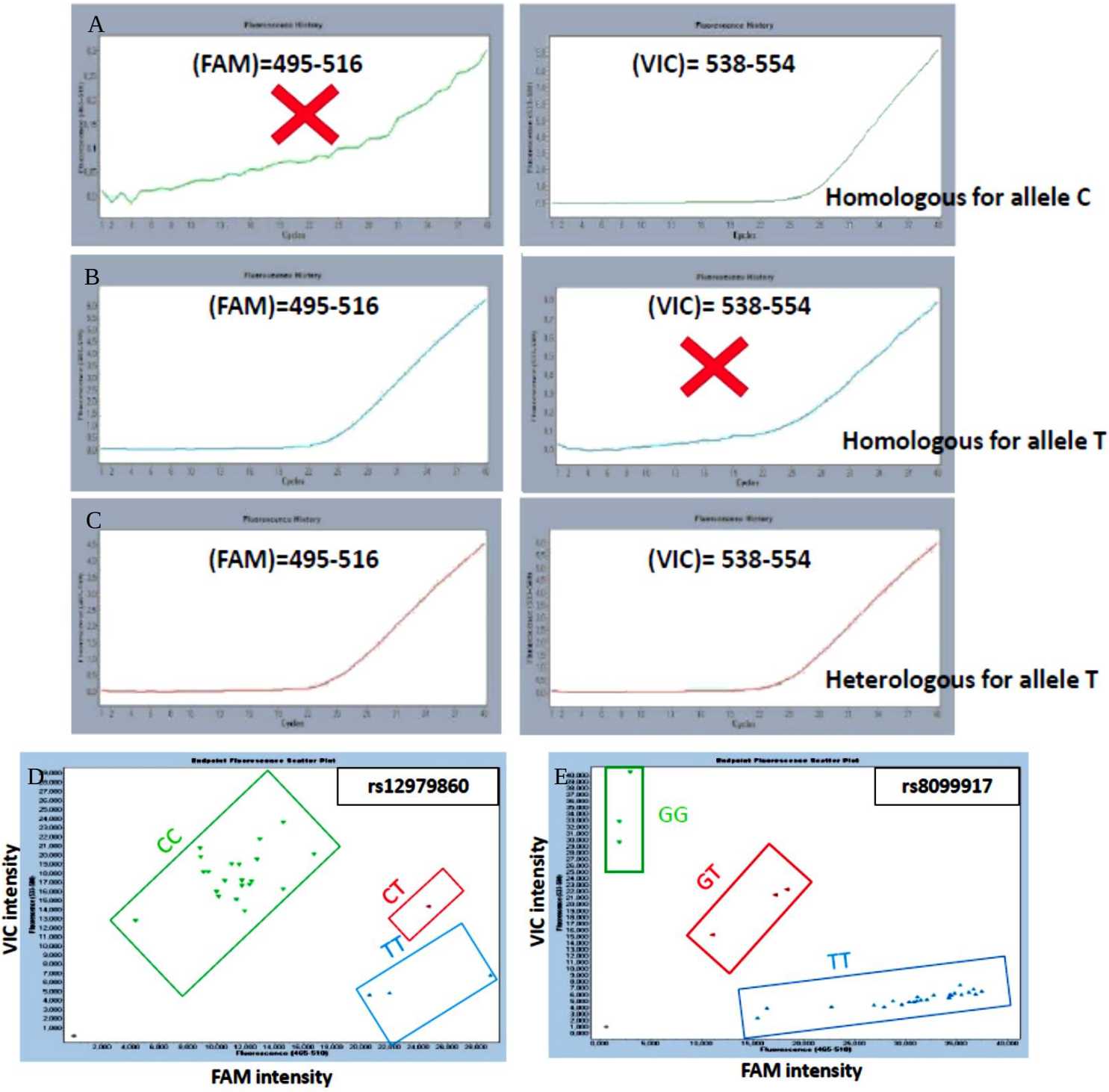

carried TT allele). This is consistent with the previous studies that rs12979860 has more

Figure 3.11. Establishment of TaqMan assay for IL28b allele discrimination (A, B) represents the fluorescence intensity for homologous allele. (C) The florescence intensity of the heterologous allele. (D, E) Scatter blot for the SNPs.

predictive values than rs8099917, and that all relapsed patients had non-CC genotype.

Table 1:IL28b SNPs genotyping

Patient ID	SNP rs8099917	SNP rs12979860
1	GG	TT
2	GG	CT
3	GG	CT
4	GG	TT
6	GG	CT
7	TT	CT
5	TT	CT

3.3. Discussion

Chronic infection with hepatitis C is still a major worldwide health problem. For almost two decades, interferon-ribavirin dual therapy was the only drug available for HCV treatment (Heim 2012). Since the application of DAAs in combination with interferon-Ribavirin, a progress has been made in the cure rates of genotype 1 infected patients (Wakita 2007, Jang and Chung 2011). Drug resistance appeared as a major challenge hinders successful treatment with protease inhibitors, therefore the establishment of reliable assay arose as a need to evaluate resistant variants. The first PIs approved were BOC and TLV, both are linear ketoamide and administrated in combination with IFN-RBV. The first generation of PIs including BOC and TLV are characterized by a low genetic barrier, meaning that one single amino acid change might confer drug resistance (Halfon and Locarnini 2011, Schiering, D'Arcy et al. 2011, Wartelle-Bladou, Le Folgoc et al. 2012) .

In the beginning, we wanted to genotype NS3 variants at baseline, during and post-treatment. In relapsed patients, we used population and clonal sequencing to identify NS3 variants in pre-treatment samples. In most cases, we did not have a pre-treatment sample, therefore we could not compare the sequence changes in relation to the baseline sequence. Nevertheless, the sequencing method and geno2phenoHCV analysis tool enabled us to identify, the NS3 resistant variants, the resistant value and the cross-resistant to other inhibitors. In our cohort, we have identified novel substitutions at 156 (D156P), 168 (D168I/V) and 174 (N174G/R/S/L). Moreover, we identified known mutations that confer resistance to PIs, those include substitutions of residue 36 (V36A/M/L), 54 (T54S), 80 (Q80K), 132 (I132V) 155 (R155K) and 156 (A156T). The known mutations that were observed most frequently in NS3 in patient isolates were V36M and R155K. While the most frequent novel substitutions were at amino acid N174 with the replacement to G, R, S, L.

In spite of that, the method was useful in the determination of resistant variants in both naive and during treatment, lacking the pre-treatment samples hindered our ability to know whether those mutations pre-exist prior PI therapy, or they were mutated under PI treatment.

Phenotyping of HCV resistant samples

HCV replicon system has been proven a useful tool to study the efficacy of anti -HCV compounds. Therefore, a modified replicon system named (shuttle vector) was used for the phenotyping assay. The shuttle vector developed by insertion of three adaptive mutations (E1202G + T1280I+K1846T). In addition, two restriction sites (Cla1 and Asc1) were created for NS3 shuttling, and for the control, defective parental vector Asc1 was inserted to the replicon (Qi, Bae et al. 2009, Imhof and Simmonds 2010). The replicative capacity of the control defective replicon decreased to 43% related to the parental replicon Con-1 ET. For the shuttling procedure, we amplified NS3 protease domain using a primer that contains the E1202G adaptive mutation. Then the PCR product of NS3P was ligated into the shuttle vector. Given that all resistant mutations reside within the NS3P domain, besides the technical challenges of cloning of the whole NS3PH domain, we decided to amplify the NS3P domain instead of the whole length NS3/4A domain.

In this study, we used Huh7-Lunet cells to determine the replication fitness and the sensitivity of mutants to PIs. Huh7-Lunet cell line is a highly permissive hepatoma cell line to HCV, this cell line was developed by infecting Huh7 cells and treat the cells with IFN (Robinson, Yang et al. 2010). Replication fitness of resistant variants defined as the ability of the mutations to replicate in relation to wild-type replication fitness (Halfon and Locarnini 2011, Lassmann, Arumugaswami et al. 2013). Given that the fitness is an important determinant of the amount of new viral transcripts accumulates in the hepatocytes, we determined the replication fitness of resistant variants. Using a transient transfection approach, we clearly saw that constructs containing resistant variants lost the replication fitness compared to the wild type. The results generally confirm previous results showed that in the presence of resistant mutations the virus will have less replication fitness. Of note, the replication fitness results that based on transient replicon system might be underestimated, that is we miss the role of those resistant variants on the late steps of the virus replication cycle. To estimate the sensitivity of resistant mutants, we determined the IC50 of BOC and TLV for both the wild type Con-1 ET and Con-1 ET 1xAsc and the resistant variants. Based on sequencing results we identified seven resistant variants in the NS3 domain, those mutations have different levels of resistance to both BOC and TLV. However, (Q80K), (R155K), (D168I) and (R155K) variants have high resistant values,

suggesting that those substitutions have big effect on substrate or enzyme binding, consistent with the notion these mutations have cross-resistance to different PIs(Shiryaev, Cheltsov et al. 2012, Lassmann, Arumugaswami et al. 2013, Solund, Krarup et al. 2014) . A previous study showed that R155K mutation counteracts the binding to BOC and TLV. The residues A156 located in the P-side of the active site, and when a mutation occurs in this position, this cause weakness of the binding between NS3 and the inhibitor (Shiryaev, Cheltsov et al. 2012, Xue, Wang et al. 2012).

Taken together, our results confirmed the sensitivity of the phenotyping assay in the determination of the resistant values of resistant variants. Moreover, it agrees with previous clinical studies for both BOC and TLV. Overall, we could attribute the failure of triple therapy to the presence of the resistant mutations which were either pre-exist or selected under PI pressure.

GWAS analysis is a successful approach to identify important polymorphism genotypes and their relation to disease pathogenesis (Clark, 2011; Lange, 2011). In 2009, several GWAS studies showed the association of IL28b polymorphisms HCV clearance or persistence. Notably, the strongest associations were for SNPs located genetic polymorphism near the IL28B locus on a chromosome, namely rs12979860, rs8099917. As mentioned earlier in the introduction part, patients carry the unfavorable allele rs12979860 (T/T), are fewer responders to IFN based therapy. The role of the different polymorphisms in disease progression is still conflicting, in one study (Asselah, 2012; Barreiro, 2011) they showed that patients with unfavourable allele have higher risk of developing liver fibrosis and cirrhosis, while (Tillmann, 2011; Thomas, 2009) showed that patients with favourable allele have higher progression to fibrosis. Given the importance of several IL28b polymorphisms, we decided to include IL28b polymorphisms in our study as a host genetic predictor in HCV clinical outcome. Due to the high homology between the IL2b and IL28A, first, we have established a TaqMan-based assay for SNPs genotyping and confirmed the genotypes by sequencing. In total, we genotyped 33 human DNA samples for both rs12979860, rs8099917 polymorphisms, then we confirmed the genotype with sequencing. Our results showed 100% matching with the sequencing results. Thus, we used TaqMan-based assay to determine the association between IL28b SNPs and the poor response in patients treated with triple therapy. When we genotyped 7 non-responder patients for rs8099917 and rs12979860**,** we found that five patients carried GG allele, while two patients had TT allele for rs8099917. In

addition, the genotype distribution for SNP rs12979860 alleles in patients were all non-CC allele (3 out of the 5 patients carrying rs8099917 GG allele carried rs12979860 CT while 2 patients carried TT allele). This is consistent with the previous studies that rs12979860 has more predictive values than rs8099917, and that all relapsed patients had non-CC genotype.

In order to determine the association between IL28b SNPs and the poor response in patients treated with triple therapy. In total 7 non-responder patients were genotyped for rs8099917 and rs12979860**.** Five patients carried GG allele, while 2 patients had TT allele for rs8099917. In addition, the genotype distribution for SNP rs12979860 alleles in patients were all non-CC allele (3 out of the 5 patients carrying rs8099917 GG allele carried rs12979860 CT while 2 patients carried TT allele). Furthermore, we confirmed that rs12979860 has more predictive values than rs8099917 and that all relapsed patients had non-CC genotype. Taken together, we have established a fast and sensitive assay for IL28b polymorphisms genotyping, and that our results confirm the previous observations of the high predictive value of the rs12979860 with the clinical outcome.

3.4. Summary

Approximately 75% HCV patients develop chronic infection and this might lead to severe illness, including cirrhosis and hepatocellular carcinoma. In 2011 the first direct-acting antiviral agents (DAAs) protease inhibitors BOC (Victrelis) and TLV (Incivek) were approved. The novel standard of care therapy, which consists of BOC or TLV in combination with PEG–IFNα - ribavirin raised the cure rates of HCV genotype 1 infected patients up to 70%. However, drug-resistance emergence arises as a major challenge to effective antiviral therapy. Taking advantage of the availability of in vitro systems that support HCV replication, we used this system to establish a phenotyping resistance testing for PIs. Thus, we could establish genotyping and phenotyping assays to characterize the resistant variants. We determined substitutions of residue 36 (V36A/M/L), 54 (T54S), 80 (Q80K), 132 (I132V) 155 (R155K), 156 (A156T) in both patient samples exposed to Boceprevir/TLV, and naÏve patient samples. In addition, we identified novel substitutions with potential resistance, they located at 156 (D156P), 168 (D168I/V) and 174 (N174G/R/S/L).

We used Huh7-Lunet cells to determine the replication fitness and the sensitivity of mutants to PIs. Thus, the phenotyping assay revealed that, mutations at (V36M, R155K), (A36L, 156T),

(Q80K) and (V36M, R155K), are associated with low resistant value, whereas (V36L, I132V, A156), (R155K), (D168I), (V36A), (V36M, T54S, R155K) are associated with moderate levels of resistance. For TLV, the following substitutions have low resistance levels, (V36M, R155K), (A36L, 156T), (Q80K) and (V36M, R155K, Q80K). Those with (R155K), (V36L, I132V, A156) and (V36M, T54S, R155K) have an intermediate resistance. And those (Q80K), (R155K), (D168I) and (R155K) have high resistant values. Moreover, BOC and TLV share similar resistance profile. We also noted that the replication fitness of resistant variants dropped compared to the wild type. Taken together, we confirmed the sensitivity of the phenotyping assay in the determination of different resistance values. Moreover, the resistance associated with different variants are correlated with the therapy failure in those patients.

4. Part II: Crystallization of HCV NS5b polymerase and structure determination

4.1.1. Cloning and expression of HCV NS5b

To amplify the HCV NS5b region, viral RNA was isolated from a genotype 4a patient sample, and RT-PCR was carried out using One-step RT-PCR amplification kit. PCR product was purified with PCR purification kit and ligated to pET30b (+) expression vector. The ligation product was then transformed into *E. coli* BL21 (DE3) competent cells and subsequently cultured in LB media. The engineered pET30b-NS5b construct was confirmed by sequencing. Confirmed construct was then used for protein expression, a pre-culture containing transformed E.coli with pET30b-NS5b construct was allowed to grow at 37°C overnight and then used to re-inoculate LB media, and the culture was monitored till the Optical density (OD) reached to 0.6-0.8. The protein induction was done by addition of 1mM isopropyl l-L-D-thiogalactoside (IPTG), bacterial culture was allowed to grow at 32°C for 6h. The culture was harvested and the subjected to purification.

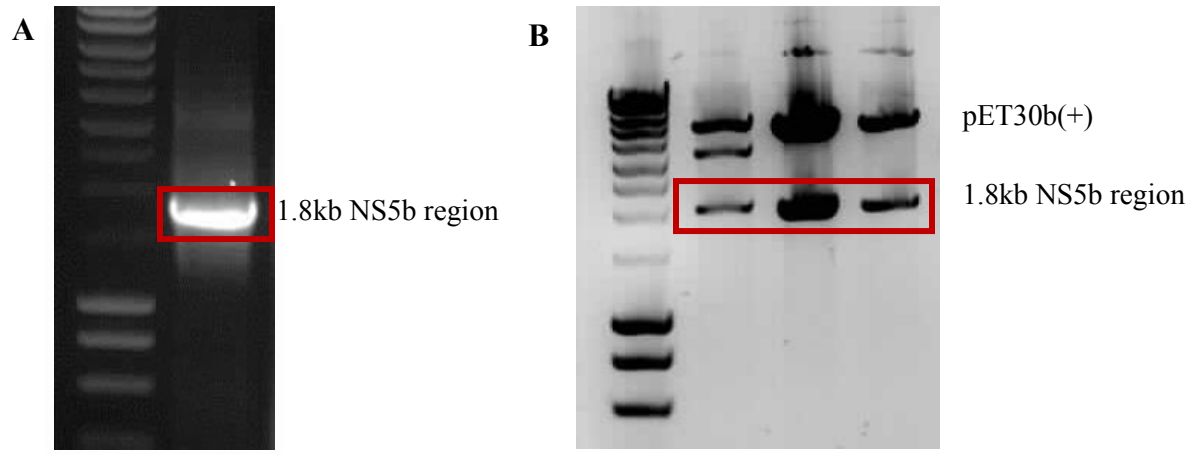

Figure 4.1. NS5b cloning and expression (A) NS5b was PCR amplified and cloned into pET30b (+) vector. (B) different pET30b-NS5b colonies were picked and amplified, followed by restriction analysis to check for the insertion of the NS5b domain.

4.1.2. HCV His-Tagged NS5b protein purification

Protein expression and solubility

In an initial trial for protein expression and HCV NS5b proteins, HCV NS5b protein expression was done in small culture, and then along with solubility were checked as the following, the

bacterial cell pellet was sonicated on ice and then cell suspension was cleared by centrifugation. Clear lysate was applied to Ni-NTA column, allowed to trap his tagged HCV NS5b protein, Figure 4.2.B, shows that HCV NS5b protein expressed in a soluble form, lanes (1-2) represent clear lysates before application on Ni-NTA column, lane 3, is the flow through, lanes (4-10) represent eluted protein with different imidazole concentrations.

4.1.3. Large scale production and Ni-NTA column purification

In order to produce enough proteins, we scaled up the bacterial culture, and then performed the expression as above, and then the crude clear lysate was applied on the Ni-Resin using AKTA. In order to elute the his-tagged protein, protein was eluted by optimized gradient elution buffer (Figure 4.2.A), the blue line in the chromatogram represents his-tagged HCV NS5b protein, purity of the tagged protein was checked by SDS-PAGE, one fraction from peak one was loaded, and then every second fraction from peak two were subjected to electrophoresis. His-tagged NS5b protein showed no contamination with other proteins.

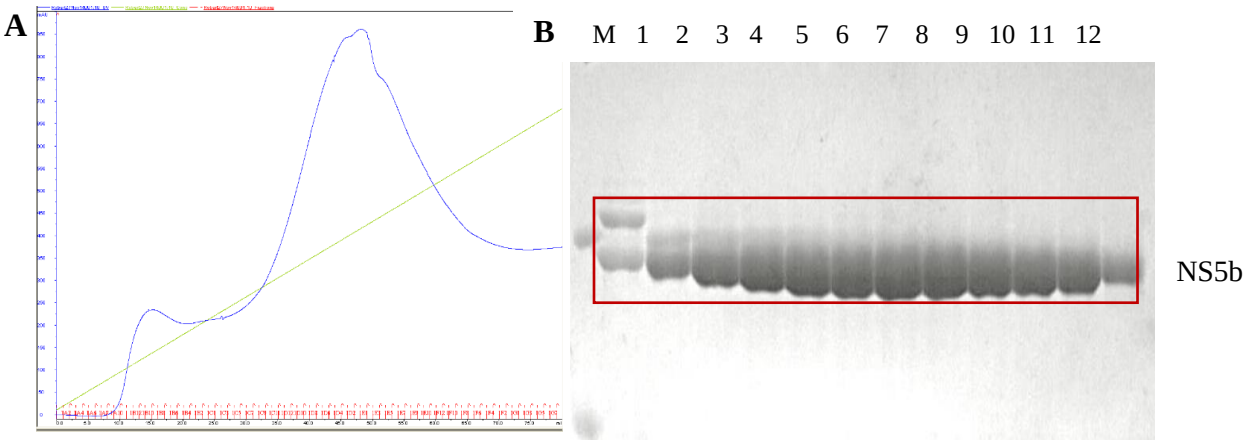

Figure 4.2. The Chromatogram and SDS-PAGE of NS5b protein (A) Crude clear lysate was run through the Ni-Resin using AKTA in order to eluate the His-tagged protein, the blue line represents the His-tagged proteins. And the light green line represents the percentage of the elution buffer. (B) To check purified His-Tagged NS5b protein, lane (2) contains protein from the first peak, lanes from (3-12) represent every second fraction of the second peak were subjected to electrophoresis.

4.1.4. Size exclusion chromatography of NS5b

In order to reach 95% purification to meet the pre-crystallization criteria, protein fractions from AKTA purification were pooled and subjected to second purification step, the protein was purified by cation exchange chromatography, the blue line represents the purified protein Figure 4.3.A. To verify the protein purity, eluted protein fractions were subjected to electrophoresis, NS5b protein showed high purity, Figure 4.3.B, Fractions in lanes (1-7) showed a second shadowed band above the specific protein, while fractions in lanes (8-14), showed pure protein. Then fractions with high purity were pooled and concentrated by centrifugation up to 4mg/ml before the precipitates start to appear and then dialyzed against lysis buffer to get rid of the undesired salts. Proteins were then shocked by liquid nitrogen and were frozen for further crystallization experiments.

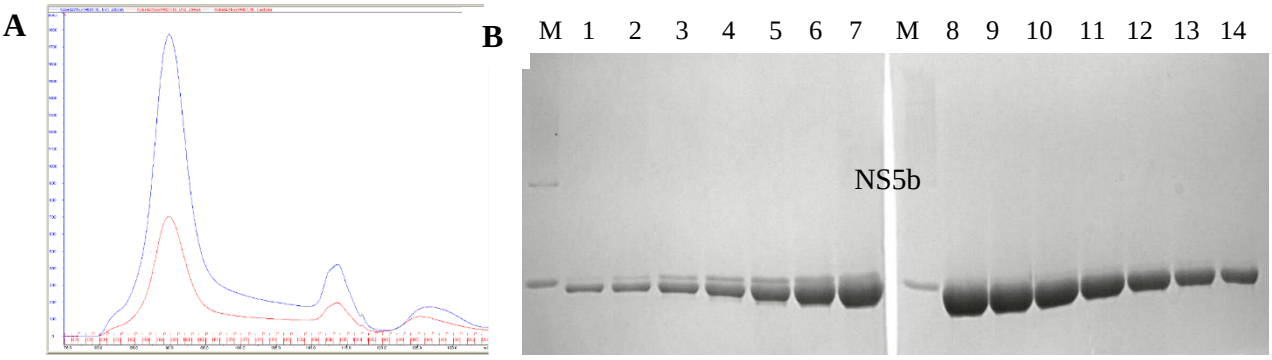

Figure 4.3. Size exclusion chromatography and SDS-PAGE analysis of HCV NS5b (A) LC-MS chromatogram of NS5b protein on a Superdex200 gel filtration column, the blue line represents the eluted NS5b protein. (B) Elution profile of NS5b protein NS5b protein, each lane contains a fraction from the first peak, the molecular mass of the NS5b is 65kDa.

4.1.5. Comparison of the NS5b protein crystallization on earth and under microgravity conditions

Frozen protein sample was thawed and CrystalCards were filled with the protein, one card for the ground control and one for the microgravity.

4.1.6. NS5b protein crystallization in the control earth card

After 21 days, the Crystal Card was screened for crystals, low magnification microscopic image shows Figure 4.4.A channels containing droplets mixture of buffer, precipitant and protein, and then higher magnification was used to check the crystal formation Figure 4.4.B, some aggregates were observed with no crystals formed in the cards. The returned Crystal card, which exposed to microgravity conditions for 21 days in the ISS, was checked for crystal formation. Figure 4.4.C shows red circles marked crystal-like structure in the microgravity card, (Figure 4.4.D and E) shows higher magnification of crystal-like structure. The crystal-like structure could be of protein, buffer or impurities.

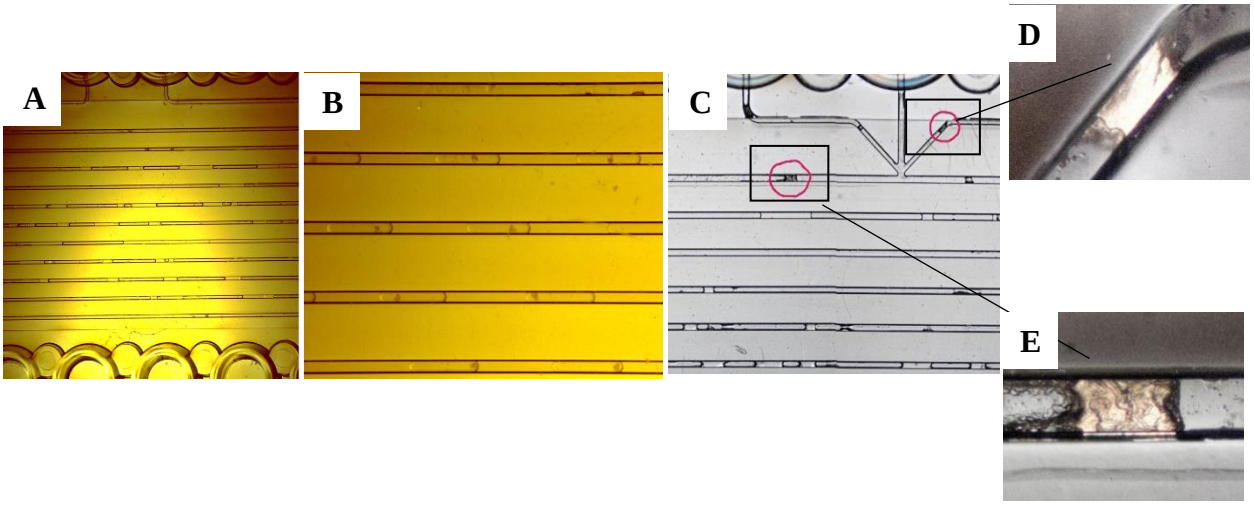

Figure 4.4. Crystallization of NS5b protein on the earth and under microgravity conditions (A) picture taken with low magnification for the ground CrystalCard, shows the capillaries containing solution droplets. (B) higher magnification of the ground card shows some aggregates in the card with no crystals were formed in the card. (C) shows a low magnification for the microgravity card, some crystal like shape were observed in the card. (D and E) show the crystal like using higher magnification, crystals could be aggregates of buffer, impurities or proteins.

4.1.7. Further crystallization tests and optimization

Since the crystals formed on the microgravity CrystalCard did not lead to crystals could be used for X-ray diffraction, we further tested and optimized the crystallization conditions. For this purpose, the protein was freshly expressed and purified. The initial crystallization screening of

NS5b was set up at 292 K using 4 mg/ml of protein with a nano-drop dispenser in sitting-drop 96-well plates and commercial screens. Optimization was performed using the sitting-drop vapor diffusion method at 292 K in 24-well plates. The crystals of NS5b appeared after 2-3 days and required another few days to grow to the final size (Figure 4.5). The biggest crystals were obtained from PEG 550 MME as a precipitating agent. Although the quality of the crystals was not good we managed to perform X-ray experiment and collect satisfactory quality data set. Diffraction data was collected on the ID30 beamline (ESRF, Grenoble, France). Data collection was performed at 100 K. The dataset was indexed and integrated using XDS and scaled using SCALA. Intensities were converted to structure-factor amplitudes using the program TRUNCATE. Table 1 summarizes data collection and processing statistics.

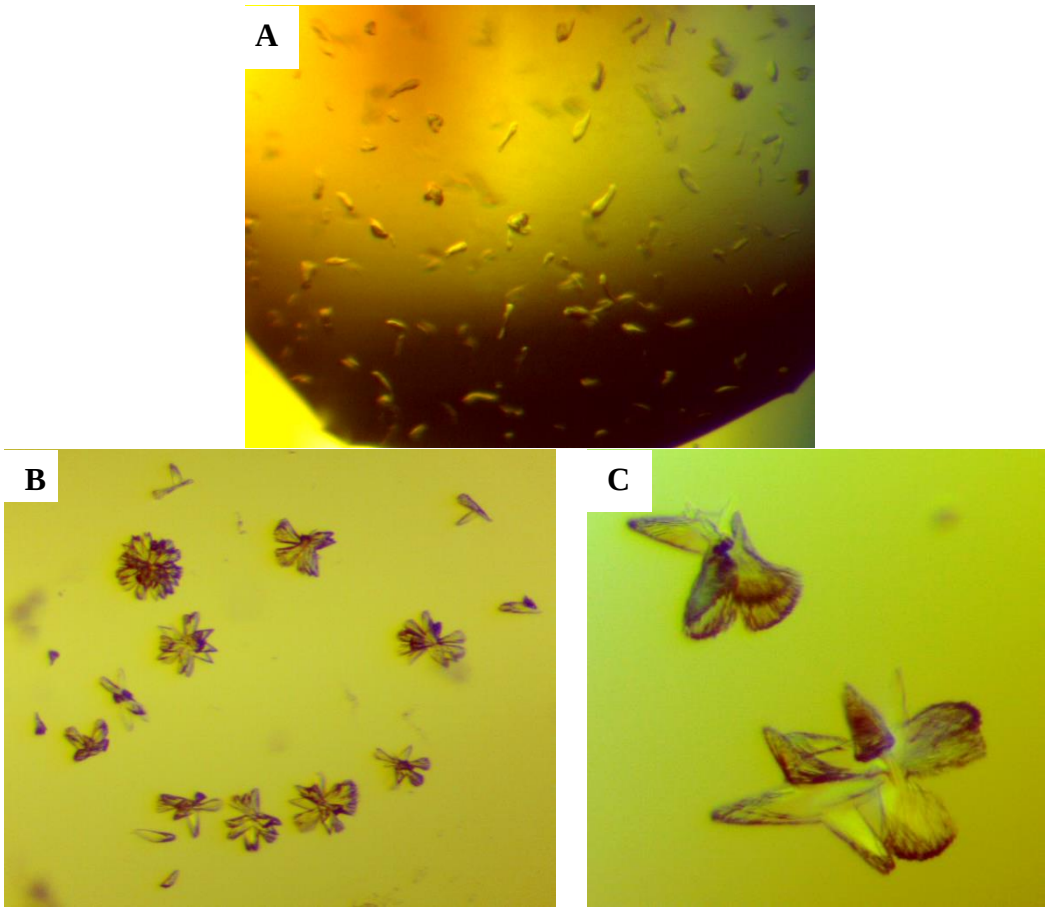

Figure 4.5. Optimization of NS5b protein crystallization Rod crystals appeared 2-3 days and required another few days before they grow to the final size. The largest crystals were obtained by addition of PEG 550 MME as a precipitating agent. (A) Overview of the well contains the largest formed crystals. (B and C) different magnification of the NS5b crystals.

4.1.8. Structure determination and refinement

The structure of NS5b was solved by molecular replacement using the crystal structure of the RNA-dependent RNA polymerase from hepatitis C virus (PDB code: 1C2P, Lesburg et al., 1999) as a search model. Both proteins share 75% sequence identity. Model building was performed in COOT. The refinement was done in REFMAC5 using the maximum likelihood target function including TLS parameters. The current model is characterized by R and Rfree factors of 22.4% and 32.2% (Table 4.1). The stereochemical analysis of the model was done in PROCHECK and MolProbity.

4.1.9. Structure comparison to the closest genotype

Structural comparison of the Egyptian genotype HCV NS5V protein with the closest homolog HCV RNA polymerase genotype 1a shows r.m.s. deviation of 1 Å with the sequence identity between the compared proteins of 74 %. Figure 4.6. shows the overlap of both structures.

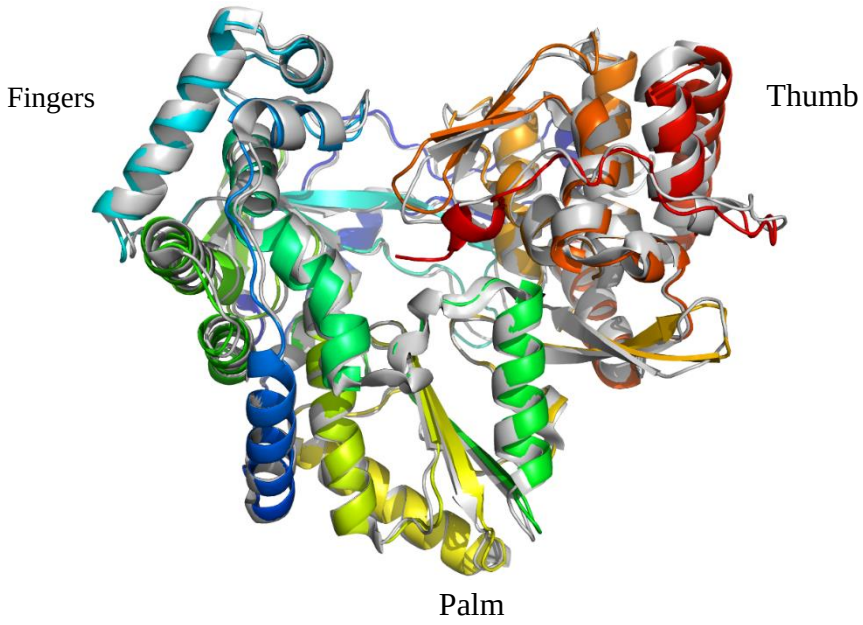

Figure 4.6. Superposition of Egyptian genotype 4 HCV NS5b protein (shown as rainbow ribbon) with the closest homologue, HCV RNA polymerase genotype 1a (Biswal et all. 2005; PDB code 1YVZ) shown as gray ribbon.

Table 4.1. Data collection and refinement statistics

Data collection	
Space group	$P2_12_12_1$
Cell dimensions	
a, *b*, *c* (Å)	63.3, 87.1, 96.7
α, β, γ (°)	90, 90, 90
Resolution (Å)	50–3.17 (3.25–3.17)
R_{merge}	13.1 (77.1)
$I / \sigma I$	9.7 (2.1)
Completeness (%)	99.7 (99.9)
Refinement	
Resolution (Å)	3.17
No. reflections	9,025
R_{work} / R_{free}	22.4 / 32.2

4.2. Discussion

Biological macromolecular crystallography is a fundamental method used to study biological molecules such as proteins, viruses, and nucleic acids. Scanning for the right crystallization conditions is essential for obtaining crystals of good quality for x-ray diffraction (Ke and Doudna 2004, McPherson 2004). Several steps involved in the determination of 3D structure by X-ray diffraction, target macromolecule cloning, expression and purification, screening of crystallization conditions; diffraction data collection; structure determination; analysis of the structural model. In the beginning of our study, the aim was to crystalize the HCV-NS5b protein by using the ISS protein crystallization facility and compare the crystals formed in microgravity to the earth formed ones.

Despite the presence of several crystal structures covering HCV-NS5b of different genotypes, none of them is for genotype4. HCV NS5b is an important target for the development of new therapies for the improved treatment of HCV infection. Recently, many pan-genotypic drugs target NS5b approved with efficiency up to 95% in naïve patients (Degasperi and Aghemo 2014, Asselah and Marcellin 2015, Bunchorntavakul and Reddy 2015, Loustaud-Ratti, Debette-Gratien et al. 2016, Nakamura, Kanda et al. 2016).

In order to proceed with the first step of protein crystallization, we cloned either full length or truncated NS5b macromolecule into the bacterial expression vector (pET30b+). The pet30b+ vector contains a T7 promoter for overexpression in E. coli strain BL21(DE3). Although we were able to successfully express truncated NS5b in a soluble form using IPTG induction, we were not able to express a full-length NS5b in bacterial cells. That is consistent with previous studies which showed the difficulty in the expression of the NS5b full length in bacteria, one possible reason is the presence of membrane-anchor domain (Huang, Sineva et al. 2004, Wang, Johnson et al. 2004). On the basis of the expression results, the over-expressed NS5B-truncstd protein was used for further purification and crystallization. Initial experiments showed that NS5b-T protein could be purified and concentrated up to 16mg/ml.

Given that gravity negatively influences the growth protein crystals, initial attempts to grow protein crystals in microgravity were conducted. Results obtained from early space shuttle missions showed improvement in the quality of the microgravity-grown crystals compared to the earth ones. This encouraged scientists to develop and optimize conditions and devices for

crystallization in space (Giege 2013, Takahashi, Ohta et al. 2013, McPherson and DeLucas 2015).

For microgravity conditions, we choose the Microcapillary Protein Crystallization System (MPCS) (also called Plug Make). The characteristic of this system is that it allows getting crystals from as tiny as µL of protein per experiment. MPCS permits mixing of different concentrations of protein, buffer, precipitate and carrier fluid, this would increase the chance of protein crystallization.

The concentrated frozen protein was thawed and loaded into the crystal cards, one was used for 1g control and the other prepared for travel to the microgravity conditions in the ISS (Gerdts, Elliott et al. 2008, Gerdts, Stahl et al. 2010) .

Unfortunately, no pictures were obtained for the crystal card on the ISS, the card was examined after the return journey to the earth.

After 25 days of the launch, the crystal card returned back to the earth and both crystal cards, the ISS, and the control 1g were checked for crystal growth.

Comparison of both cards revealed the formation of crystals in the ISS card, while no crystals were formed on the earth card.

Because of technical difficulties we could not perform X-ray diffraction on the crystals, thus we could not confirm whether formed crystals were protein, buffer aggregates or dirt. At present, there is still no compelling hypotheses that can anticipate protein crystallization conditions. Consequently, further screening and optimization for crystallization parameters are required. For screening purposes, we used crystallization plates with 96 microwells, in which each well contains one precipitant, followed by an automated stage that allows for dispensing the same amount of protein in each well. This strategy is advantageous in obtaining the best conditions for growing crystals. Since temperature is one parameter which can influence crystals formation, it was necessary to control for crystallization temperature. As the most common temperatures for crystallization are 4°C and 22°C (Bartling et al. 2005), we placed the plates either at room temperature 22°C.

In the initial crystallization screening experiment, crystals were obtained in the presence of PEG 550 MME. The determination of the right conditions followed by crystallization in a 24 well crystallization plate. Protein crystals formed either as a single needle-like structure or as microcrystal aggregates which likely originate from one nucleation site. The microscope

observation of crystals showed that the quality of crystals external appearance is promising for x-ray diffraction. To harvest crystals for crystallography, we carefully opened the plate, and gently harvest them using Nylon loops, crystals were immediately cryo frozen into liquid nitrogen. Crystals stored in liquid nitrogen until X-ray diffraction.

For diffraction data collection, crystals were mounted and illuminated by the X-ray beam generated by synchrotron sources. The dataset of diffraction images taken for crystals showed that most crystals diffracted to an average of 3.1 Å resolution. The calculated factors including space group, cell dimension reflect the quality of resolution data. This poor quality of the diffraction data could be attributed to the lack of protein crystals homogeneity, which believed to be the case for protein crystals. Generally, protein crystals diffract at 1.5 to 4 Å resolution, and thus the diffraction dataset quality reduced with misalignment of the crystal lattice.

For the establishment of the NS5b structural model, we processed the X-ray diffraction data by Molecular Replacement approach (Abergel 2013). This method can be used to solve the unknown crystal structure if there is any known similar solved protein structure. In the case of genotype4a HCV-NS5b protein modeling, several models covering other genotypes are available. We built the model based on a homologous genotype 1a HCV-NS5b model. Identical to other HCV-NS5b polymerases, the HCV-NS5b of genotype4a comprises of six conserved subdomains, the analogy structure indicates that fingers, palm, and thumb are in close interaction, which contracts the flexibility between the subdomains (Biswal, Cherney et al. 2005, Powdrill, Bernatchez et al. 2010, Karam, Powdrill et al. 2014). However, previous models of HCV-NS5b revealed the presence of several conformations when in complex with the template. Unfortunately, as we did not perform NS5b template co-crystallization, we still miss the other confirmations.

4.3. Summary

The structural determination of viruses on the atomic level illustrates the virus nature arrangement, this consequently led to the interpretation of the virus life cycle, pathogenesis and potential targets for drug development. Numerous approaches are utilized for structure determination including, X-ray crystallography, electron microscopy, and NMR. Several 3D structures of HCV structural and structural proteins are available. The 3D structure of HCV NS5b reveals that it has six conserved motifs, furthermore, it folds in fingers, palm and thumb subdomains. Microgravity provides an opportunity for different areas of research such as

biotechnology. Thus, we used microgravity to study protein crystal growth of HCV-NS5b protein of genotype 4a.

At first, for microgravity conditions, we selected the Microcapillary Protein Crystallization System (MPCS), which allows obtaining crystals from as little amount of protein per experiment. Comparison of crystallization in microgravity and gravity revealed the formation of crystals in the ISS card, while no crystals were formed on the earth card. Because of technical difficulties we could not perform X-ray diffraction on the crystals. At present, no compelling hypotheses can anticipate protein crystallization conditions. Therefore, we went for further optimization for crystallization parameters to obtain crystals suitable for X-ray diffraction.

Once we obtained protein crystals of good quality, crystals were illuminated by the X-ray beam generated by synchrotron sources. The dataset of diffraction images taken for crystals showed that most crystals diffracted to an average of 3.1 Å resolution. The calculated factors including space group, cell dimension reflect the quality of resolution data. This poor quality of the diffraction data could be attributed to the lack of protein crystals homogeneity, which believed to be the case for protein crystals. Generally, protein crystals diffract at 1.5 to 4 Å resolution, and thus the diffraction dataset quality reduced with misalignment of the crystal lattice.

For NS5b structural modeling, we processed the X-ray diffraction data by Molecular Replacement approach. Identical to other HCV-NS5b polymerases, the HCV-NS5b of genotype4a comprises of six conserved subdomains, the analogy structure indicates that fingers, palm, and thumb are in close interaction, which contracts the flexibility between the subdomains. However, previous models of HCV-NS5b revealed the presence of several conformations when in complex with the template. Unfortunately, as we did not perform NS5b template co-crystallization, we still miss the other protein confirmations.

5. Part III: The role of tripartite motif family members (TRIM) in mediating susceptibility to HCV infection

5.1. Characterization of TRIMs in hepatocytes

Multiple TRIM proteins play a role in restricting viral infection such as retroviruses infection, by inducing IFN response, regulating RPRs and/or interacting directly with viral proteins.

5.1.1. TRIM genes regulation upon HCV infection

A number of host factors are regulated by HCV infection either directly or indirectly, previous studies have shown some innate immune factors manipulated by HCV infection. To investigate TRIMs roles in HCV infection, we used different hepatoma cell lines that support either HCV infection or replication. Huh7.5 cells are highly permissive for HCV infection, the high permissiveness results from a mutation (Thr-55-Iso) in the RIG-I gene (retinoic acid-inducible gene I, which impairs interferon signaling).

We searched the literature to check for the TRIMs which expressed by hepatocytes. Human gene array for the transcriptional levels including TRIMs was investigated in Huh7.5 HCV-infected cells. A number of TRIM genes were upregulated upon HCV infection including some TRIMs such as TRIM5, 14 and 25 with a known anti-viral effect on viruses such as HIV and SeV. TRIM31 showed the highest expression level in HCV-infected cells (Figure 5.2.A). A panel of TRIMs showed down-regulation upon HCV infection, including TRIM43, 44 which have been identified by another group (Li, Zhang et al. 2014). The gene array was done at the one-time point, 72 hours post HCV (JC-1) infection. Therefore, further characterization of TRIMs regulation upon HCV infection or interferon stimulation were performed.

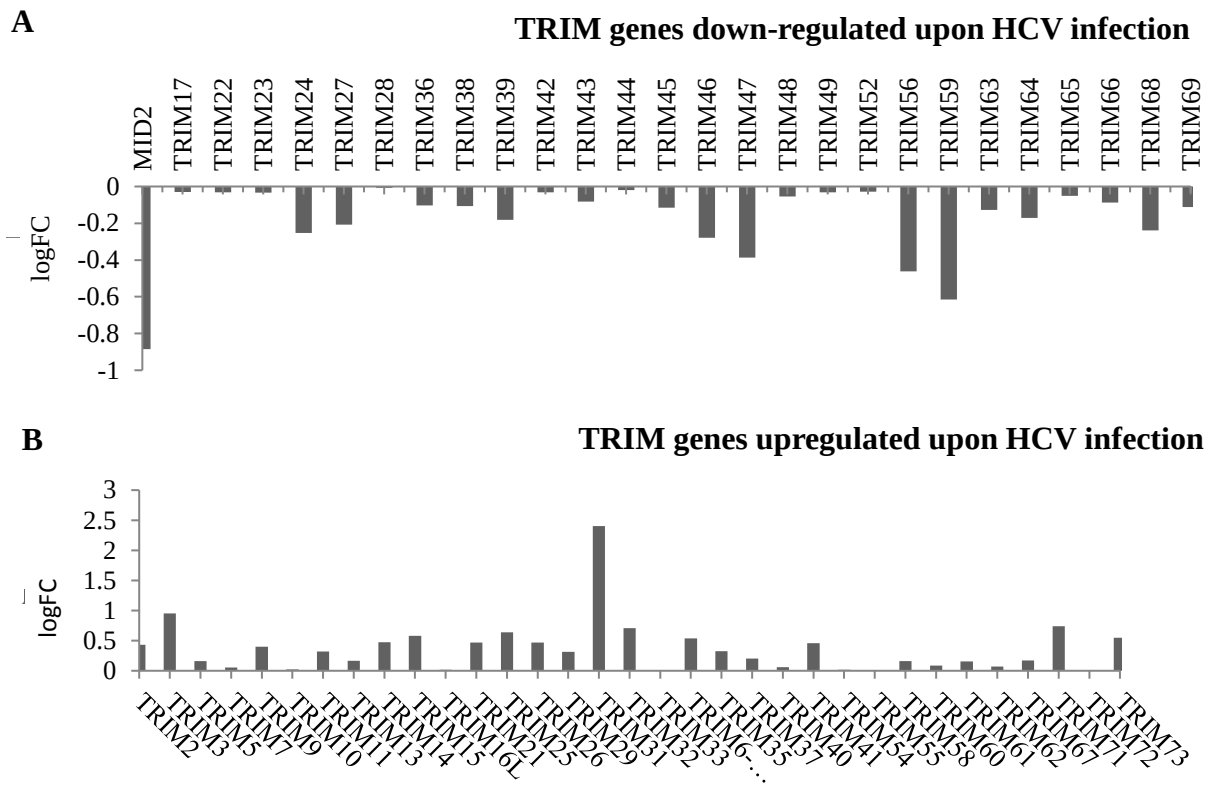

Figure 5.2. The gene array of TRIM genes in HCV infected Huh7.5 cells Huh7.5 cells were cultivated and then infected with HCV (Jc1 strain) for 72 hours. RNA from infected and uninfected cells was extracted and TRIM gene array was done. (A) Shows TRIM genes that are upregulated upon HCV infection. (B) Shows the TRIM genes which are downregulated upon HCV infection.

5.1.2. Expression kinetics of TRIM genes in Huh7 hepatoma cells

In order to perform a study on TRIM family roles in HCV infection, first, we checked the TRIM gene expression at different time points after interferon treatment or HCV infection in Huh7 cells. We screened 33 TRIMs which expressed in hepatoma cells or hepatoma cell lines and the housekeeping gene b-actin. The quantitative RT-PCR showed (Figure 5.3.A) showed the impact of IFN treatment on TRIM gene expression. The induction kinetics was divided into three groups, early (6 hours), intermediates (24-48 hours) and late (72-96 hours). TRIMs such as TRIM 7, 9, 21 and 40 showed early up-regulation kinetics, while TRIM5 and 14 showed intermediate kinetics at 24 hours post stimulation, other TRIM genes such as TRIM 1 showed late kinetics and reached the peak at 96 hours post IFN treatment.

Interestingly, in case of HCV infection (Figure 5.3.B), TRIM 9 and 11 showed early kinetics, and then decline after 48 hours and increased again late at 72-96 hours post infection, while TRIMs such as TRIM 5, 14, 52 and others showed intermediate kinetics, and finally TRIM 1 and 7 showed late kinetics and reached peak at 96 hours post infection.

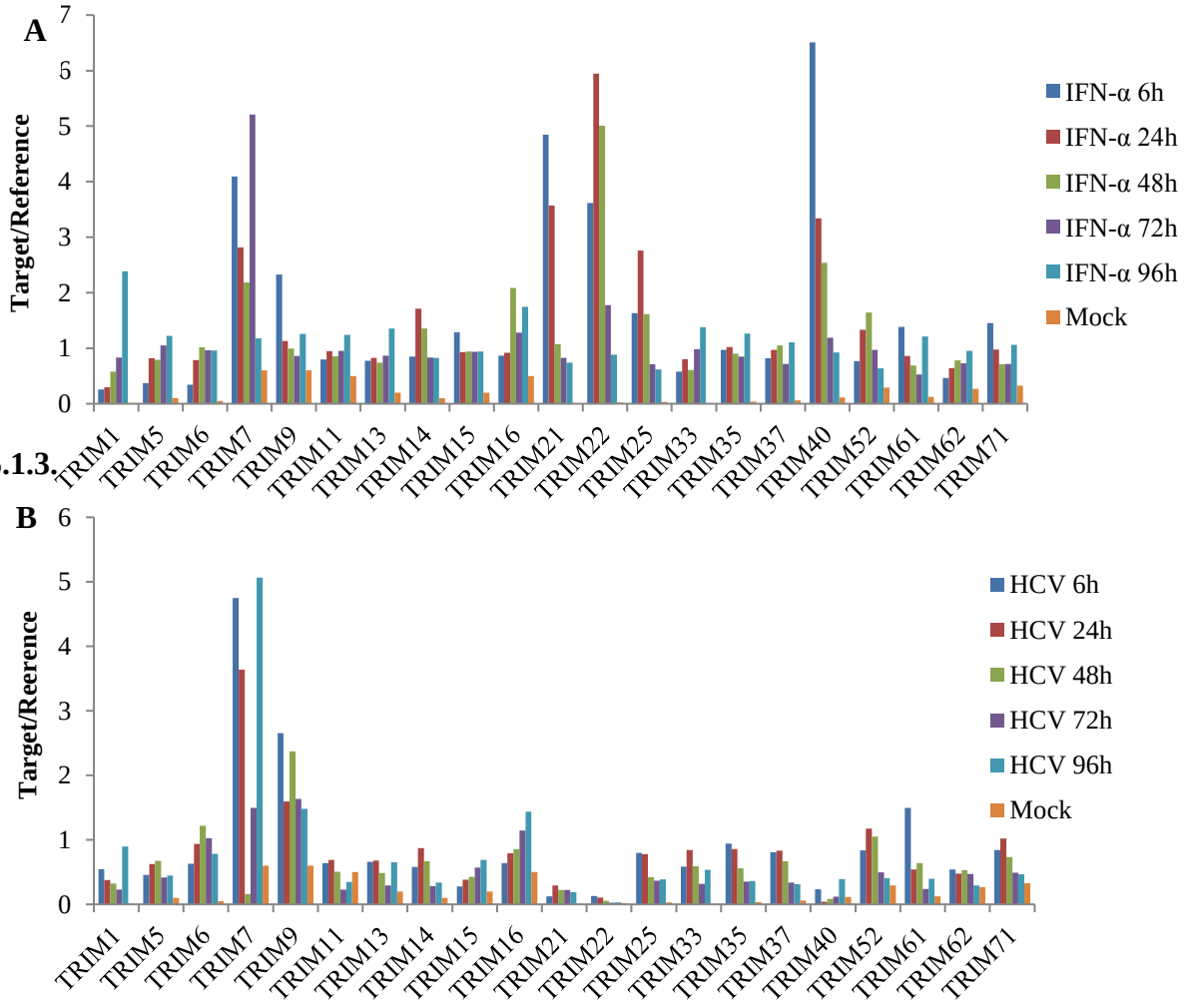

5.1.3.

Figure 5.3. TRIM gene expression at different time points Huh7 cells were seeded and then either (A) treated with interferon-α or (B) infected with HCV (0.1 MOI) for different durations. RNA was extracted and cDNA was prepared from all samples at the same time. TRIM genes which expressed in hepatoma cells or hepatoma cell lines were quantified and normalized to GAPDH.

5.1.4. TRIM gene expression in primary hepatocytes

As hepatoma cell lines are transformed cells and could have changes in the RNA, we used pure primary hepatocytes to confirm the TRIM gene expression profile. The main drawback of this model is the scarcity of resources and the poor susceptibility to HCV infection. Primary hepatocytes were obtained and seeded at ($1x10^5$) density, and then infected with HCV five MOI (JC-1 strain), treated with IFN-α or infected-treated (Figure 5.3).

Cells were then intensively washed and lysed for RNA extraction and TRIM genes quantification. When we analyzed the TRIM gene expression, a number of TRIMs were undetectable such as TRIM 22, 62, 76 and 71. Upon HCV infection, TRIM1 was downregulated compared to the uninfected control, where it showed upregulation in HCV24h-IFN 72h infected/treated cells, while TRIM 1 showed upregulation at 72h of IFN treatment. As the infectivity of PHHs is not clear, we attributed the upregulation of TRIM 1 in HCV24h-IFN 72h to the interferon treatment (Figure 5.4).

In PHHs, 14 TRIMs (TRIM 5,7,9,11,13,14,15,21,25,33,34,35,40 and 55) showed upregulation upon IFN-alpha treatment, either early at 6hours or late 72 hours post stimulation, we also included NIP10 as a positive control for in interferon stimulation. As mentioned earlier, because of the poor PHHs infectivity, we cannot conclude about the regulation of TRIMs by HCV infection in this model. Among these genes, we selected the ones aligned with previous experiments such as TRIM 5, 9, 14 and 25 for further studies (Figure 5.4).

Although IFN induces several TRIM genes which might trigger a broad antiviral response, it is not clear whether antiviral TRIMs solely induced by IFN or by other stimuli associated with the antiviral activity.

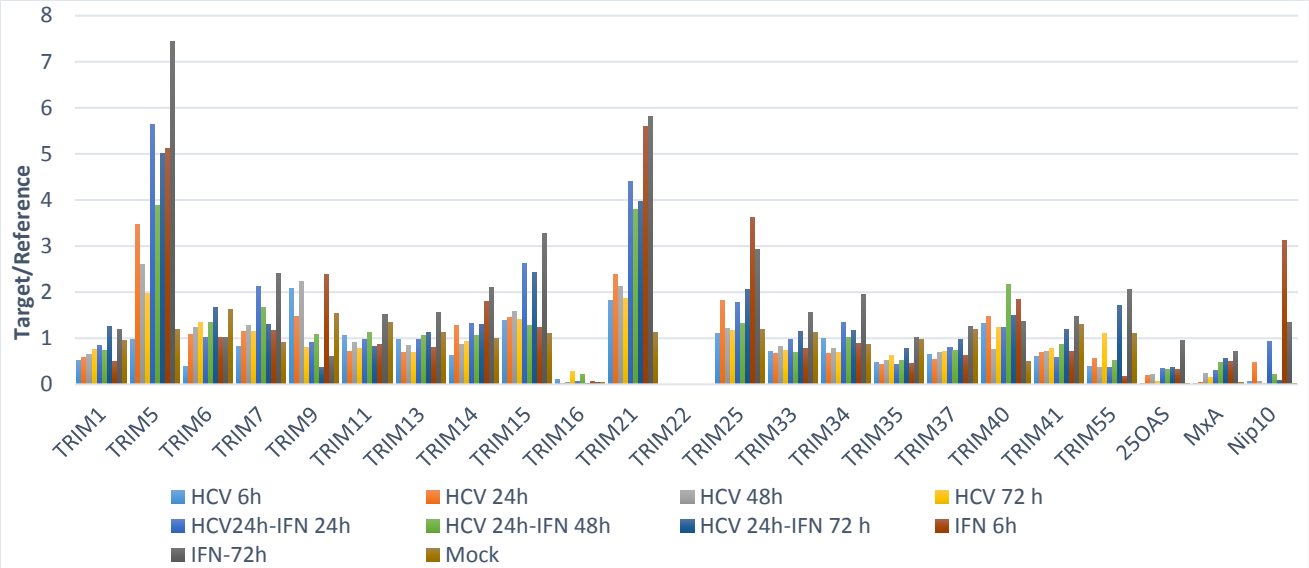

Figure 5.4. TRIM gene expression in PHHs cells were seeded at ($1x10^5$) density, cells were then either infected with HCV five MOI (JC-1 strain) or treated with IFN-alpha or infected-treated for different durations. RNAs were extracted, RT-qPCR used to quantify TRIM gene expression and normalized to GAPDH.

5.2. The antiviral effect of TRIMs on HCV infection and replication

Previous work identified two possible antiviral mechanisms of TRIMs, either by interacting directly with viral proteins or inducing IFNs and cytokines by modulating the signaling pathway. The antiviral mechanisms of most TRIMs are unknown, while few are well studied such as TRIM5, it functions in mediating the restriction of HIV infection, this occurs via its interaction with core protein and destabilization of the virus.

So, to test the role of selected TRIMs in HCV replication and infection we used HCV reporter replicon cell line (ED43) harboring ED43-genotype4a isolate. The ED43 replicon is a bicistronic vector with a F-Luc reporter gene.

5.2.1.1. TRIM5 restricts HCV viral replication and infection

As shown in the schematic representation (figure 5.4.A), ED43 replicon cells were seeded and then transiently transfected with increasing amount of TRIM5 or pcDNA3.1 control plasmids (Figure 5.5.B). 72 hours later, cells were lysed and F-Luc was measured and normalized to

untransfected control. The overexpression of TRIM5 results in a decrease in HCV replication in a dose-dependent manner (figure 5.5.C).

To further test the effect of TRIM5 on HCV infection, we performed infection experiment using HEPepG2-HFL. The advantages of using this cell line are that it expresses the liver-specific microRNA, miR-122 along with the entry factor, CD81, so they support the entire HCV life cycle. Moreover, unlike Huh7.5, HepG2-HFL has intact RIG-I system which leads to a robust IFN response.

Briefly, HepG2-HFL cells were seeded, 24 hours later cells were infected with HCVcc (JC1) with MOI of 0.1, 48 hours later cells were transiently transfected with increasing amounts of TRIM5 plasmid, control plasmid or left untreated. Then, 48 hours later supernatants were collected for TCID50 (to test the extracellular virus production), and cells were lysed for RNA extraction, HCV viral genome, and TRIM5 expression were quantified by qRT-PCR (Figure 5.6.A). As expected from our replicon cell model, we observed a reduction in viral genome production with increasing amount of TRIM5 transfection dose (Figure 5.6.C). In addition, supernatants were collected and titrated for TCID50, showed very little infectivity in transfected cells compared to the untransfected or plasmid control ones (Figure 5.6.D).

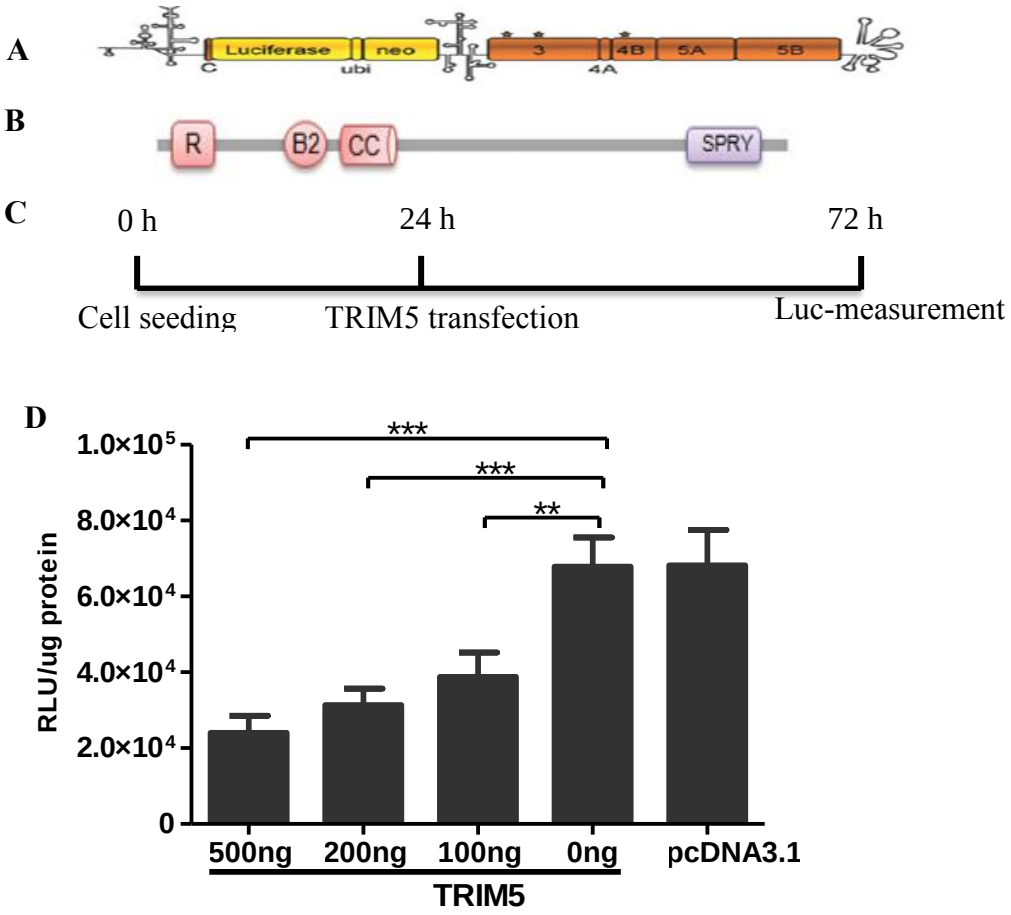

Figure 5.5. Effect of TRIM proteins overexpression on HCV replication (A) Experimental representation of HCV replicon construct stably expresses in the used in the replicon cells used in our experiments. (B) Schematic representation of TRIM5 protein domains. (C) Experimental set up shows that cells were seeded and then after 24 hours transfected with 500, 200, 100, 0 ng of TRIM5 and, and cells were lysed for F-Luc as a representative measurement for HCV replication. (D) F-luc measurement normalized to protein content (RLU).

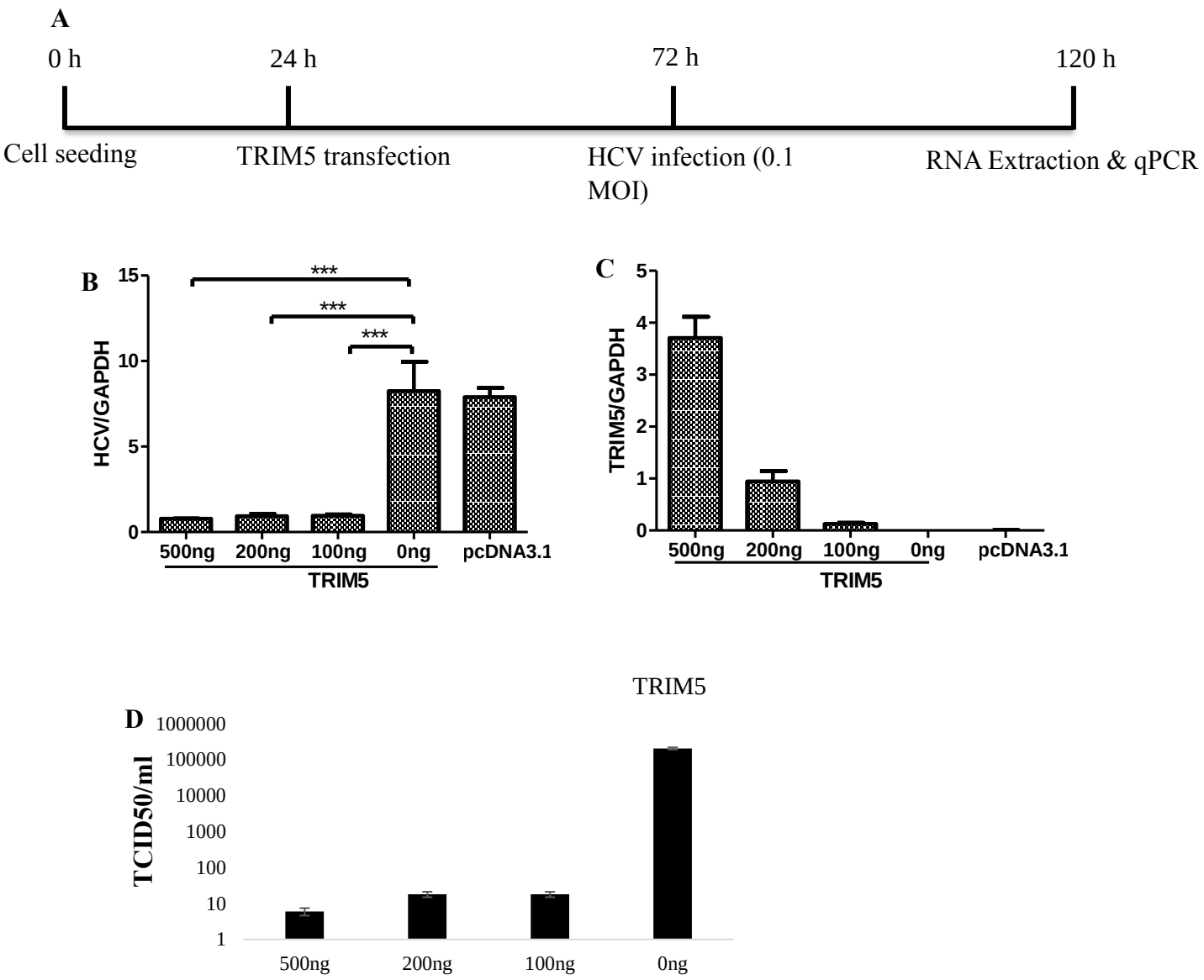

Figure 5.6. TRIM5 overexpression restricts HCV infection (A) HepG2-HFL cells were seeded (1×10^5)/well in a 12 well plate. Cells were then transfected with TRIM5, 48 hours later cells were infected with HCV at a MOI of 0.1. After 48hours, supernatants were collected for TCID50 and cells were lysed and RNA was analyzed for the expression of TRIM5 and HCV genome. (B) HCV genome quantification by qRT-PCR. (C) TRIM5 expression quantified by qRT-PCR. (D) supernatants were titrated and virus titers were determined using TCID50.

5.2.1.2. TRIM9 role in HCV infection

A recent study revealed that TRIM9 act as a negative regulator of NF-κB in brain cells (Shi, Cho et al. 2014), this negative regulation of NF-κB might be beneficial for HCV to escape the immune system. In order to check the role of TRIM9 in HCV infection, we performed replication and infection based experiments.

Figure 5.7.A shows a schematic representation of TRIM9, it consists of RING, B-box, coiled-coil and SPRY domains. To examine the effect of TRIM9 expression on HCV replication, ED43 cells were seeded, 24 hours later cells were transfected with the TRIM9 plasmid. After 48 hours, cells were lysed and F-Luc and protein content (Figure 5.6.B). TRIM9 expression inhibits HCV replication in a dose-dependent manner (Figure 5.7.C).

To further examine the effect of TRIM9 expression on HCV infection, HepG2-HFL cells were seeded and then transfected with TRIM9 plasmid, 48 hours later, cells were infected with HCV at (0.1 MOI), and then cells were left for another 48 hours before they analyzed for Intra and extracellular HCV infection, supernatants were collected for TCID50 and lysed cells were RNA extractions and RT-qPCR analysis. As shown in (Figure 5.7.B-C), HCV viral genome was strongly reduced with the increasing amount of TRIM9 expression. TCID50 results showed that TRIM9 overexpression does decrease the HCV infectivity, which confirms the TRIM9 anti-HCV effect on HCV (Figure 5.7.D).

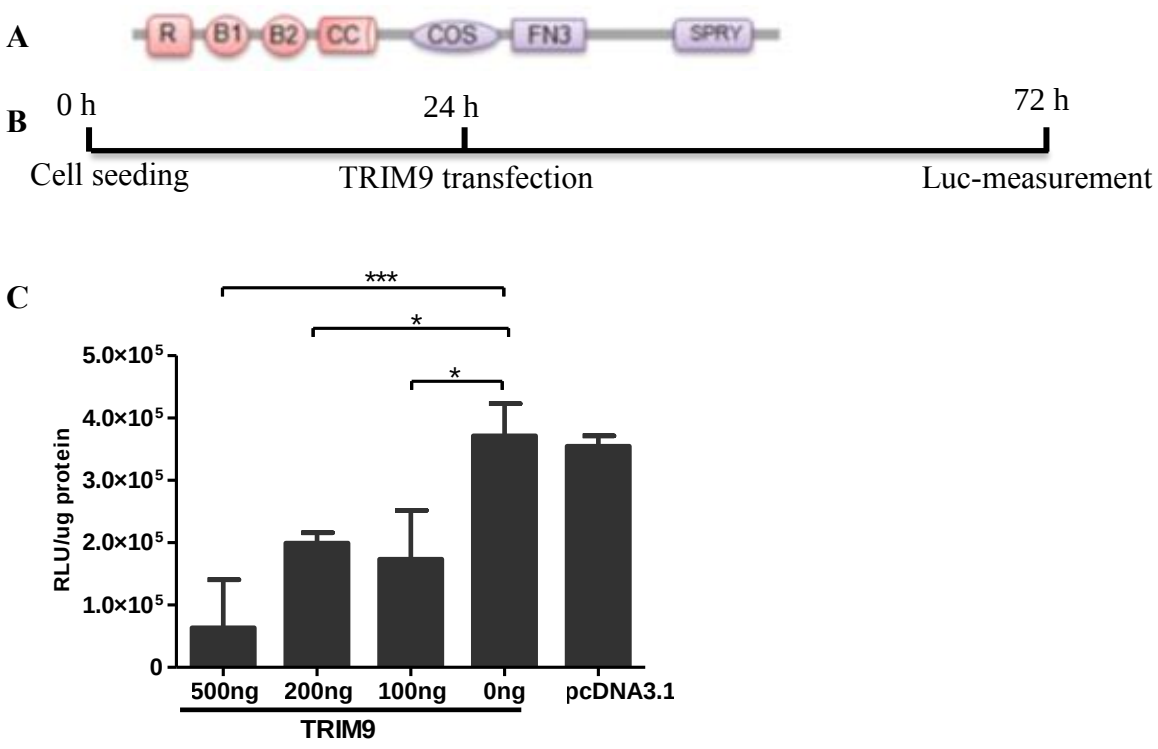

Figure 5.7. TRIM9 overexpression effect on HCV replication (A) Schematic representation of TRIM9 domains. (B) ED43 replicon cells were seeded and then transfected with TRIM9 construct, control or left un-transfected, 48 hours later cells were lysed (C) HCV replication reduction measured as F-Luc normalized to protein content.

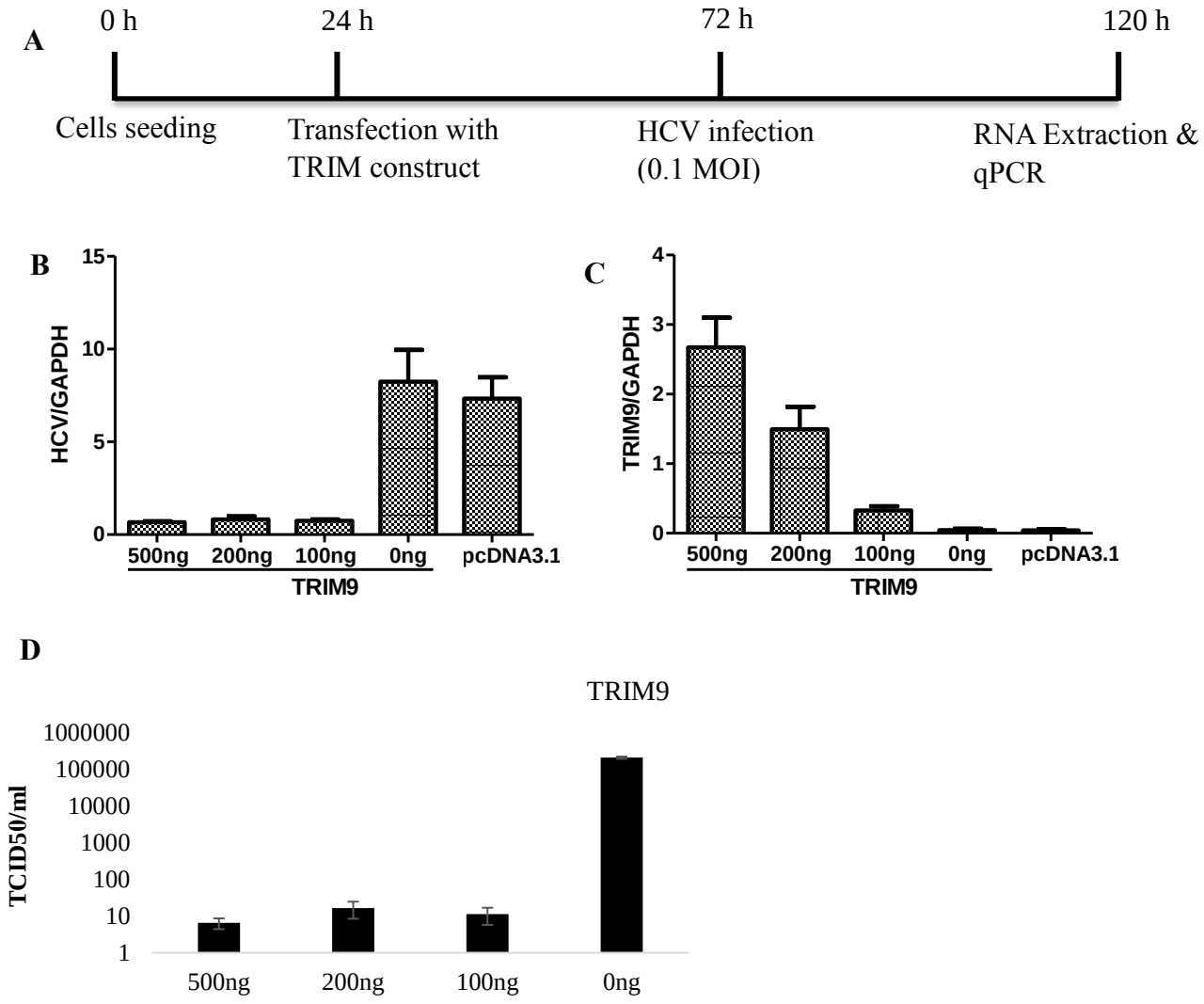

Figure 5.8. TRIM9 overexpression in HepG2-HFL hepatoma cell line restricts HCV infection (A) experimental representation, HepG2-HFL cells were seeded (1×10^5)/well in a 12 well plate. Cells were then transfected with TRIM9, 48 hours later cells were infected with HCV at a MOI of 0.1. After 48hours, supernatants were collected for TCID50 and cells were lysed and RNA was analyzed for the expression of TRIM5 and HCV genome. (B) HCV genome quantification by qRT-PCR. (C) TRIM9 expression quantified by qRT-PCR. (D) supernatants were titrated and virus titers were determined using TCID50.

5.2.1.3. TRIM14 overexpression influence on HCV infection

TRIM14 is a protein belongs to the family of the TRIM proteins with a conserved domain architecture (known as RBCC) that is characterized by RING (R) finger domain, one or two B-box domains (B1 and B2), a Coiled-coil domain and a variable C-terminus (Meroni and Diez-Roux 2005). Similar to TRIM family protein, TRIM14 is involved in the innate immune response, upon viral infection, TRIM14 triggers the IFN and NF-κB pathways activation. Briefly, TRIM14 activation occurs via facilitation the link between NEMO and MAVS, this resulted in amplification of the innate immune response (Zhou, Jia et al. 2014)In order to determine whether TRIM14 has an anti-HCV activity. We transfected HCV replicon cells with increasing amounts of TRIM14 constructs after the cells were lysed and F-Luc measured (Figure 5.9.A). As shown in Figure 5.9.B, over-expression of the TRIM14 in HCV replicon cells resulted in a decrease of HCV virus replication in a dose-dependent manner.

To further examine the effect of TRIM14 on the HCV infection, cells were seeded followed by transfection with increasing amounts of TRIM14 or control plasmid, and then cells were infected with HCV cc (MOI= 0.1) Figure 5.10.A. After that intracellular HCV genome was quantified by qPCR Figure 5.10.B and extracellular virus secretion was evaluated by TCID50 (Figure 5.10.D). Figure 5.10.B-C shows that expression of TRIM14 resulted in a decrease of the HCV infection as quantified by qPCR. The effect of TRIM14 overexpression is confirmed by the decrease in extracellular virus quantification (Figure 5.10.D). Taken together, TRIM14 overexpression restricts HCV replication and infection.

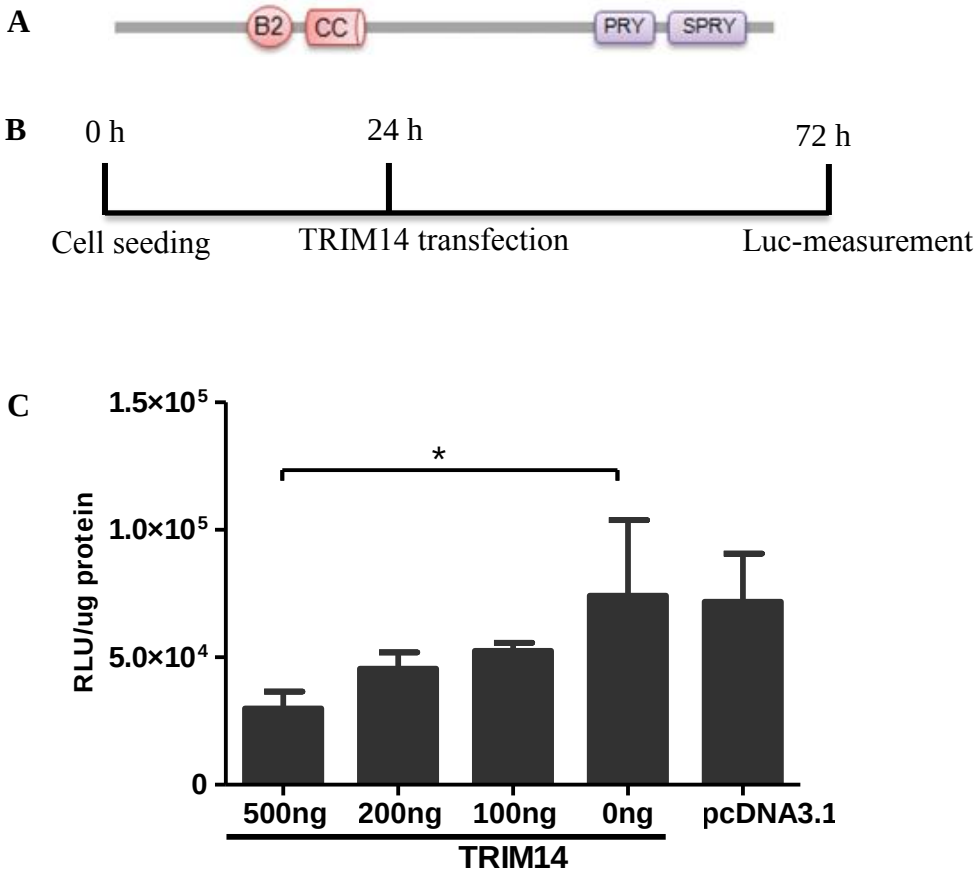

Figure 5.9. Effect TRIM14 overexpression on HCV replication (A) Schematic representation of TRIM14 domains. (B) ED43 replicon cells were seeded and then transfected with TRIM14 construct, control or left un-transfected, 48hours later cells were lysed and F-luc was measured. (C) The graph shows the HCV replication reduction measured as F-Luc normalized to protein content.

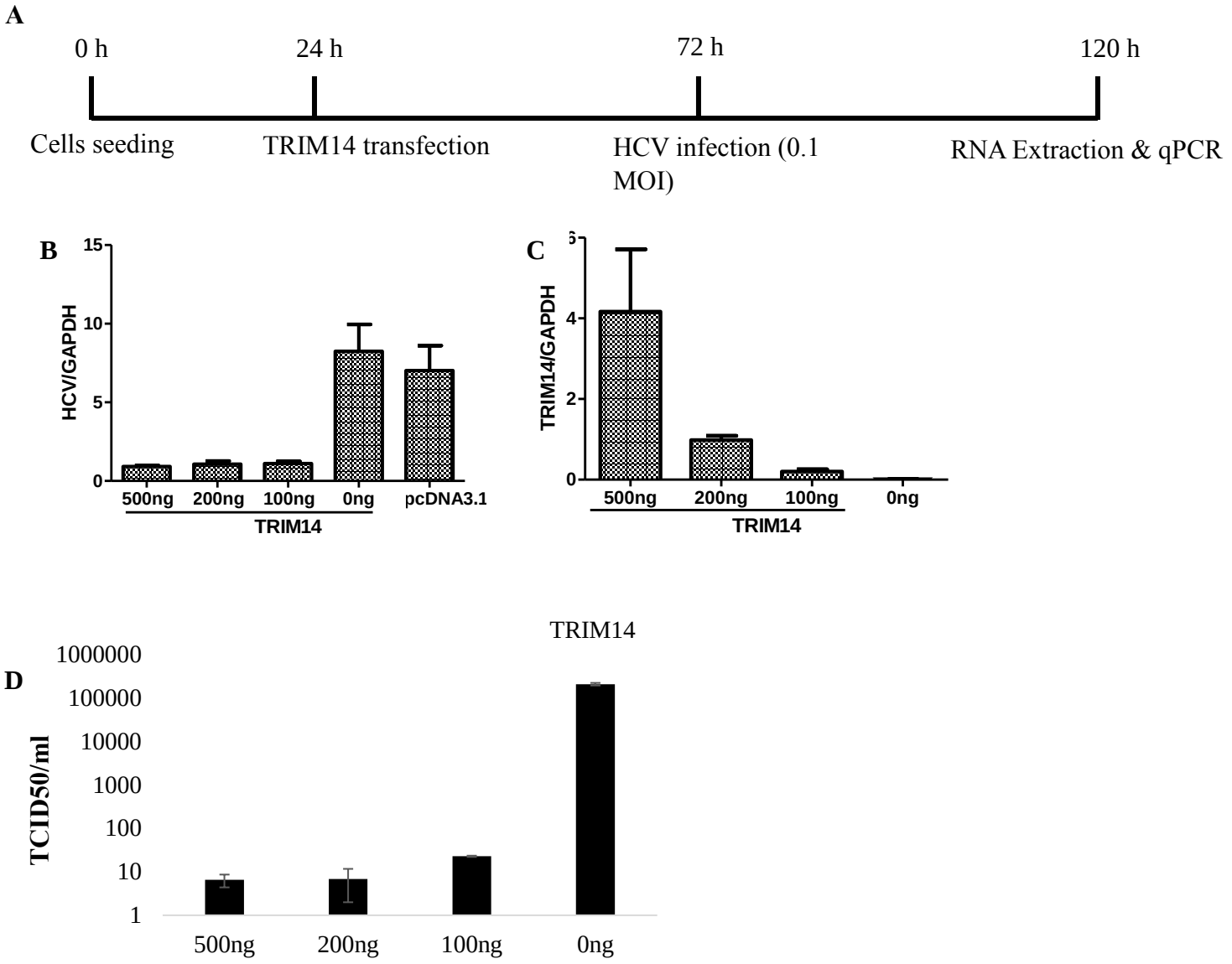

Figure 5.9. TRIM14 overexpression reduced the HCV infection in HepG2-HFL cells (A) experimental representation, HepG2-HFL cells were seeded (1×10^5)/well in a 12 well plate. Cells were then transfected with TRIM5, 48hours later cells were infected with HCV at MOI of 0.1. After 48 hours, supernatants were collected for TCID50 and cells were lysed and RNA was analyzed for the expression of TRIM14 and HCV genome. (B) HCV genome quantification by qRT-PCR. (C) TRIM5 expression quantified by qRT-PCR. (D) supernatants were titrated and virus titers were determined using TCID50.

5.2.1.4. TRIM25 effectively inhibits HCV replication and infection

TRIM25 belongs to the C-IV TRIM proteins family, TRIM25 is abundantly expressed in placenta and uterus, highly expressed in the thyroid gland, aorta and spleen and low in most other tissues. In addition, TRIM25 is an IFN-inducible gene. Recently, it was shown that TRIM25 plays an important role in innate immunity regulation, notably in RIG-I pathway regulation. It interacts with (CARD) domain of RIG-I through its PRYSPRY region, this results in ubiquitination of RIG-I and, consequently, induction of type I IFN, production and activation of NF-κB. Interestingly, TRIM25 inhibits HIV and MLV late stage of viral replication and may play a role in HBV viral restriction.

As described in (Figure 5.10.A), TRIM25 consists of N-terminal RING domain, one or two B-boxes, and a coiled-coil region. To characterize the role of TRIM25 in HCV replication and infection, we performed an experiment where we seeded replicon cells ED43 and then transfected with increasing concentrations of TRIM25 plasmid or control plasmid for 48 hours and then F-Luc was measured and normalized to protein content (Figure 5.10.B). Our results showed that HCV replication was reduced in the TRIM25 transfected cells compared to the untransfected ones (Figure 5.10.C), we did not notice differences between the 100 and 200 ng transfections.

Next, we performed an infection experiment to test the effect of TRIM25 on HCV infection. As described in Figure 5.11.A, we transfected HepG2-HFL-HCV infected cells with TRIM25 plasmid, then supernatants and cell lysates were used for analysis. First, by RT-PCR we did observe a tremendous decrease in HCV genome in TRIM25 transfected cells compared to control plasmid or untransfected cells (Figure 5.11.B-C). TCID50 results confirmed the reduction in the HCV infection as seen in (Figure 5.11.D). These results strongly suggest that overexpression of TRIM25 protein acts as anti-HCV protein.

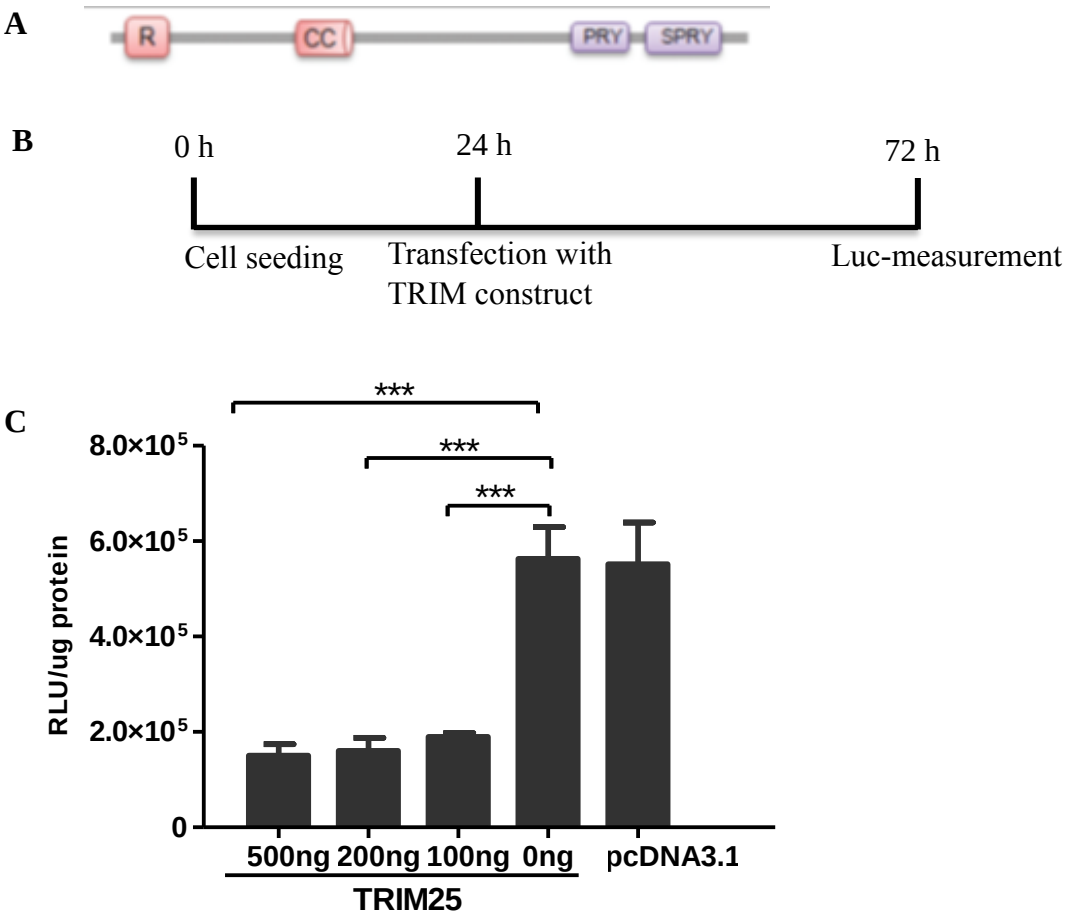

Figure 5.10. TRIM25 overexpression effect on HCV replication (A) Schematic representation of TRIM25 domains. (B) ED43 replicon cells were seeded and then transfected with TRIM25 construct, control or left un-transfected. After48hours, cells were lysed and F-luc was measured. (C) graph shows the HCV replication measured as F-Luc normalized to protein content.

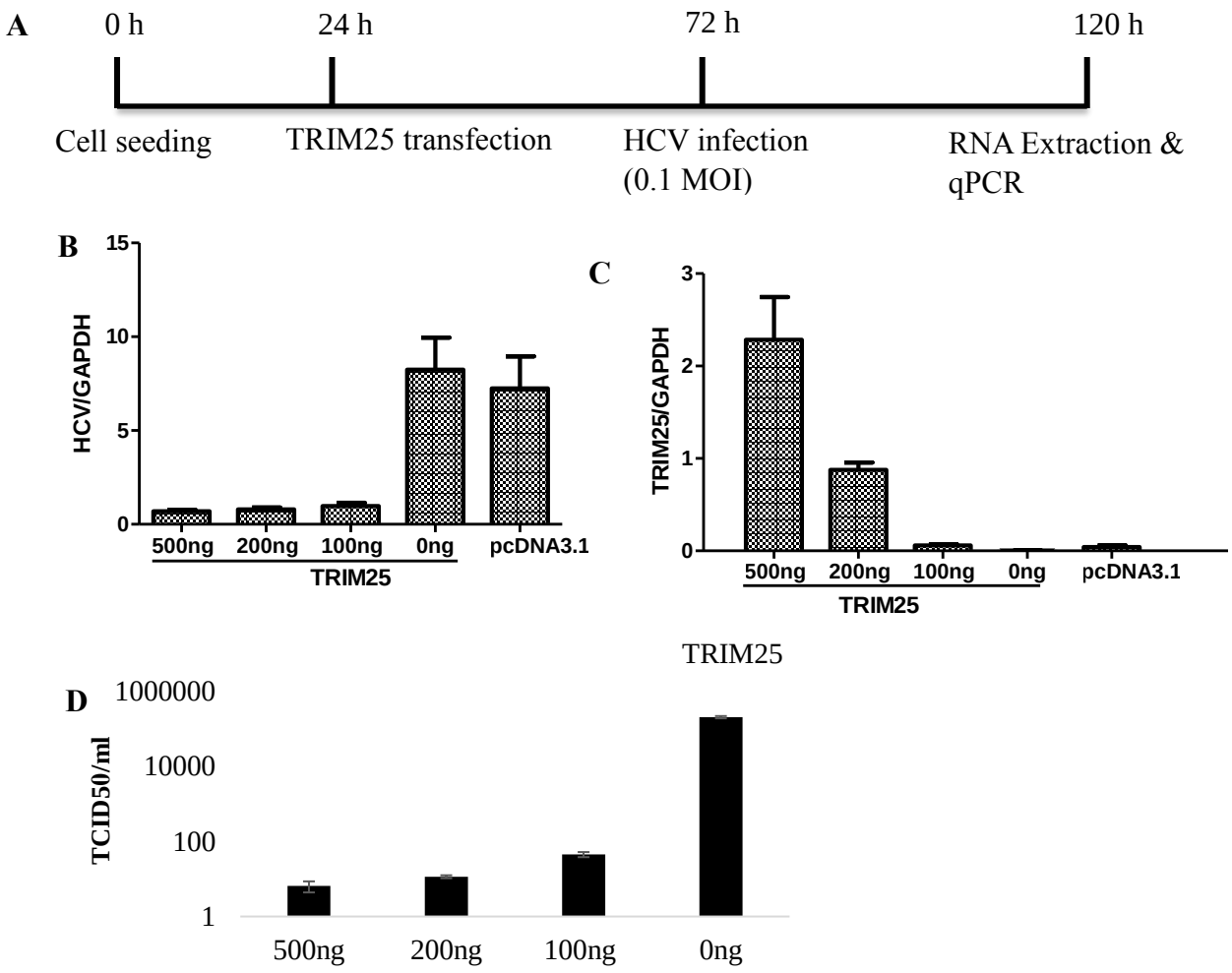

Figure 5.11. TRIM25 overexpression in HepG2-HFL hepatoma cell line restricts HCV infection (A) HepG2-HFL cells were seeded (1×10^5)/well in a 24 well plate. Cells were then transfected with TRIM25, 48 hours later cells were infected with HCV at a MOI of 0.1. 48hours later, supernatants were collected for TCID50 and cells were lysed and RNA was analyzed for the expression of TRIM25 and HCV genome. (B) HCV genome quantification by qRT-PCR. (C) TRIM25 expression quantified by qRT-PCR, (D) supernatants were titrated and virus titers were determined using TCID50.

5.3. Effect of TRIM proteins overexpression on type I IFN response

We previously showed that TRIM5, 9, 14 and 25 overexpression restricts HCV replication and infection in the *in vitro* system. So we decided to investigate the role of those TRIMs in the IFN response. Therefore, cells were transiently co-transfected with IFN-β-luc promoter and 100 ng of TRIM or control plasmids. 48 hours later, cells were infected with HCV of 0.1 MOI (Figure 5.12.A). We found that TRIMs overexpression activated the IFN-β responsive promoter with the highest activation for the TRIM25 Figure. 1D). To further investigate whether TRIMs regulate IFN- β production via IRF3 and NF-κB. Cells were co-transfected with IFN-sensitive response element (ISRE), which is an IRF3-dependent promoter and individual TRIM plasmids or control ones (Figure 5.12.A), TRIM25 significantly stimulated the ISRE, while the TRIM5, 9 and 14 moderately increased the ISRE response compared to the control ones (Figure 5.12.C). We then checked the NF-κB promoter activation as another marker for the IFN pathway activation, the results showed a significant activation of NF-κB promoter in cells transfected with TRIM5, 14 and 25, whereas in cells transiently transfected with TRIM9, NF-κB remained unchanged (Figure 5.12.D).

In sum, TRIMs over-expression during HCV infection can regulate direct or indirect activation of IFN pathway, which suggest a possible mechanism of TRIM proteins in controlling HCV infection.

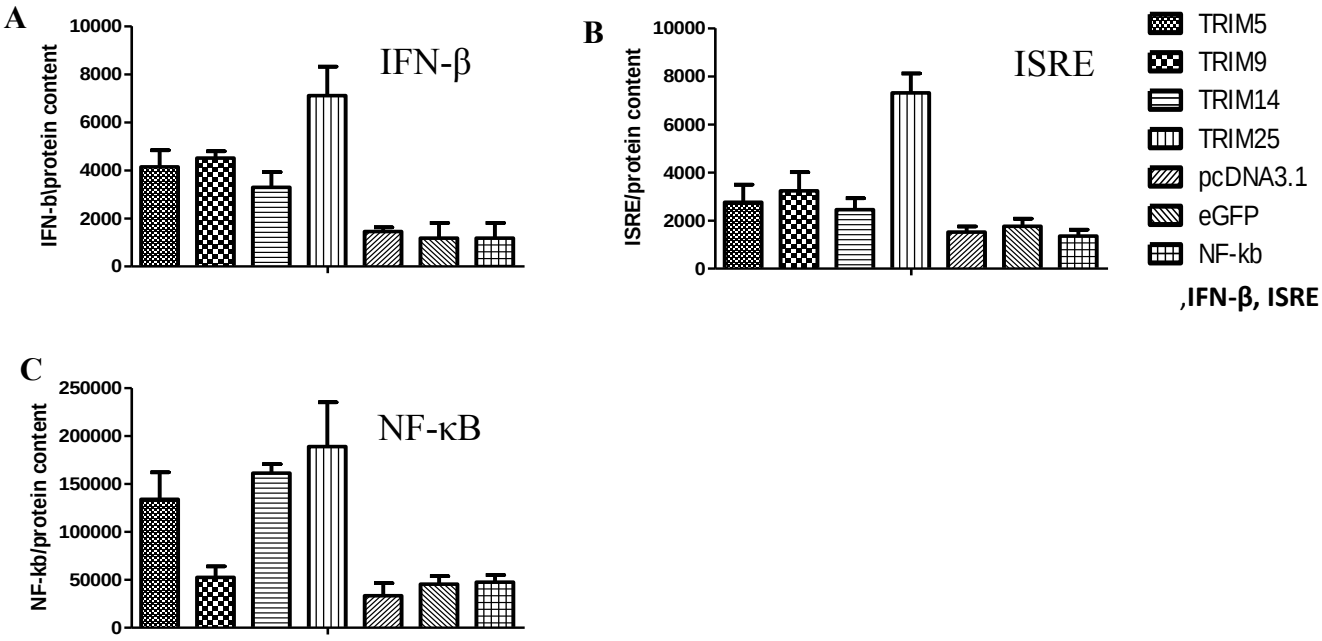

Figure 5.12. Type I IFN response is activated by TRIM proteins overexpression: Cells were transfected with (A) IFN-β. (B) ISRE or (C) NF-κB reporter plasmids along with control plasmids or an individual TRIM5, 9, 14 or 25 plasmid, and then cells were infected with HCV (JC-1). After 48 hours, cells were lysed and the promotor activity was determined by measuring the luciferase activity.

5.3.1. HCV regulatory effect on IFN response (*in vitro*)

To confirm that the IFN regulatory effect is a result of TRIMs and not from HCV infection, we investigated the effect of TRIM protein overexpression on type 1 IFN in presence or absence of HCV infection. Thus, we transfected the cells with an IFN-β, ISRE or NF-κB along with one of the TRIM plasmids. After, 48 hours cells were infected with HCV (JC-1 strain) at 0.1 MOI, as seen in Figure 5.13. Consistent with the previous results, the induction of IFN-β, ISRE, and NF-κB promoters results from TRIM proteins overexpression. As shown in the promoter assay

(Figure 5.13.B-D) HCV infection has no effect on IFN-β promoter activation, whereas it has a little down-regulatory effect on ISRE and NF-κB. Collectively, these results suggest that TRIM5, 9, 14 and 25 play a positive role in mediating the anti-HCV response.

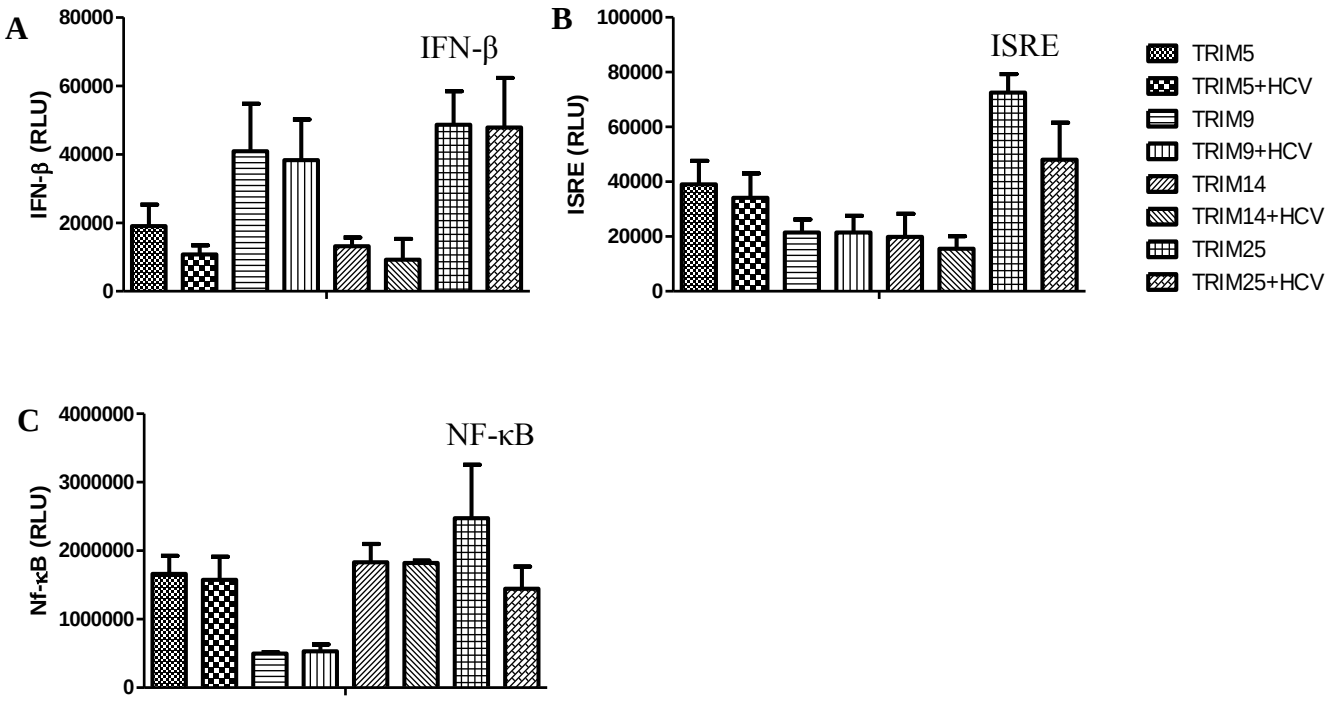

Figure 5.13. Effect of HCV infection on type 1 IFN response cells were transfected with indicated TRIMs along with IFN-β, ISRE or NF-κB reporter plasmids. After 48 hours, cells left uninfected or infected with HCV. And then cells were analyzed for promoter activities. (B) IFN-β activity, HCV slightly supress the TRIM5 and 14 activities. (C) ISRE and (D) the activity of NF-κB was counteracted by HCV infection in case of TRIM25 transfection.

5.3.2. Effects of HCV infection on IFN-β signaling pathway

To further determine the effect of HCV infection on IFN-β pathway, cells were transfected with IFN-β, ISRE or NF-κB luciferase reporter plasmids, and then promoter activities were determined at different time points after HCV infection (Figure 5.14.A-C). The activation of the

IFN-β reporter (Figure 5.14.A) was decreased upon infection and reached the lowest activity at 96 hours post infection.

In contrast, ISRE activity increased upon infection and reached the maximum at 24 hours post HCV infection and it dropped at 96 hours post infection (Figure 5.14.B). In agreement with IFN-β reporter results, HCV infection down-regulates NF-κB promoter activity over the course of HCV infection (Figure 5.14.C). Together, these results indicate that HCV has a negative effect on the IFN-β signaling pathway.

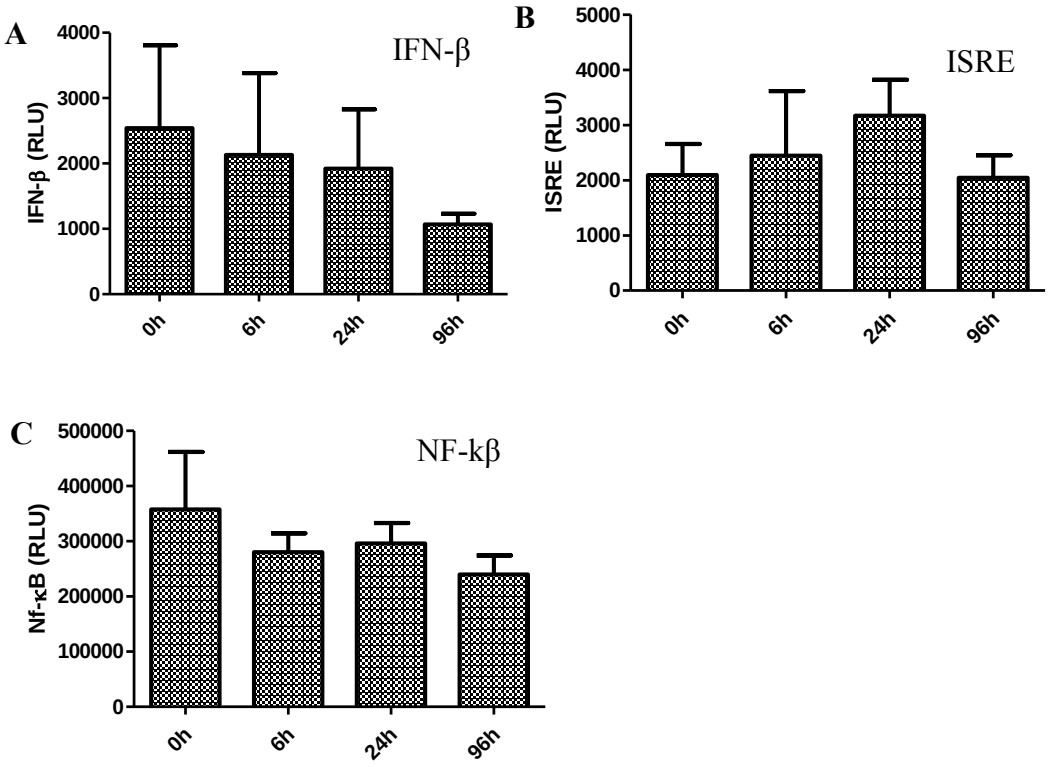

Figure 5.14. HCV infection negatively regulates IFN-β pathway: Cells were transfected with IFN-β, ISRE or NF.kβ. After 24 hours, cells were infected with HCV for different durations, 0, 6, 24 and 96 hours. Followed by cell lysis and F-Luc measurement (A) Shows the activation pattern of IFN-β. (B) Activation of ISRE. (C) Activation of NF-kβ promotor. Luciferase activities were normalized to protein content.

5.3.3. Kinetic stimulation of IFN-β response upon IFN-α treatment

To investigate how IFN-β signaling pathway is regulated, we did a transfection experiment where we transfected cells with IFN-β, ISRE or NF-κB promoter plasmids, and then cells were treated with IFN-α for different durations. We analyzed the IFN-β promoter activity using luciferase assay measurement, IFN-β promoter activity was activated at 6 hours post treatment, and it dropped below the control level at 24hours post-treatment, whereas at 96 hours post treatment the promoter partially gained the activation (Figure 5.15.A). Consistent with IFN promoter activation pattern, both ISRE and NF-κB showed fast kinetics and induced at 6 hours post treatment, at 24 hours the activation dropped below the untreated values and then regained the basal levels at 96 hours post treatment (Figure 5.15.B-C).

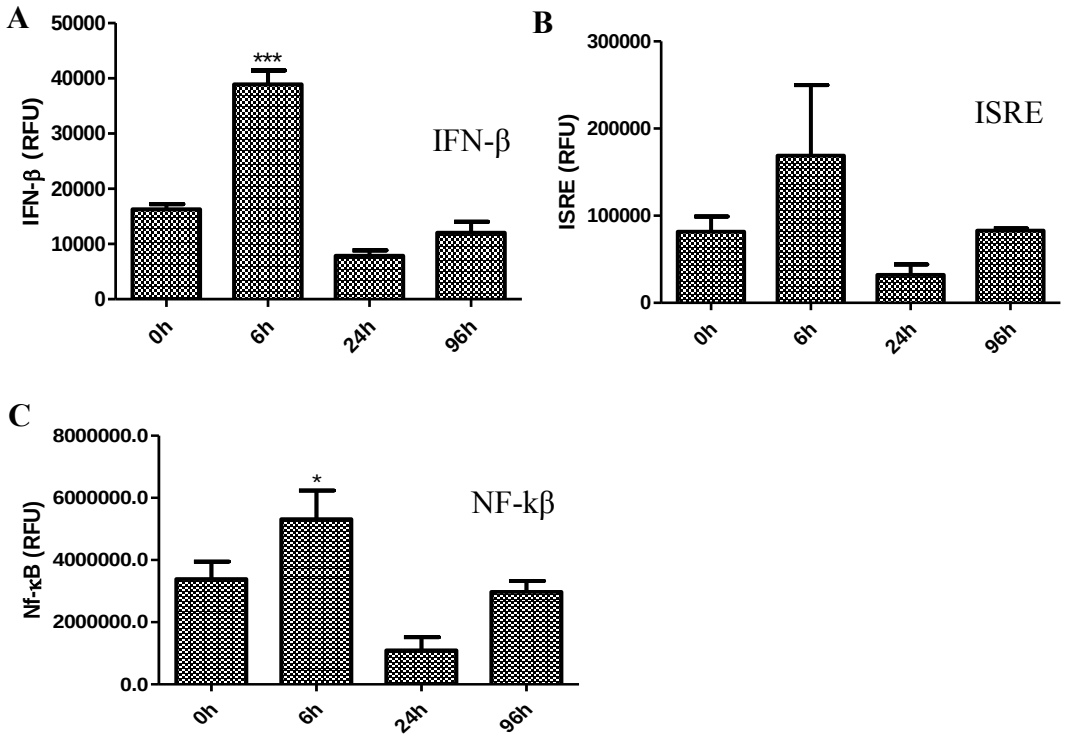

Figure 5.15. Kinetic stimulation of IFN-β pathway Cells were transfected with one of the reporter plasmids IFN-β, ISRE or NF-κB, and then cells were treated with IFN-α for different durations, 0, 6, 24 and 96 hours. Cells were then lysed and F-Luc was measured. (A) Shows the activation pattern of IFN-β. (B) Activation of ISRE. (C) Activation of NF-kβ promotor. Luciferase activities were normalized to protein content.

5.4. TRIM proteins and innate immune regulation

5.4.1. TRIM5 and innate immune response regulation

As we showed previously, TRIM5 was induced in hepatoma cell lines upon IFN treatment. Moreover, the transient overexpression of TRM5 in HepG2-HFL hepatoma cell line results in restriction of HCV infection as quantified by qRT-PCR and TCID50 experiments. To gain insight into the TRIM5 regulation of the innate immune response, we performed an experiment to quantify for the following innate immune elements, RIG-I (the dsRNA receptor), MAVS (the mitochondrial protein that participates in the anti-viral signaling pathway), TRIF (adaptors molecule), which in turn leads to induction of IFN-β. In Figure 5.16. B, RIG-I was significantly upregulated in cells transfected with TRIM5. In addition, MAVS was upregulated in cells transfected with TRIM5 (Figure 5.16.C). In agreement with that, overexpression of TRIM5 resulted in significant increase in TRIF (Figure 5.16.D). Nevertheless, as expected IFN-β was increased in transfected cells (Figure 5.16.E). From the above results, we could conclude that TRIM5 overexpression can activate the IFN signaling pathway at different levels upstream IFN-β.

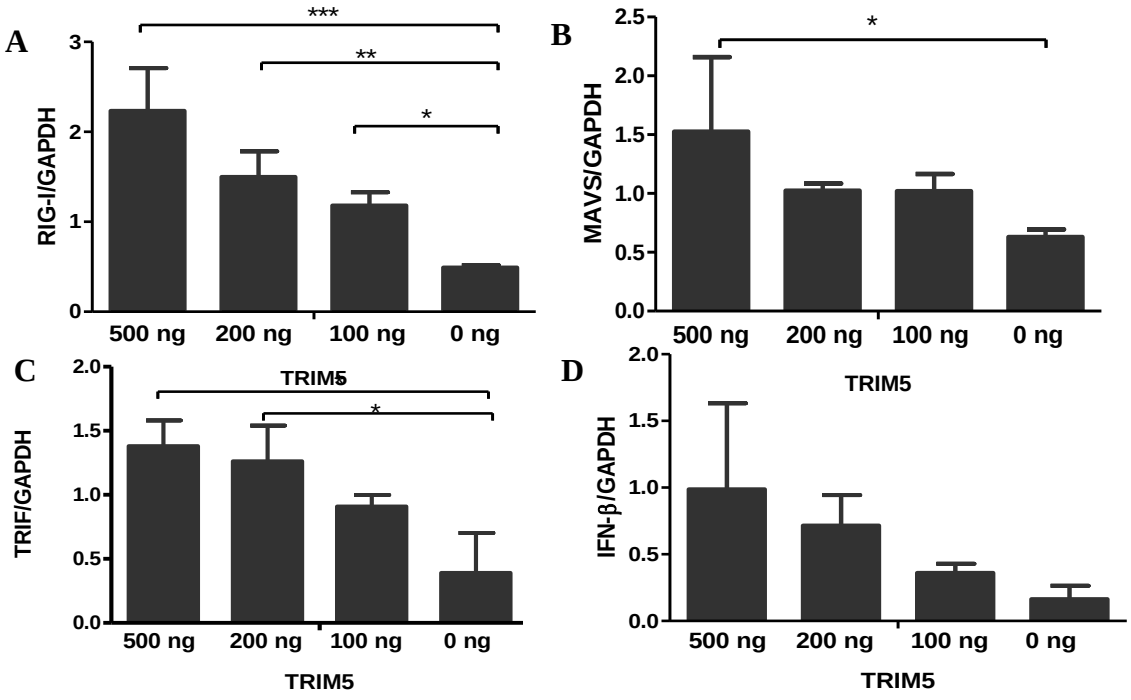

Figure 5.16. TRIM5 overexpression regulates IFN pathway: Cells were transfected with increasing amounts of TRIM5 (500, 200, 100 or 0 ng). After 48 hours, cells were infected with HCV (0.1 MOI). 48 hours post infection, cells were lysed and RNA was extracted, RNA was analyzed for the expression of (A) RIG-I. (B) MAVs. (C) TRIF and (D) IFN-β. Data are mean values ± SD. *p<0.05,**p<0.01,***p<0.001.

5.4.2. TRIM9 regulation of the innate immune response

In the previous section, we observed a correlation between the TRIM9 overexpression and the decrease of HCV replication and infection. Therefore, we investigated the activation of the IFN pathway at different levels including RIG-I, MAVS, TRIF, and IFN-β. Overexpression of TRIM9 upregulated RIG-I (Figure 5.17.B), whereas overexpression of TRIM9 upregulated MAVS expression and the upregulation was inversely correlated with TRIM9 transection dose (Figure 5.17.C). Although TRIF expression was upregulated in response to TRIM9 overexpression, the upregulation was not correlated with the transfection dose (Figure 5.17.D). However, the upregulation of RIG-I, MAVS and TRIF was not clearly dosed dependent, when we checked for IFN-β, we found that the expression increased in transfected cells in a dose-dependent manner (Figure5.17.E). Taken together, these results suggest a potential role of TRIM9 in IFN induction and restriction of HCV.

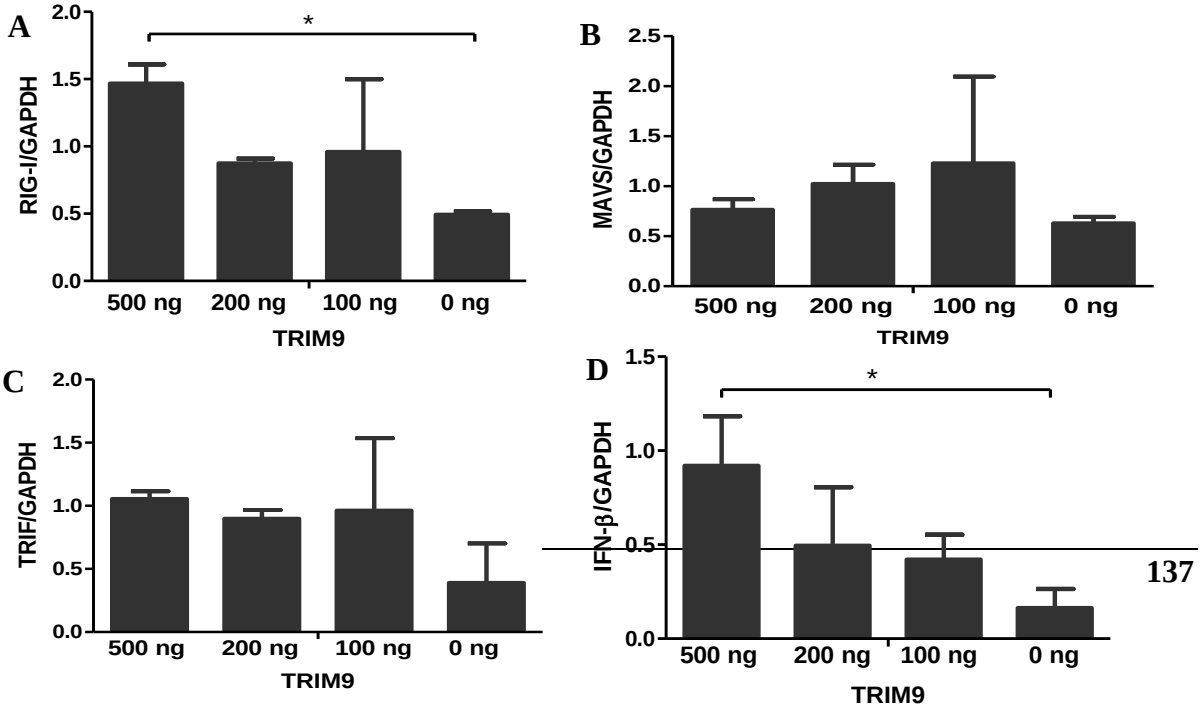

Figure 5.17. TRIM9 overexpression effect on the IFN pathway Cells were transfected with increasing amounts of TRIM9 (500, 200, 100 or 0 ng). After 48 hours, cells were infected with HCV (0.1 MOI). 48 hours post infection, cells were lysed and RNA was extracted, RNA was analyzed for the expression of (A) RIG-I. (B) MAVs. (C) TRIF and (D) IFN-β. Data are mean values ± SD. *p<0.05,**p<0.01,***p<0.001.

5.4.3. TRIM14 activates the immune response at different levels upstream the IFN-β

Considering our results that TRIM14 can decrease HCV replication and infection, we hypothesized that it could induce the IFN-β signaling. Thus, we checked for the regulation upstream the IFN-β by qRT-PCR analysis. As shown in Figure 5.18.B, transfection of cells with TRIM14 remarkably increased the expression of RIG-I. Consistent with that, TRIM14 overexpression increased MAVS, TRIF and IFN-β expression (Figure 5.18. C-E). These results indicate that TRIM14 mediates the IFN signaling at different levels.

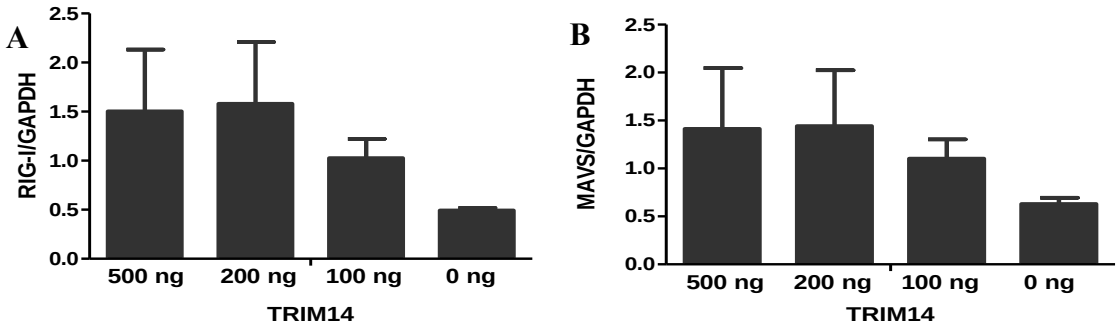

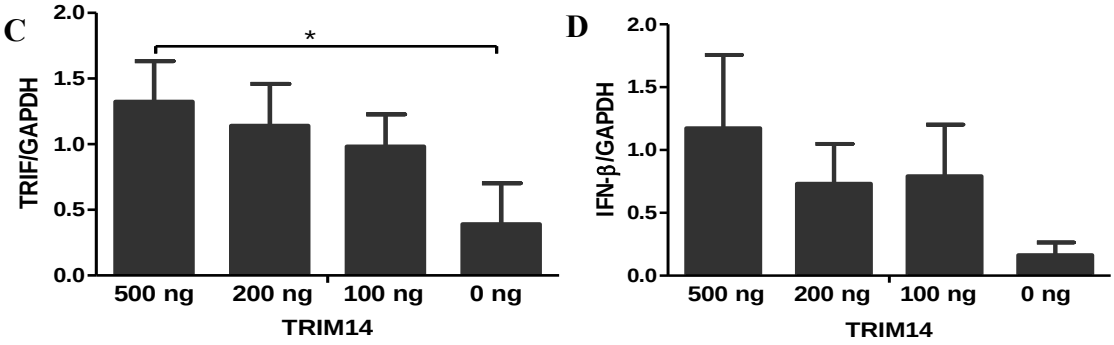

Figure 5.18. TRIM14 overexpression effect on the IFN pathway Cells were transfected with increasing amounts of TRIM14 (500, 200, 100 or 0 ng). After 48 hours, cells were infected with HCV (0.1 MOI). 48 hours post infection, cells were lysed and RNA was extracted, RNA was analyzed for the expression of (A) RIG-I. (B) MAVs. (C) TRIF and (D) IFN-β. Data are mean values ± SD. *p<0.05,**p<0.01,***p<0.001.

5.4.4. TRIM25 activates the immune response at different levels

We have shown previously that TRIM25 is ISG and is implicated in the inhibition of HCV replication and infection. To assess the role of TRIM25 in the IFN-β signaling pathway, we performed an experiment to investigate the effect of TRIM25 overexpression on the IFN-β signaling. In agreement with previous studies which showed TRIM25 as an important regulator of RIG-I, our results indicate that TRIM25 significantly increased RIG-I expression (Figure 5.19.B). We also checked for MAVS expression, transfected cells have a remarkable increase in TRIM25 transfected cells, with a significant expression using 500ng of TRIM. In parallel, quantification of TRIF in cells transfected with TRIM25 showed a significant increase in the TRIF expression compared to negative control. Consistent with the expression of previous markers, the expression levels of IFN-β showed a significant increase in TRIM25 transfected cells.

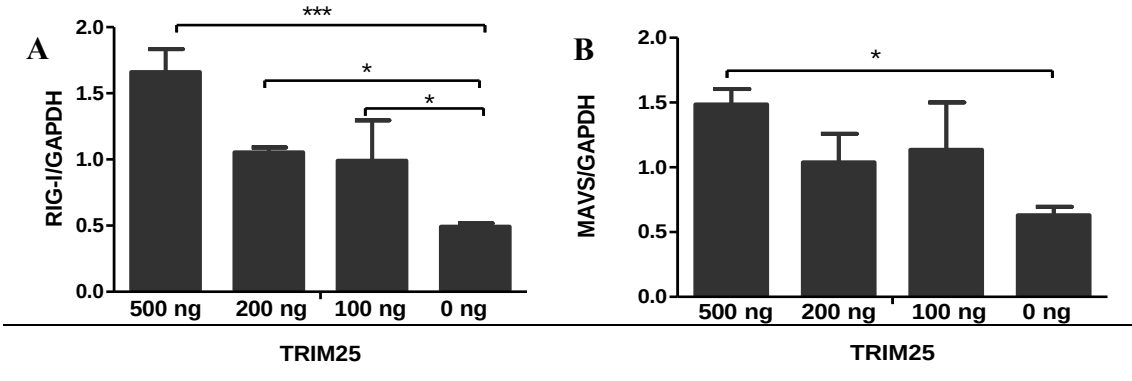

C **D**

Figure 5.19. TRIM25 overexpression effect on the IFN pathway Cells were transfected with increasing amounts of TRIM25 (500, 200, 100 or 0 ng). After 48 hours, cells were infected with HCV (0.1 MOI). 48 hours post infection, cells were lysed and RNA was extracted, RNA was then analyzed for the expression of (A) RIG-I. (B) MAVS. (C) TRIF and (D) IFN-β. Data are mean values ± SD. *p<0.05,**p<0.01,***p<0.001.

5.5. Discussion

Type I IFNs fighting viral infections by regulating a large number of cellular molecules such as ISGs. Although several ISGs are well characterized, not all have been fully investigated in terms of their roles in antiviral mechanisms (Helbig, Lau et al. 2005, Jiang, Guo et al. 2008, Schoggins and Rice 2011, Schoggins, Wilson et al. 2011) . It is possible that multiple ISGs involved in the interference with different stages of the viral replication cycle (Schoggins, Wilson et al. 2011, Metz, Reuter et al. 2013). Therefore, characterization of individual ISGs and their potential roles are important to understand their involvement in pathogenesis and IFNs antiviral mechanism.

Here we chose to focus on TRIM family protein, the initial findings from the gene array revealed that HCV infection regulates a panel of TRIM genes in the in vitro model, suggesting that TRIMs might act as an anti-viral molecule. Interestingly, the upregulated TRIM genes including (TRIM5, 14 and 25), were identified before to have antiviral activity against several viruses such as HIV and SeV (Neamati 2001, Pertel, Hausmann et al. 2011, Westbrook and Dusheiko 2014, Lascano, Uchil et al. 2016).

While we believe that TRIMs are likely played different roles in controlling viral infections, their role in HCV infection is not yet clear. Using our array data along with literature search, we could identify the genes of interest for further investigations.

We considered two approaches to identify TRIMs with anti-HCV activity, the first determination of the induction profile of TRIMs using interferon, a second determination of TRIM regulation upon HCV infection in cell culture.

We analyzed the induction kinetics of selected TRIMs, TRIM 7, 9, 21 and 40 have rapid induction kinetics, while TRIM5 and 14 have intermediate kinetics peaking at 24 hours, and TRIM 1 have slow kinetics and reached a peak at 96 hours post IFN treatment. In the course of HCV infection, the kinetic peaks of TRIM5, 7, 14 and 40 overlap with the expression pattern post IFN treatment. Notably, TRIM21, 22 and 40 have a high expression level, one possibility is that HCV tends to establish a mechanism to downregulate them. Because hepatoma cell lines are transformed cells, we checked for TRIMs expression in PHHs, our analysis noted upregulation of 14 TRIMs (TRIM5,7,9,11,13,14,15,21,25,33,34,35,40 and 55) at different time points post IFN treatment. Considering that PHHs are poorly infectible, and the quantification of the viral genome was not clearly determined, it is not obvious how HCV regulates TRIMs expression in this model.

Among overlapped TRIMs from different experiments, we selected TRIM5, 9, 14 and 25 to further study their role in HCV infection.

Our data showed that TRIM5 is one of the most highly induced Type 1 IFN TRIMs in PHHs and hepatoma cells. Several studies revealed that TRIM5 restricts various retroviral infections, such as HIV and SeV (James, Keeble et al. 2007, Pertel, Hausmann et al. 2011, Lascano, Uchil et al. 2016). However, the antiviral activity of TRIM5 is well studied, no information are available on its role in HCV infection. Therefore, we explored the TRIM5 role in HCV infection in two parts: first, we used an overexpression approach to determine the effect on HCV replication cycle in both replicon and HCVcc system, next we continued to determine the efficiency of TRIM5 activation on multiple molecules in the IFN signaling pathway.

We showed that TRIM5 overexpression significantly decreased HCV replication in both a replicon and infection (HCVcc) based tests. Thus, we suggest that TRIM5 restricts multiple steps

in the HCV replication cycle, we confirmed that TRIM5 inhibits replication when TRIM5 transfected into replicon cells in a dose-dependent manner. Further infection experiment revealed a significant decrease in intracellular HCV genome RNA level in TRIM5 transfected cells, in addition, our TCID50 assay showed that secreted viral particles were significantly diminished when TRIM5 was expressed in the cells. Comment from other literature… These observations reflect, the anti-viral activity of TRIM5 in HCV infection. Yet, we could not rule out the effect on the early (e.g: entry) and the late (e.g: assembly) steps of HCV infection cycle.

Before we analyze the activation of ISRE, IFN-β, and NF-κB reporter promotes by several TRIMs, we studied the regulation kinetic pattern in the presence of either IFN-alpha or HCV. We demonstrated that the ISRE, IFN-β, and NF-κB promoters were activated upon IFN treatment, and peaked the maximum at 6 hours post-treatment, and then dropped at 24 hours followed by gaining increase at 96 hours post treatment. In contrast, during HCV infection, IFN-β promoter activation dropped, these results also suggest that the presence of HCV inhibited the activation of the IFN-β promoter in our experiments. Same is true for NF-κB promoter activation, we have observed a gradual decline in the activation after HCV infection. While, ISRE promoter activation increased and reached the maximum at 24 hours post infection, then dropped in the later time points indicating that HCV might establish a defense mechanism to overcome the immune mechanisms.

Subsequent to the identification of TRIM5 as anti-HCV molecule, we wanted to check its ability to activate IFN-β promoter, NF-κB responsive promoter, and ISRE in reporter assays. In the presence of HCV infection, overexpression of TRIM5 enhanced the induction of ISRE and NF-κB by approximately 1 fold, while IFN-β was induced by 2 folds. When we used same conditions to check the induction in the absence of HCV infection, we found that the induction of NF-κB and ISRE is the same in both presence and absence of HCV, whereas IFN-β was higher in the absence of HCV infection.

To understand whether TRIM5 regulates the innate immune responses, we investigated several marker molecules in the antiviral innate immunity. TRIM5 upregulates the RIG-I viral recognition receptor, and the downstream molecule MAVS, moreover TRIM5 transfection upregulates TRIF adaptor molecule and the IFN-β. Taken together, these observations suggest

that TRIM5 positively regulates IFN signaling pathway (Rajsbaum, Stoye et al. 2008, Rajsbaum, Albrecht et al. 2012, Ovsyannikova, Haralambieva et al. 2013, Zhu, Liu et al. 2016).

As mentioned earlier TRIM9 has two isoforms TRIM9s and TRIM9I, the short isoform poses anti-viral activity and enhances the expression of ISGs (Qin, Liu et al. 2016). Therefore, further series of experiments aimed to identify the role of TRIM9 in HCV infection were performed. In HCV replicon cell line, overexpression of TRIM9 led to a significant reduction in the virus replication as measured by the reporter assay. Then we further sought to determine the effect of TRIM9 on HCV infection using the HCVcc based system. As we expected TRIM9 overexpression resulted in a significant decrease in HCV infection, this decrease was in both, the intracellular HCV genomic RNA level and the extracellular virus secretion.

First reports about TRIM9 identified TRIM9 as a brain-specific molecule (Tanji, Kamitani et al. 2010), then further characterization showed that it is widely expressed in several tissues in the human body. A previous study indicated that TRIM9 expression is reduced in damaged brains of Parkinson's disease and Lewy body dementia patients (Tanji, Kamitani et al. 2010, Yang, Li et al. 2014), and this decrease is associated with a dramatic increase of NF-κB . The study also revealed that, TRIM9 act as a negative regulator of NF-κB in brain cells via targeting b-TrCP SCF complex which regulates NF-κB (Shi, Cho et al. 2014). Another study showed that overexpression of TRIM9 hindered virus infection in particular VSV, this could be attributed to the enhancements of IRF3 and IFN-β signaling (Qin, Liu et al. 2016). Thus, we determined the regulatory mechanism of TRIM9 on the innate immune signaling during HCV infection in vitro. In our HCVcc infection system, when TRIM9 was overexpressed in the cells, we were able to see enhancements in both IFN-β and ISRE promotors' activation, whereas NF-κB promotor stayed unchanged, this partially agrees with the previous study which indicated the negative regulatory role of TRIM9 on NF-κB. Nevertheless, the analysis of the TRIM9 effect on ISRE, IFN-β and NF-κB promoters in the absence of HCV infection, showed an overlapped pattern with the previously determined in the presence of HCV infection. The second set of innate molecular markers including RIG-I, MAVS, TRIF and finally IFN-β were analyzed. The RIG-I dsRNA molecular receptor and IFN-β were up-regulated in TRIM9 transfected cells in a dose-dependent manner. Independent of TRIM9 transfection does, TRIF adaptor molecule expression was upregulated in transfected cells. Unlike, RIG-I and IFN-β, MAVS expression was reversely

correlated with TRIM9 transfection dose. We could argue that the overall upregulation of different molecules attributed in the IFN-β signaling pathway, is one possible explanation for inhibiting HCV infection in our study.

Similar to other selected TRIMs, TRIM14 was highly expressed upon IFN-alpha treatment in HCV replicon cells, Huh7 cells, and PHHs. Therefore, we first analyzed the effect of TRM14 overexpression on HCV infection cycle. In line with another study, TRIM14 overexpression impaired HCV virus replication and infection. Our results based on both HCV replicon and HCVcc systems. This is similar to the observations made before for several ISGs including TRIM14, in which an overexpression approach was performed for individual ISGs, in that TRIM14 showed an inhibition of HCV replication (Jiang, Guo et al. 2008, Metz, Reuter et al. 2013). Nevertheless, the mechanism of TRIM14 associated with HCV replication reduction is still not determined. To determine whether TRIM14 mediates IFN-β pathway activation, we analyzed the ISRE, IFN-β, and NF-κB promoter activation during TRIM14 overexpression. Thus, while TRIM14 led to an enhancement of both IFN-β and NF-κB promoters' activities, the ISRE promoter activity remained unchanged. Consequently, we wanted to test what influence TRIM14 overexpression have on the RIG-I, MAVS, TRIF and IFN-β expression level in relation to HCV infection. Overexpression of TRIM14, increased mRNA expression levels of RIG-I, MAVS, TRIF and IFN-β demonstrating that TRIM14 triggers the IFN antiviral response. Together, this proposes an explanation of the decline of HCV replication in our study.

As stated earlier, TRIM25 is able to cooperate with the CARD domains of RIG-I which facilitate RIG-I activation of MAVS. This interaction then facilitates downstream signaling and the production of IFNβ (Gack, Shin et al. 2007, Castanier, Zemirli et al. 2012, Rajsbaum, Albrecht et al. 2012). Our results indicated that TRIM25 is induced upon IFN treatment or HCV viral infection. Thus, in order to determine the role of TRIM25 in HCV infection, we performed an overexpression experiment where we overexpressed TRIM25 in both HCV replicons cells and in HCV infection settings. Thus, TRIM25 led to a reduction of HCV replication and infection. This was accompanied by the activation of several promoter activations such as ISRE, IFN-β, and NF-κB, which suggests its anti-viral role against HCV infection. Additionally, we tested the effect of TRIM25 overexpression on several molecules in the IFN signaling pathway. All markers including HCV recognition receptor RIG-I, adaptor molecule TRIF, MAVS, and IFN-β showed a

significant increase in the expression level upon TRIM25 transfection. Collectively, this activation is required for elimination of HCV infection, agrees with previous findings which revealed that TRIM25 possess anti-viral activity which attributed to the activation of the IFN-β signaling pathway.

5.6. Summary

TRIM family members have been implicated in several functions such as cell differentiation, apoptosis, neurogenesis, muscular physiology and innate immune responses. Multiple TRIM proteins play a role in restricting viral infection such as retroviruses infection, by inducing IFN response, regulate RPRs and/or interacting directly with viral proteins. Thus, we sought to study the role of TRIMs in HCV infection. Screening of TRIMs revealed that HCV infection regulates a panel of TRIM genes in the in *vitro* model, suggesting that TRIMs might act as a anti-viral molecule. Interestingly, the upregulated TRIM genes including (TRIM5, 14 and 25), were identified before to have antiviral activity against several viruses such as HIV and SeV. While we believe that TRIMs are likely played different roles in controlling viral infections, their role in HCV infection is not yet clear. We could identify the genes of interest for further investigations. Therefore, we hypothesized that those TRIMs play anti-HCV activities. In our study, we choose to focus on (TRIM5, TRIM9, TRIM14 and TRIM25).

We indicated that TRIM5 overexpression significantly decreased HCV replication in both a replicon and infection (HCVcc) based system. Thus, we suggest that TRIM5 restricts multiple steps in the HCV replication cycle, we confirmed that TRIM5 inhibits replication when TRIM5 transfected into replicon cells in a dose-dependent manner. Further infection experiment revealed a significant decrease in intracellular HCV genome RNA level in TRIM5 transfected cells, in addition, our TCID50 assay showed that secreted viral particles were significantly diminished when TRIM5 was expressed in the cells. These observations reflect the anti-viral activity of TRIM5 in HCV infection. Yet, we could not rule out the effect on the early (e.g: entry) and the late (e.g: assembly) steps of HCV infection cycle. In this model, TRIM5 upregulates the RIG-I viral recognition receptor and the downstream molecule MAVS, moreover TRIM5 transfection upregulates TRIF adaptor molecule and the IFN-β. Taken together, these observations suggest that TRIM5 positively regulates IFN signaling pathway.

For TRIM9, overexpression led to a significant reduction in the virus replication as measured by the reporter assay. Further analysis showed that the effect of TRIM9 extends to the whole virus replication system as illustrated by HCVcc based system. A former study showed that overexpression of TRIM9 hindered virus infection in particular VSV, this could be attributed to the enhancements of IRF3 and IFN-β signaling. Our analysis of the innate immune regulatory role of TRIM9 on the revealed enhancements in both IFN-β and ISRE promotors' activation, whereas NF-κB promotor stayed unchanged, this partially agrees with the previous study which indicated the negative regulatory role of TRIM9 on NF-κB. Nevertheless, the analysis of the TRIM9 effect on ISRE, IFN-β and NF-κB promoters in the absence of HCV infection, showed an overlapped pattern with the previously determined in the presence of HCV infection.

TRIM14 was highly expressed upon IFN-α treatment in HCV replicon cells, Huh7 cells, and PHHs. In our study, TRIM14 overexpression impaired HCV virus replication and infection. This is similar to the observations made before for several ISGs including TRIM14, in that TRIM14 showed an inhibition of HCV replication Nevertheless, the mechanism of TRIM14 associated with HCV replication reduction is still not determined. To determine whether TRIM14 mediates IFN-β pathway activation, we analyzed the ISRE, IFN-β, and NF-κB promoter activation during TRIM14 overexpression. Thus, while TRIM14 led to an enhancement of both IFN-β and NF-κB promoters' activities. Overexpression of TRIM14 increased expression levels of RIG-I, MAVS, TRIF and IFN-β. Together, this demonstrates that TRIM14 triggers the IFN antiviral response leading to the decline of HCV replication.

TRIM25 is able to cooperate with the CARD domains of RIG-I which facilitate RIG-I activation of MAVS. Thus, overexpression of TRIM25 in both HCV replicons cells and in HCV infection settings. This was accompanied by the activation of several promoter activations such as ISRE, IFN-β, and NF-κB, which suggests its anti-viral role against HCV infection. Additionally, TRIM25 transfection enhances the expression levels of the RIG-I receptor, adaptor molecule TRIF, MAVS, and IFN-β. Collectively, this activation is required for elimination of HCV infection, agrees with previous findings which revealed that TRIM25 possess anti-viral activity which attributed to the activation of the IFN-β signaling pathway.

6. Chapter VI References

Abergel, C. (2013). "Molecular replacement: tricks and treats." Acta Crystallogr D Biol Crystallogr **69**(Pt 11): 2167-2173.

Afdhal, N., K. R. Reddy, D. R. Nelson, E. Lawitz, S. C. Gordon, E. Schiff, R. Nahass, R. Ghalib, N. Gitlin, R. Herring, J. Lalezari, Z. H. Younes, P. J. Pockros, A. M. Di Bisceglie, S. Arora, G. M. Subramanian, Y. Zhu, H. Dvory-Sobol, J. C. Yang, P. S. Pang, W. T. Symonds, J. G. McHutchison, A. J. Muir, M. Sulkowski, P. Kwo and I. O. N. Investigators (2014). "Ledipasvir and sofosbuvir for previously treated HCV genotype 1 infection." N Engl J Med **370**(16): 1483-1493.

Alloush, J. and N. Weisleder (2013). "TRIM proteins in therapeutic membrane repair of muscular dystrophy." JAMA Neurol **70**(7): 928-931.

Anderson, A. C. (2003). "The Process of Structure-Based Drug Design." Chemistry & Biology **10**(9): 787-797.

Ansaldi, F., A. Orsi, L. Sticchi, B. Bruzzone and G. Icardi (2014). "Hepatitis C virus in the new era: perspectives in epidemiology, prevention, diagnostics and predictors of response to therapy." World J Gastroenterol **20**(29): 9633-9652.

Asselah, T., S. De Muynck, P. Broet, J. Masliah-Planchon, M. Blanluet, I. Bieche, M. Lapalus, M. Martinot-Peignoux, O. Lada, E. Estrabaud, Q. Zhang, A. El Ray, D. Vidaud, M. P. Ripault, N. Boyer, P. Bedossa, D. Valla, M. Vidaud and P. Marcellin (2012). "IL28B polymorphism is associated with treatment response in patients with genotype 4 chronic hepatitis C." J Hepatol **56**(3): 527-532.

Asselah, T. and P. Marcellin (2015). "Optimal IFN-free therapy in treatment-naive patients with HCV genotype 1 infection." Liver Int **35 Suppl 1**: 56-64.

Balagopal, A., D. L. Thomas and C. L. Thio (2010). "IL28B and the control of hepatitis C virus infection." Gastroenterology **139**(6): 1865-1876.

Barreiro, P., J. A. Pineda, N. Rallon, S. Naggie, L. Martin-Carbonero, K. Neukam, A. Rivero, J. M. Benito, A. Caruz, E. Vispo, A. Camacho, J. Medrano, J. McHutchison and V. Soriano (2011). "Influence of interleukin-28B single-nucleotide polymorphisms on progression to liver cirrhosis in human immunodeficiency virus-hepatitis C virus-coinfected patients receiving antiretroviral therapy." J Infect Dis **203**(11): 1629-1636.

Bartenschlager, R., A. Kaul and S. Sparacio (2003). "Replication of the hepatitis C virus in cell culture." Antiviral Research **60**(2): 91-102.

Bartenschlager, R., V. Lohmann and F. Penin (2013). "The molecular and structural basis of advanced antiviral therapy for hepatitis C virus infection." Nat Rev Microbiol **11**(7): 482-496.

Bartenschlager, R., F. Penin, V. Lohmann and P. Andre (2011). "Assembly of infectious hepatitis C virus particles." Trends Microbiol **19**(2): 95-103.

Barth, H. (2015). "Hepatitis C virus: Is it time to say goodbye yet? Perspectives and challenges for the next decade." World J Hepatol **7**(5): 725-737.

Bartosch, B., A. Vitelli, C. Granier, C. Goujon, J. Dubuisson, S. Pascale, E. Scarselli, R. Cortese, A. Nicosia and F. L. Cosset (2003). "Cell entry of hepatitis C virus requires a set of co-receptors

that include the CD81 tetraspanin and the SR-B1 scavenger receptor." J Biol Chem **278**(43): 41624-41630.

Beltra, J. C. and H. Decaluwe (2016). "Cytokines and persistent viral infections." Cytokine.

Binder, J., S. Tetangco, M. Weinshank, K. Maegley, L. Lingardo, W. Diehl, R. Love, A. K. Patick and G. J. Smith, 3rd (2011). "Development of hepatitis C virus chimeric replicons for identifying broad spectrum NS3 protease inhibitors." Antiviral Res **91**(2): 102-111.

Biswal, B. K., M. M. Cherney, M. Wang, L. Chan, C. G. Yannopoulos, D. Bilimoria, O. Nicolas, J. Bedard and M. N. James (2005). "Crystal structures of the RNA-dependent RNA polymerase genotype 2a of hepatitis C virus reveal two conformations and suggest mechanisms of inhibition by non-nucleoside inhibitors." J Biol Chem **280**(18): 18202-18210.

Boltjes, A., D. Movita, A. Boonstra and A. M. Woltman (2014). "The role of Kupffer cells in hepatitis B and hepatitis C virus infections." J Hepatol **61**(3): 660-671.

Boudinot, P., L. M. van der Aa, L. Jouneau, L. Du Pasquier, P. Pontarotti, V. Briolat, A. Benmansour and J. P. Levraud (2011). "Origin and evolution of TRIM proteins: new insights from the complete TRIM repertoire of zebrafish and pufferfish." PLoS One **6**(7): e22022.

Bowen, D. G. and C. M. Walker (2005). "Adaptive immune responses in acute and chronic hepatitis C virus infection." Nature **436**(7053): 946-952.

Bunchorntavakul, C. and K. R. Reddy (2015). "Review article: the efficacy and safety of daclatasvir in the treatment of chronic hepatitis C virus infection." Aliment Pharmacol Ther **42**(3): 258-272.

Cai, C., H. Masumiya, N. Weisleder, N. Matsuda, M. Nishi, M. Hwang, J. K. Ko, P. Lin, A. Thornton, X. Zhao, Z. Pan, S. Komazaki, M. Brotto, H. Takeshima and J. Ma (2009). "MG53 nucleates assembly of cell membrane repair machinery." Nat Cell Biol **11**(1): 56-64.

Caillet-Saguy, C., P. C. Simister and S. Bressanelli (2011). "An objective assessment of conformational variability in complexes of hepatitis C virus polymerase with non-nucleoside inhibitors." J Mol Biol **414**(3): 370-384.

Calistri, A., D. Munegato, I. Carli, C. Parolin and G. Palu (2014). "The ubiquitin-conjugating system: multiple roles in viral replication and infection." Cells **3**(2): 386-417.

Carruthers, C. W., Jr., C. Gerdts, M. D. Johnson and P. Webb (2013). "A microfluidic, high throughput protein crystal growth method for microgravity." PLoS One **8**(11): e82298.

Castanier, C., N. Zemirli, A. Portier, D. Garcin, N. Bidere, A. Vazquez and D. Arnoult (2012). "MAVS ubiquitination by the E3 ligase TRIM25 and degradation by the proteasome is involved in type I interferon production after activation of the antiviral RIG-I-like receptors." BMC Biol **10**: 44.

Caterina Berti, S. M., Andrea Ballabio, Alexandre Reymond1, Germana Meroni (2002). "TRIM9 is specifically expressed in the embryonic and adult nervous system." Mechanisms of Development **113** 4.

Chan, E., G. J. Towers and W. Qasim (2014). "Gene therapy strategies to exploit TRIM derived restriction factors against HIV-1." Viruses **6**(1): 243-263.

Chayama, K. and C. N. Hayes (2015). "HCV Drug Resistance Challenges in Japan: The Role of Pre-Existing Variants and Emerging Resistant Strains in Direct Acting Antiviral Therapy." Viruses **7**(10): 5328-5342.

Chayen, N. E. (2004). "Turning protein crystallisation from an art into a science." Curr Opin Struct Biol **14**(5): 577-583.

Chen, C. H. and M. L. Yu (2010). "Evolution of interferon-based therapy for chronic hepatitis C." Hepat Res Treat **2010**: 140953.

Chen, Y., S. Wang, Z. Yi, H. Tian, R. Aliyari, Y. Li, G. Chen, P. Liu, J. Zhong, X. Chen, P. Du, L. Su, F. X. Qin, H. Deng and G. Cheng (2014). "Interferon-inducible cholesterol-25-hydroxylase inhibits hepatitis C virus replication via distinct mechanisms." Sci Rep **4**: 7242.

Choo, Y. S. and Z. Zhang (2009). "Detection of protein ubiquitination." J Vis Exp(30).

Choudhury, N. R., J. S. Nowak, J. Zuo, J. Rappsilber, S. H. Spoel and G. Michlewski (2014). "Trim25 Is an RNA-Specific Activator of Lin28a/TuT4-Mediated Uridylation." Cell Rep **9**(4): 1265-1272.

Chung, R. T., M. Gale, Jr., S. J. Polyak, S. M. Lemon, T. J. Liang and J. H. Hoofnagle (2008). "Mechanisms of action of interferon and ribavirin in chronic hepatitis C: Summary of a workshop." Hepatology **47**(1): 306-320.

Cormier, E. G., F. Tsamis, F. Kajumo, R. J. Durso, J. P. Gardner and T. Dragic (2004). "CD81 is an entry coreceptor for hepatitis C virus." Proceedings of the National Academy of Sciences **101**(19): 7270-7274.

Crotty, S., C. E. Cameron and R. Andino (2001). "RNA virus error catastrophe: direct molecular test by using ribavirin." Proc Natl Acad Sci U S A **98**(12): 6895-6900.

Curry, S., P. Qiu and X. Tong (2008). "Analysis of HCV resistance mutations during combination therapy with protease inhibitor boceprevir and PEG-IFN alpha-2b using TaqMan mismatch amplification mutation assay." J Virol Methods **153**(2): 156-162.

de Silva, S. and L. Wu (2011). "TRIM5 acts as more than a retroviral restriction factor." Viruses **3**(7): 1204-1209.

Degasperi, E. and A. Aghemo (2014). "Sofosbuvir for the treatment of chronic hepatitis C: between current evidence and future perspectives." Hepat Med **6**: 25-33.

DiFrancesco, J. M. and J. M. Olson (2015). "The economics of microgravity research." npj Microgravity **1**: 15001.

DiMattia, M., L. Govindasamy, H. C. Levy, B. Gurda-Whitaker, A. Kalina, E. Kohlbrenner, J. A. Chiorini, R. McKenna, N. Muzyczka, S. Zolotukhin and M. Agbandje-McKenna (2005). "Production, purification, crystallization and preliminary X-ray structural studies of adeno-associated virus serotype 5." Acta Crystallogr Sect F Struct Biol Cryst Commun **61**(Pt 10): 917-921.

Donaldson, E. F., P. R. Harrington, J. J. O'Rear and L. K. Naeger (2015). "Clinical evidence and bioinformatics characterization of potential hepatitis C virus resistance pathways for sofosbuvir." Hepatology **61**(1): 56-65.

Dorner, M., J. A. Horwitz, B. M. Donovan, R. N. Labitt, W. C. Budell, T. Friling, A. Vogt, M. T. Catanese, T. Satoh, T. Kawai, S. Akira, M. Law, C. M. Rice and A. Ploss (2013). "Completion of the entire hepatitis C virus life cycle in genetically humanized mice." Nature **501**(7466): 237-241.

Du Pasquier, L. (2009). "Fish 'n' TRIMs." J Biol **8**(5): 50.

Eksteen, B. (2011). "Infections and the liver." Dig Dis **29**(2): 184-190.

Elabd, S., G. Meroni and C. Blattner (2016). "TRIMming p53's anticancer activity." Oncogene.

Elbaz, T., M. El-Kassas and G. Esmat (2015). "New era for management of chronic hepatitis C virus using direct antiviral agents: A review." J Adv Res **6**(3): 301-310.

Elhefnawi, M., M. ElGamacy and M. Fares (2012). "Multiple virtual screening approaches for finding new hepatitis C virus RNA-dependent RNA polymerase inhibitors: structure-based screens and molecular dynamics for the pursue of new poly pharmacological inhibitors." BMC Bioinformatics **13 Suppl 17**: S5.

Falkowska, E., R. J. Durso, J. P. Gardner, E. G. Cormier, R. A. Arrigale, R. N. Ogawa, G. P. Donovan, P. J. Maddon, W. C. Olson and T. Dragic (2006). "L-SIGN (CD209L) isoforms differently mediate trans-infection of hepatoma cells by hepatitis C virus pseudoparticles." J Gen Virol **87**(Pt 9): 2571-2576.

Ferenci, P. (2004). "Predicting the therapeutic response in patients with chronic hepatitis C: the role of viral kinetic studies." J Antimicrob Chemother **53**(1): 15-18.

Firdaus, R., A. Biswas, K. Saha, A. Mukherjee, F. Pal, S. Chaudhuri, A. Chandra, A. Konar and P. C. Sadhukhan (2014). "Modulation of TLR 3, 7 and 8 expressions in HCV genotype 3 infected individuals: potential correlations of pathogenesis and spontaneous clearance." Biomed Res Int **2014**: 491064.

Fournier, C., G. Duverlie and S. Castelain (2013). "Are trans-complementation systems suitable for hepatitis C virus life cycle studies?" J Viral Hepat **20**(4): 225-233.

Friebe, P. and R. Bartenschlager (2009). "Role of RNA structures in genome terminal sequences of the hepatitis C virus for replication and assembly." J Virol **83**(22): 11989-11995.

Gack, M. U., Y. C. Shin, C. H. Joo, T. Urano, C. Liang, L. Sun, O. Takeuchi, S. Akira, Z. Chen, S. Inoue and J. U. Jung (2007). "TRIM25 RING-finger E3 ubiquitin ligase is essential for RIG-I-mediated antiviral activity." Nature **446**(7138): 916-920.

Gale, M., Jr. and E. M. Foy (2005). "Evasion of intracellular host defence by hepatitis C virus." Nature **436**(7053): 939-945.

Gaudieri, S., A. Rauch, K. Pfafferott, E. Barnes, W. Cheng, G. McCaughan, N. Shackel, G. P. Jeffrey, L. Mollison, R. Baker, H. Furrer, H. F. Gunthard, E. Freitas, I. Humphreys, P. Klenerman, S. Mallal, I. James, S. Roberts, D. Nolan and M. Lucas (2009). "Hepatitis C virus drug resistance and immune-driven adaptations: relevance to new antiviral therapy." Hepatology **49**(4): 1069-1082.

Gerdts, C. J., M. Elliott, S. Lovell, M. B. Mixon, A. J. Napuli, B. L. Staker, P. Nollert and L. Stewart (2008). "The plug-based nanovolume Microcapillary Protein Crystallization System (MPCS)." Acta Crystallogr D Biol Crystallogr **64**(Pt 11): 1116-1122.

Gerdts, C. J., G. L. Stahl, A. Napuli, B. Staker, J. Abendroth, T. E. Edwards, P. Myler, W. Van Voorhis, P. Nollert and L. J. Stewart (2010). "Nanovolume optimization of protein crystal growth using the microcapillary protein crystallization system." J Appl Crystallogr **43**(Pt 5): 1078-1083.

Giege, R. (2013). "A historical perspective on protein crystallization from 1840 to the present day." FEBS J **280**(24): 6456-6497.

Gokhale, N. S., C. Vazquez and S. M. Horner (2014). "Hepatitis C Virus. Strategies to Evade Antiviral Responses." Future Virol **9**(12): 1061-1075.

Guglietta, S., A. R. Garbuglia, L. Salichos, L. Ruggeri, A. Folgori, M. P. Perrone, C. Camperio, V. Mellace, G. Maio, P. Maio, M. R. Capobianchi, E. Spada, N. Gargano, C. Scotta, E. Piccolella and P. Del Porto (2009). "Impact of viral selected mutations on T cell mediated immunity in chronically evolving and self limiting acute HCV infection." Virology **386**(2): 398-406.

Habjan, M., I. Andersson, J. Klingstrom, M. Schumann, A. Martin, P. Zimmermann, V. Wagner, A. Pichlmair, U. Schneider, E. Muhlberger, A. Mirazimi and F. Weber (2008). "Processing of genome 5' termini as a strategy of negative-strand RNA viruses to avoid RIG-I-dependent interferon induction." PLoS One **3**(4): e2032.

Halfon, P. and S. Locarnini (2011). "Hepatitis C virus resistance to protease inhibitors." J Hepatol **55**(1): 192-206.

Hamamoto, I., Y. Nishimura, T. Okamoto, H. Aizaki, M. Liu, Y. Mori, T. Abe, T. Suzuki, M. M. Lai, T. Miyamura, K. Moriishi and Y. Matsuura (2005). "Human VAP-B is involved in hepatitis C virus replication through interaction with NS5A and NS5B." J Virol **79**(21): 13473-13482.

Han, R., R. Wang, Q. Zhao, Y. Han, S. Zong, S. Miao, W. Song and L. Wang (2016). "Trim69 regulates zebrafish brain development by ap-1 pathway." Sci Rep **6**: 24034.

Han, R., Q. Zhao, S. Zong, S. Miao, W. Song and L. Wang (2016). "A novel TRIM family member, trim69, regulates zebrafish development through p53-mediated apoptosis." Mol Reprod Dev.

Hardy, R. W., J. Marcotrigiano, K. J. Blight, J. E. Majors and C. M. Rice (2003). "Hepatitis C Virus RNA Synthesis in a Cell-Free System Isolated from Replicon-Containing Hepatoma Cells." Journal of Virology **77**(3): 2029-2037.

Hatakeyama, S. (2011). "TRIM proteins and cancer." Nat Rev Cancer **11**(11): 792-804.

Heim, M. H. (2012). "Interferons and hepatitis C virus." Swiss Med Wkly **142**: w13586.

Heim, M. H. and R. Thimme (2014). "Innate and adaptive immune responses in HCV infections." J Hepatol **61**(1 Suppl): S14-25.

Helbig, K. J., D. T. Lau, L. Semendric, H. A. Harley and M. R. Beard (2005). "Analysis of ISG expression in chronic hepatitis C identifies viperin as a potential antiviral effector." Hepatology **42**(3): 702-710.

Hofmann, W. P. and S. Zeuzem (2011). "A new standard of care for the treatment of chronic HCV infection." Nat Rev Gastroenterol Hepatol **8**(5): 257-264.

Huang, L., J. Hwang, S. D. Sharma, M. R. Hargittai, Y. Chen, J. J. Arnold, K. D. Raney and C. E. Cameron (2005). "Hepatitis C virus nonstructural protein 5A (NS5A) is an RNA-binding protein." J Biol Chem **280**(43): 36417-36428.

Huang, L., E. V. Sineva, M. R. Hargittai, S. D. Sharma, M. Suthar, K. D. Raney and C. E. Cameron (2004). "Purification and characterization of hepatitis C virus non-structural protein 5A expressed in Escherichia coli." Protein Expr Purif **37**(1): 144-153.

Hwang, J., L. Huang, D. G. Cordek, R. Vaughan, S. L. Reynolds, G. Kihara, K. D. Raney, C. C. Kao and C. E. Cameron (2010). "Hepatitis C virus nonstructural protein 5A: biochemical characterization of a novel structural class of RNA-binding proteins." J Virol **84**(24): 12480-12491.

Ignatius Irudayam, J., D. Contreras, L. Spurka, A. Subramanian, J. Allen, S. Ren, V. Kanagavel, Q. Nguyen, A. Ramaiah, K. Ramamoorthy, S. W. French, A. S. Klein, V. Funari and V. Arumugaswami (2015). "Characterization of type I interferon pathway during hepatic differentiation of human pluripotent stem cells and hepatitis C virus infection." Stem Cell Res **15**(2): 354-364.

Imhof, I. and P. Simmonds (2010). "Development of an intergenotypic hepatitis C virus (HCV) cell culture method to assess antiviral susceptibilities and resistance development of HCV NS3 protease genes from HCV genotypes 1 to 6." J Virol **84**(9): 4597-4610.

Issur, M. and M. Gotte (2014). "Resistance patterns associated with HCV NS5A inhibitors provide limited insight into drug binding." Viruses **6**(11): 4227-4241.

Ito, K., K. Higami, N. Masaki, M. Sugiyama, M. Mukaide, H. Saito, Y. Aoki, Y. Sato, M. Imamura, K. Murata, H. Nomura, S. Hige, H. Adachi, K. Hino, H. Yatsuhashi, E. Orito, S. Kani, Y. Tanaka and M. Mizokami (2011). "The rs8099917 polymorphism, when determined by a suitable genotyping method, is a better predictor for response to pegylated alpha interferon/ribavirin therapy in Japanese patients than other single nucleotide polymorphisms associated with interleukin-28B." J Clin Microbiol **49**(5): 1853-1860.

Izquierdo, L., F. Helle, C. Francois, S. Castelain, G. Duverlie and E. Brochot (2014). "Simeprevir for the treatment of hepatitis C virus infection." Pharmgenomics Pers Med **7**: 241-249.

James, L. C., A. H. Keeble, Z. Khan, D. A. Rhodes and J. Trowsdale (2007). "Structural basis for PRYSPRY-mediated tripartite motif (TRIM) protein function." Proc Natl Acad Sci U S A **104**(15): 6200-6205.

Janardhan, S. V. and N. S. Reau (2015). "Should NS5A inhibitors serve as the scaffold for all-oral anti-HCV combination therapies?" Hepat Med **7**: 11-20.

Jang, J. Y. and R. T. Chung (2011). "Chronic hepatitis C." Gut Liver **5**(2): 117-132.

Jiang, D., H. Guo, C. Xu, J. Chang, B. Gu, L. Wang, T. M. Block and J. T. Guo (2008). "Identification of three interferon-inducible cellular enzymes that inhibit the replication of hepatitis C virus." J Virol **82**(4): 1665-1678.

Jilg, N., W. Lin, J. Hong, E. A. Schaefer, D. Wolski, J. Meixong, K. Goto, C. Brisac, P. Chusri, D. N. Fusco, S. Chevaliez, J. Luther, K. Kumthip, T. J. Urban, L. F. Peng, G. M. Lauer and R. T.

Chung (2014). "Kinetic differences in the induction of interferon stimulated genes by interferon-alpha and interleukin 28B are altered by infection with hepatitis C virus." Hepatology **59**(4): 1250-1261.
Kanda, T., R. Steele, R. Ray and R. B. Ray (2007). "Hepatitis C virus infection induces the beta interferon signaling pathway in immortalized human hepatocytes." J Virol **81**(22): 12375-12381.
Karam, P., M. H. Powdrill, H. W. Liu, C. Vasquez, W. Mah, J. Bernatchez, M. Gotte and G. Cosa (2014). "Dynamics of hepatitis C virus (HCV) RNA-dependent RNA polymerase NS5B in complex with RNA." J Biol Chem **289**(20): 14399-14411.
Katze, M. G., Y. He and M. Gale, Jr. (2002). "Viruses and interferon: a fight for supremacy." Nat Rev Immunol **2**(9): 675-687.
Kayali, Z. and W. N. Schmidt (2014). "Finally sofosbuvir: an oral anti-HCV drug with wide performance capability." Pharmgenomics Pers Med **7**: 387-398.
Ke, A. and J. A. Doudna (2004). "Crystallization of RNA and RNA-protein complexes." Methods **34**(3): 408-414.
Khan, A. G., J. Whidby, M. T. Miller, H. Scarborough, A. V. Zatorski, A. Cygan, A. A. Price, S. A. Yost, C. D. Bohannon, J. Jacob, A. Grakoui and J. Marcotrigiano (2014). "Structure of the core ectodomain of the hepatitis C virus envelope glycoprotein 2." Nature **509**(7500): 381-384.
Kim, T. Y., P. F. Siesser, K. L. Rossman, D. Goldfarb, K. Mackinnon, F. Yan, X. Yi, M. J. MacCoss, R. T. Moon, C. J. Der and M. B. Major (2015). "Substrate trapping proteomics reveals targets of the betaTrCP2/FBXW11 ubiquitin ligase." Mol Cell Biol **35**(1): 167-181.
Krieger, M. (2001). "Scavenger receptor class B type I is a multiligand HDL receptor that influences diverse physiologic systems." Journal of Clinical Investigation **108**(6): 793-797.
Lamarre, D., P. C. Anderson, M. Bailey, P. Beaulieu, G. Bolger, P. Bonneau, M. Bos, D. R. Cameron, M. Cartier, M. G. Cordingley, A. M. Faucher, N. Goudreau, S. H. Kawai, G. Kukolj, L. Lagace, S. R. LaPlante, H. Narjes, M. A. Poupart, J. Rancourt, R. E. Sentjens, R. St George, B. Simoneau, G. Steinmann, D. Thibeault, Y. S. Tsantrizos, S. M. Weldon, C. L. Yong and M. Llinas-Brunet (2003). "An NS3 protease inhibitor with antiviral effects in humans infected with hepatitis C virus." Nature **426**(6963): 186-189.
Lange, C. M. and S. Zeuzem (2011). "IL28B single nucleotide polymorphisms in the treatment of hepatitis C." J Hepatol **55**(3): 692-701.
Lascano, J., P. D. Uchil, W. Mothes and J. Luban (2016). "TRIM5 Retroviral Restriction Activity Correlates with the Ability To Induce Innate Immune Signaling." J Virol **90**(1): 308-316.
Lassmann, B., V. Arumugaswami, K. W. Chew and M. J. Lewis (2013). "A new system to measure and compare hepatitis C virus replication capacity using full-length, replication competent viruses." J Virol Methods **194**(1-2): 82-88.
Lau, J. Y., R. C. Tam, T. J. Liang and Z. Hong (2002). "Mechanism of action of ribavirin in the combination treatment of chronic HCV infection." Hepatology **35**(5): 1002-1009.
Lauer, G. M. (2013). "Immune responses to hepatitis C virus (HCV) infection and the prospects for an effective HCV vaccine or immunotherapies." J Infect Dis **207 Suppl 1**: S7-S12.

Le Pogam, S., J. M. Yan, M. Chhabra, M. Ilnicka, H. Kang, A. Kosaka, S. Ali, D. J. Chin, N. S. Shulman, P. Smith, K. Klumpp and I. Najera (2012). "Characterization of hepatitis C virus (HCV) quasispecies dynamics upon short-term dual therapy with the HCV NS5B nucleoside polymerase inhibitor mericitabine and the NS3/4 protease inhibitor danoprevir." Antimicrob Agents Chemother **56**(11): 5494-5502.

Leng, J. and J. B. Salmon (2009). "Microfluidic crystallization." Lab Chip **9**(1): 24-34.

Li, M., X. Liu, Y. Zhou and S. B. Su (2009). "Interferon-lambdas: the modulators of antivirus, antitumor, and immune responses." J Leukoc Biol **86**(1): 23-32.

Li, Q., Y. Y. Zhang, S. Chiu, Z. Hu, K. H. Lan, H. Cha, C. Sodroski, F. Zhang, C. S. Hsu, E. Thomas and T. J. Liang (2014). "Integrative functional genomics of hepatitis C virus infection identifies host dependencies in complete viral replication cycle." PLoS Pathog **10**(5): e1004163.

Lindh, M., M. Lagging, M. Farkkila, N. Langeland, K. Morch, S. Nilsson, G. Norkrans, C. Pedersen, M. R. Buhl, J. Westin and K. Hellstrand (2011). "Interleukin 28B gene variation at rs12979860 determines early viral kinetics during treatment in patients carrying genotypes 2 or 3 of hepatitis C virus." J Infect Dis **203**(12): 1748-1752.

Liu, W. L., W. C. Su, C. W. Cheng, L. H. Hwang, C. C. Wang, H. L. Chen, D. S. Chen and M. Y. Lai (2007). "Ribavirin up-regulates the activity of double-stranded RNA-activated protein kinase and enhances the action of interferon-alpha against hepatitis C virus." J Infect Dis **196**(3): 425-434.

Lorber, B. (2002). "<The crystallization of biological macromolecules under microgravity.pdf>." Biochimica et Biophysica Acta **1599** 8.

Loustaud-Ratti, V., M. Debette-Gratien, J. Jacques, S. Alain, P. Marquet, D. Sautereau, A. Rousseau and P. Carrier (2016). "Ribavirin: Past, present and future." World J Hepatol **8**(2): 123-130.

M S Smyth, J. H. J. M. (2000). "x Ray crystallography." J Clin Pathol:Mol Pathol **53**(1): 7.

Ma, H., V. Leveque, A. De Witte, W. Li, T. Hendricks, S. M. Clausen, N. Cammack and K. Klumpp (2005). "Inhibition of native hepatitis C virus replicase by nucleotide and non-nucleoside inhibitors." Virology **332**(1): 8-15.

Macdonald, A. and M. Harris (2004). "Hepatitis C virus NS5A: tales of a promiscuous protein." J Gen Virol **85**(Pt 9): 2485-2502.

Majumdar, T., S. Chattopadhyay, E. Ozhegov, J. Dhar, R. Goswami, G. C. Sen and S. Barik (2015). "Induction of interferon-stimulated genes by IRF3 promotes replication of Toxoplasma gondii." PLoS Pathog **11**(3): e1004779.

Malito, E., A. Carfi and M. J. Bottomley (2015). "Protein Crystallography in Vaccine Research and Development." Int J Mol Sci **16**(6): 13106-13140.

Mandell, M. A., A. Jain, J. Arko-Mensah, S. Chauhan, T. Kimura, C. Dinkins, G. Silvestri, J. Munch, F. Kirchhoff, A. Simonsen, Y. Wei, B. Levine, T. Johansen and V. Deretic (2014). "TRIM proteins regulate autophagy and can target autophagic substrates by direct recognition." Dev Cell **30**(4): 394-409.

Mandell, M. A., T. Kimura, A. Jain, T. Johansen and V. Deretic (2014). "TRIM proteins regulate autophagy: TRIM5 is a selective autophagy receptor mediating HIV-1 restriction." Autophagy **10**(12): 2387-2388.

Manns, M. P. and T. von Hahn (2013). "Novel therapies for hepatitis C - one pill fits all?" Nat Rev Drug Discov **12**(8): 595-610.

Manns, M. P., H. Wedemeyer and M. Cornberg (2006). "Treating viral hepatitis C: efficacy, side effects, and complications." Gut **55**(9): 1350-1359.

Marascio, N., C. Torti, M. Liberto and A. Foca (2014). "Update on different aspects of HCV variability: focus on NS5B polymerase." BMC Infect Dis **14 Suppl 5**: S1.

Marin, I. (2012). "Origin and diversification of TRIM ubiquitin ligases." PLoS One **7**(11): e50030.

Masroori, N., N. Merindol and L. Berthoux (2016). "The interferon-induced antiviral protein PML (TRIM19) promotes the restriction and transcriptional silencing of lentiviruses in a context-specific, isoform-specific fashion." Retrovirology **13**: 19.

Mayhoub, A. S. (2012). "Hepatitis C RNA-dependent RNA polymerase inhibitors: a review of structure-activity and resistance relationships; different scaffolds and mutations." Bioorg Med Chem **20**(10): 3150-3161.

McPherson, A. (2004). "Introduction to protein crystallization." Methods **34**(3): 254-265.

McPherson, A. and L. J. DeLucas (2015). "Microgravity protein crystallization." npj Microgravity **1**: 15010.

Meroni, G. and G. Diez-Roux (2005). "TRIM/RBCC, a novel class of 'single protein RING finger' E3 ubiquitin ligases." Bioessays **27**(11): 1147-1157.

Metz, P., A. Reuter, S. Bender and R. Bartenschlager (2013). "Interferon-stimulated genes and their role in controlling hepatitis C virus." J Hepatol **59**(6): 1331-1341.

Meylan, E., J. Curran, K. Hofmann, D. Moradpour, M. Binder, R. Bartenschlager and J. Tschopp (2005). "Cardif is an adaptor protein in the RIG-I antiviral pathway and is targeted by hepatitis C virus." Nature **437**(7062): 1167-1172.

Miki, D., H. Ochi, A. Takahashi, C. N. Hayes, Y. Urabe, H. Abe, T. Kawaoka, M. Tsuge, N. Hiraga, M. Imamura, Y. Kawakami, H. Aikata, S. Takahashi, N. Akuta, F. Suzuki, K. Ikeda, H. Kumada, Y. Karino, J. Toyota, T. Tsunoda, M. Kubo, N. Kamatani, Y. Nakamura and K. Chayama (2013). "HLA-DQB1*03 confers susceptibility to chronic hepatitis C in Japanese: a genome-wide association study." PLoS One **8**(12): e84226.

Mishima, K., N. Sakamoto, Y. Sekine-Osajima, M. Nakagawa, Y. Itsui, S. Azuma, S. Kakinuma, K. Kiyohashi, A. Kitazume, K. Tsuchiya, M. Imamura, N. Hiraga, K. Chayama, T. Wakita and M. Watanabe (2010). "Cell culture and in vivo analyses of cytopathic hepatitis C virus mutants." Virology **405**(2): 361-369.

Mohd Hanafiah, K., J. Groeger, A. D. Flaxman and S. T. Wiersma (2013). "Global epidemiology of hepatitis C virus infection: new estimates of age-specific antibody to HCV seroprevalence." Hepatology **57**(4): 1333-1342.

Moradpour, D. and H. E. Blum (2004). "A primer on the molecular virology of hepatitis C." Liver Int **24**(6): 519-525.

Moriishi, K. and Y. Matsuura (2007). "Evaluation systems for anti-HCV drugs." Adv Drug Deliv Rev **59**(12): 1213-1221.

Mosley, R. T., T. E. Edwards, E. Murakami, A. M. Lam, R. L. Grice, J. Du, M. J. Sofia, P. A. Furman and M. J. Otto (2012). "Structure of hepatitis C virus polymerase in complex with primer-template RNA." J Virol **86**(12): 6503-6511.

Nakamoto, S., T. Kanda, S. Wu, H. Shirasawa and O. Yokosuka (2014). "Hepatitis C virus NS5A inhibitors and drug resistance mutations." World J Gastroenterol **20**(11): 2902-2912.

Nakamura, M., T. Kanda, Y. Haga, R. Sasaki, S. Wu, S. Nakamoto, S. Yasui, M. Arai, F. Imazeki and O. Yokosuka (2016). "Sofosbuvir treatment and hepatitis C virus infection." World J Hepatol **8**(3): 183-190.

Nakamuta, M., T. Fujino, R. Yada, Y. Aoyagi, K. Yasutake, M. Kohjima, K. Fukuizumi, T. Yoshimoto, N. Harada, M. Yada, M. Kato, K. Kotoh, A. Taketomi, Y. Maehara, M. Nakashima and M. Enjoji (2011). "Expression profiles of genes associated with viral entry in HCV-infected human liver." J Med Virol **83**(5): 921-927.

Napolitano, L. M., E. G. Jaffray, R. T. Hay and G. Meroni (2011). "Functional interactions between ubiquitin E2 enzymes and TRIM proteins." Biochem J **434**(2): 309-319.

Napolitano, L. M. and G. Meroni (2012). "TRIM family: Pleiotropy and diversification through homomultimer and heteromultimer formation." IUBMB Life **64**(1): 64-71.

Neamati, N. (2001). "Structure-based HIV-1 integrase inhibitor design: a future perspective." Expert Opin Investig Drugs **10**(2): 281-296.

Nenasheva, V. V., G. V. Kovaleva, N. V. Khaidarova, E. V. Novosadova, E. S. Manuilova, S. A. Antonov and V. Z. Tarantul (2014). "Trim14 overexpression causes the same transcriptional changes in mouse embryonic stem cells and human HEK293 cells." In Vitro Cell Dev Biol Anim **50**(2): 121-128.

Nenasheva, V. V., G. V. Kovaleva, L. V. Uryvaev, K. S. Ionova, A. V. Dedova, G. K. Vorkunova, S. V. Chernyshenko, N. V. Khaidarova and V. Z. Tarantul (2015). "Enhanced expression of trim14 gene suppressed Sindbis virus reproduction and modulated the transcription of a large number of genes of innate immunity." Immunol Res **62**(3): 255-262.

Newby, Z. E., J. D. O'Connell, 3rd, F. Gruswitz, F. A. Hays, W. E. Harries, I. M. Harwood, J. D. Ho, J. K. Lee, D. F. Savage, L. J. Miercke and R. M. Stroud (2009). "A general protocol for the crystallization of membrane proteins for X-ray structural investigation." Nat Protoc **4**(5): 619-637.

Nexo, B. A., T. Christensen, J. Frederiksen, A. Moller-Larsen, A. B. Oturai, P. Villesen, B. Hansen, K. K. Nissen, M. J. Laska, T. S. Petersen, S. Bonnesen, A. Hedemand, T. Wu, X. Wang, X. Zhang, T. Brudek, R. Maric, H. B. Sondergaard, F. Sellebjerg, K. Brusgaard, A. L. Kjeldbjerg, H. B. Rasmussen, A. L. Nielsen, M. Nyegaard, T. Petersen, A. D. Borglum and F. S. Pedersen (2011). "The etiology of multiple sclerosis: genetic evidence for the involvement of the human endogenous retrovirus HERV-Fc1." PLoS One **6**(2): e16652.

Nisole, S., J. P. Stoye and A. Saib (2005). "TRIM family proteins: retroviral restriction and antiviral defence." Nat Rev Microbiol **3**(10): 799-808.

Ovsyannikova, I. G., I. H. Haralambieva, R. A. Vierkant, M. M. O'Byrne and G. A. Poland (2013). "Associations between polymorphisms in the antiviral TRIM genes and measles vaccine immunity." Hum Immunol **74**(6): 768-774.

Ozato, K., D. M. Shin, T. H. Chang and H. C. Morse, 3rd (2008). "TRIM family proteins and their emerging roles in innate immunity." Nat Rev Immunol **8**(11): 849-860.

Pagliaccetti, N. E. and M. D. Robek (2010). "Interferon-lambda in the immune response to hepatitis B virus and hepatitis C virus." J Interferon Cytokine Res **30**(8): 585-590.

Pai, M., R. Prabhu, A. Panebra, S. Nangle, S. Haque, F. Bastian, R. Garry, K. Agrawal, S. Goodbourn and S. Dash (2005). "Activation of interferon-stimulated response element in huh-7 cells replicating hepatitis C virus subgenomic RNA." Intervirology **48**(5): 301-311.

Park, S. H. and B. Rehermann (2014). "Immune responses to HCV and other hepatitis viruses." Immunity **40**(1): 13-24.

Pawlotsky, J. M. (2013). "NS5A inhibitors in the treatment of hepatitis C." J Hepatol **59**(2): 375-382.

Pertel, T., S. Hausmann, D. Morger, S. Zuger, J. Guerra, J. Lascano, C. Reinhard, F. A. Santoni, P. D. Uchil, L. Chatel, A. Bisiaux, M. L. Albert, C. Strambio-De-Castillia, W. Mothes, M. Pizzato, M. G. Grutter and J. Luban (2011). "TRIM5 is an innate immune sensor for the retrovirus capsid lattice." Nature **472**(7343): 361-365.

Pham, T. N., C. S. Coffin and T. I. Michalak (2010). "Occult hepatitis C virus infection: what does it mean?" Liver Int **30**(4): 502-511.

Pichlmair, A., K. Kandasamy, G. Alvisi, O. Mulhern, R. Sacco, M. Habjan, M. Binder, A. Stefanovic, C. A. Eberle, A. Goncalves, T. Burckstummer, A. C. Muller, A. Fauster, C. Holze, K. Lindsten, S. Goodbourn, G. Kochs, F. Weber, R. Bartenschlager, A. G. Bowie, K. L. Bennett, J. Colinge and G. Superti-Furga (2012). "Viral immune modulators perturb the human molecular network by common and unique strategies." Nature **487**(7408): 486-490.

Pichlmair, A. and C. Reis e Sousa (2007). "Innate recognition of viruses." Immunity **27**(3): 370-383.

Pichlmair, A., O. Schulz, C. P. Tan, T. I. Naslund, P. Liljestrom, F. Weber and C. Reis e Sousa (2006). "RIG-I-mediated antiviral responses to single-stranded RNA bearing 5'-phosphates." Science **314**(5801): 997-1001.

Pichlmair, A., O. Schulz, C. P. Tan, J. Rehwinkel, H. Kato, O. Takeuchi, S. Akira, M. Way, G. Schiavo and C. Reis e Sousa (2009). "Activation of MDA5 requires higher-order RNA structures generated during virus infection." J Virol **83**(20): 10761-10769.

Pietschmann, T., A. Kaul, G. Koutsoudakis, A. Shavinskaya, S. Kallis, E. Steinmann, K. Abid, F. Negro, M. Dreux, F. L. Cosset and R. Bartenschlager (2006). "Construction and characterization of infectious intragenotypic and intergenotypic hepatitis C virus chimeras." Proc Natl Acad Sci U S A **103**(19): 7408-7413.

Ploss, A. and J. Dubuisson (2012). "New advances in the molecular biology of hepatitis C virus infection: towards the identification of new treatment targets." Gut **61 Suppl 1**: i25-35.

Powdrill, M. H., J. A. Bernatchez and M. Gotte (2010). "Inhibitors of the Hepatitis C Virus RNA-Dependent RNA Polymerase NS5B." Viruses **2**(10): 2169-2195.

Qi, X., A. Bae, S. Liu, H. Yang, S. C. Sun, J. Harris, W. Delaney, M. Miller and H. Mo (2009). "Development of a replicon-based phenotypic assay for assessing the drug susceptibilities of HCV NS3 protease genes from clinical isolates." Antiviral Res **81**(2): 166-173.

Qian, X. J., Y. Z. Zhu, P. Zhao and Z. T. Qi (2016). "Entry inhibitors: New advances in HCV treatment." Emerg Microbes Infect **5**: e3.

Qin, Y., Q. Liu, S. Tian, W. Xie, J. Cui and R. F. Wang (2016). "TRIM9 short isoform preferentially promotes DNA and RNA virus-induced production of type I interferon by recruiting GSK3beta to TBK1." Cell Res **26**(5): 613-628.

Rajesh, S., P. Sridhar, B. A. Tews, L. Feneant, L. Cocquerel, D. G. Ward, F. Berditchevski and M. Overduin (2012). "Structural basis of ligand interactions of the large extracellular domain of tetraspanin CD81." J Virol **86**(18): 9606-9616.

Rajsbaum, R., R. A. Albrecht, M. K. Wang, N. P. Maharaj, G. A. Versteeg, E. Nistal-Villan, A. Garcia-Sastre and M. U. Gack (2012). "Species-specific inhibition of RIG-I ubiquitination and IFN induction by the influenza A virus NS1 protein." PLoS Pathog **8**(11): e1003059.

Rajsbaum, R., A. Garcia-Sastre and G. A. Versteeg (2014). "TRIMmunity: the roles of the TRIM E3-ubiquitin ligase family in innate antiviral immunity." J Mol Biol **426**(6): 1265-1284.

Rajsbaum, R., J. P. Stoye and A. O'Garra (2008). "Type I interferon-dependent and -independent expression of tripartite motif proteins in immune cells." Eur J Immunol **38**(3): 619-630.

Randall, G., L. Chen, M. Panis, A. K. Fischer, B. D. Lindenbach, J. Sun, J. Heathcote, C. M. Rice, A. M. Edwards and I. D. McGilvray (2006). "Silencing of USP18 potentiates the antiviral activity of interferon against hepatitis C virus infection." Gastroenterology **131**(5): 1584-1591.

Ranjith-Kumar, C. T., Y. Wen, N. Baxter, K. Bhardwaj and C. Cheng Kao (2011). "A cell-based assay for RNA synthesis by the HCV polymerase reveals new insights on mechanism of polymerase inhibitors and modulation by NS5A." PLoS One **6**(7): e22575.

Raymond, A., S. Lovell, D. Lorimer, J. Walchli, M. Mixon, E. Wallace, K. Thompkins, K. Archer, A. Burgin and L. Stewart (2009). "Combined protein construct and synthetic gene engineering for heterologous protein expression and crystallization using Gene Composer." BMC Biotechnol **9**: 37.

Reker, C. and K. M. Islam (2014). "Risk factors associated with high prevalence rates of hepatitis C infection in Egypt." Int J Infect Dis **25**: 104-106.

Rhodes, D. A., B. de Bono and J. Trowsdale (2005). "Relationship between SPRY and B30.2 protein domains. Evolution of a component of immune defence?" Immunology **116**(4): 411-417.

Robinson, M., H. Yang, S. C. Sun, B. Peng, Y. Tian, N. Pagratis, A. E. Greenstein and W. E. t. Delaney (2010). "Novel hepatitis C virus reporter replicon cell lines enable efficient antiviral screening against genotype 1a." Antimicrob Agents Chemother **54**(8): 3099-3106.

Rupp, D. and R. Bartenschlager (2014). "Targets for antiviral therapy of hepatitis C." Semin Liver Dis **34**(1): 9-21.

Sadler, A. J. and B. R. Williams (2008). "Interferon-inducible antiviral effectors." Nat Rev Immunol **8**(7): 559-568.

Sardiello, M., S. Cairo, B. Fontanella, A. Ballabio and G. Meroni (2008). "Genomic analysis of the TRIM family reveals two groups of genes with distinct evolutionary properties." BMC Evol Biol **8**: 225.

Sarrazin, C., E. Lathouwers, M. Peeters, B. Daems, A. Buelens, J. Witek, Y. Wyckmans, B. Fevery, T. Verbinnen, A. Ghys, M. Schlag, A. Baldini, S. De Meyer and O. Lenz (2015). "Prevalence of the hepatitis C virus NS3 polymorphism Q80K in genotype 1 patients in the European region." Antiviral Res **116**: 10-16.

Scheel, T. K. and C. M. Rice (2013). "Understanding the hepatitis C virus life cycle paves the way for highly effective therapies." Nat Med **19**(7): 837-849.

Schiering, N., A. D'Arcy, F. Villard, O. Simic, M. Kamke, G. Monnet, U. Hassiepen, D. I. Svergun, R. Pulfer, J. Eder, P. Raman and U. Bodendorf (2011). "A macrocyclic HCV NS3/4A protease inhibitor interacts with protease and helicase residues in the complex with its full-length target." Proc Natl Acad Sci U S A **108**(52): 21052-21056.

Schmidt, J., H. E. Blum and R. Thimme (2013). "T-cell responses in hepatitis B and C virus infection: similarities and differences." Emerg Microbes Infect **2**(3): e15.

Schoggins, J. W. and C. M. Rice (2011). "Interferon-stimulated genes and their antiviral effector functions." Curr Opin Virol **1**(6): 519-525.

Schoggins, J. W., S. J. Wilson, M. Panis, M. Y. Murphy, C. T. Jones, P. Bieniasz and C. M. Rice (2011). "A diverse range of gene products are effectors of the type I interferon antiviral response." Nature **472**(7344): 481-485.

Seo, J. Y., R. Yaneva and P. Cresswell (2011). "Viperin: a multifunctional, interferon-inducible protein that regulates virus replication." Cell Host Microbe **10**(6): 534-539.

Seth, R. B., L. Sun, C. K. Ea and Z. J. Chen (2005). "Identification and characterization of MAVS, a mitochondrial antiviral signaling protein that activates NF-kappaB and IRF 3." Cell **122**(5): 669-682.

Shi, M., H. Cho, K. S. Inn, A. Yang, Z. Zhao, Q. Liang, G. A. Versteeg, S. Amini-Bavil-Olyaee, L. Y. Wong, B. V. Zlokovic, H. S. Park, A. Garcia-Sastre and J. U. Jung (2014). "Negative regulation of NF-kappaB activity by brain-specific TRIpartite Motif protein 9." Nat Commun **5**: 4820.

Shiryaev, S. A., A. V. Cheltsov and A. Y. Strongin (2012). "Probing of exosites leads to novel inhibitor scaffolds of HCV NS3/4A proteinase." PLoS One **7**(7): e40029.

Simister, P., M. Schmitt, M. Geitmann, O. Wicht, U. H. Danielson, R. Klein, S. Bressanelli and V. Lohmann (2009). "Structural and functional analysis of hepatitis C virus strain JFH1 polymerase." J Virol **83**(22): 11926-11939.

Singaravelu, R., S. O'Hara, D. M. Jones, R. Chen, N. G. Taylor, P. Srinivasan, C. Quan, D. G. Roy, R. H. Steenbergen, A. Kumar, R. K. Lyn, D. Ozcelik, Y. Rouleau, M. A. Nguyen, K. J.

Rayner, T. C. Hobman, D. L. Tyrrell, R. S. Russell and J. P. Pezacki (2015). "MicroRNAs regulate the immunometabolic response to viral infection in the liver." Nat Chem Biol **11**(12): 988-993.

Snell, E. H. and J. R. Helliwell (2005). "Macromolecular crystallization in microgravity." Reports on Progress in Physics **68**(4): 799-853.

Solund, C., H. Krarup, S. Ramirez, P. Thielsen, B. T. Roge, S. Lunding, T. S. Barfod, L. G. Madsen, B. Tarp, P. B. Christensen, J. Gerstoft, A. L. Laursen, J. Bukh, N. Weis and D. group (2014). "Nationwide experience of treatment with protease inhibitors in chronic hepatitis C patients in Denmark: identification of viral resistance mutations." PLoS One **9**(12): e113034.

Spiegel, M., A. Pichlmair, L. Martinez-Sobrido, J. Cros, A. Garcia-Sastre, O. Haller and F. Weber (2005). "Inhibition of Beta interferon induction by severe acute respiratory syndrome coronavirus suggests a two-step model for activation of interferon regulatory factor 3." J Virol **79**(4): 2079-2086.

Stanley Koszelak, J. D., Cathy Leja, Robert Cudney, and Alexander McPherson (1995). "<Protein and Virus Crystal Growth on International Microgravity.pdf>." Biophysical Journal **69** 7.

Steinmann, E., C. Brohm, S. Kallis, R. Bartenschlager and T. Pietschmann (2008). "Efficient trans-encapsidation of hepatitis C virus RNAs into infectious virus-like particles." J Virol **82**(14): 7034-7046.

Sulbaran, M. Z., F. A. Di Lello, Y. Sulbaran, C. Cosson, C. L. Loureiro, H. R. Rangel, J. F. Cantaloube, R. H. Campos, G. Moratorio, J. Cristina and F. H. Pujol (2010). "Genetic history of hepatitis C virus in Venezuela: high diversity and long time of evolution of HCV genotype 2." PLoS One **5**(12): e14315.

Sun, J., R. Rajsbaum and M. Yi (2015). "Immune and non-immune responses to hepatitis C virus infection." World J Gastroenterol **21**(38): 10739-10748.

Sung, P. S., E. C. Shin and S. K. Yoon (2015). "Interferon Response in Hepatitis C Virus (HCV) Infection: Lessons from Cell Culture Systems of HCV Infection." Int J Mol Sci **16**(10): 23683-23694.

Suzuki, R., K. Saito, T. Kato, M. Shirakura, D. Akazawa, K. Ishii, H. Aizaki, Y. Kanegae, Y. Matsuura, I. Saito, T. Wakita and T. Suzuki (2012). "Trans-complemented hepatitis C virus particles as a versatile tool for study of virus assembly and infection." Virology **432**(1): 29-38.

Takahashi, S., K. Ohta, N. Furubayashi, B. Yan, M. Koga, Y. Wada, M. Yamada, K. Inaka, H. Tanaka, H. Miyoshi, T. Kobayashi and S. Kamigaichi (2013). "JAXA protein crystallization in space: ongoing improvements for growing high-quality crystals." J Synchrotron Radiat **20**(Pt 6): 968-973.

Takeda, K. and S. Akira (2004). "TLR signaling pathways." Seminars in Immunology **16**(1): 3-9.

Takeuchi, O. and S. Akira (2008). "MDA5/RIG-I and virus recognition." Curr Opin Immunol **20**(1): 17-22.

Talele, T. T., P. Arora, S. S. Kulkarni, M. R. Patel, S. Singh, M. Chudayeu and N. Kaushik-Basu (2010). "Structure-based virtual screening, synthesis and SAR of novel inhibitors of hepatitis C virus NS5B polymerase." Bioorg Med Chem **18**(13): 4630-4638.

Tamori, A., M. Enomoto and N. Kawada (2016). "Recent Advances in Antiviral Therapy for Chronic Hepatitis C." Mediators Inflamm **2016**: 6841628.

Tanaka, H., T. Umehara, K. Inaka, S. Takahashi, R. Shibata, Y. Bessho, M. Sato, S. Sugiyama, E. Fusatomi, T. Terada, M. Shirouzu, S. Sano, M. Motohara, T. Kobayashi, T. Tanaka, A. Tanaka and S. Yokoyama (2007). "Crystallization of the archaeal transcription termination factor NusA: a significant decrease in twinning under microgravity conditions." Acta Crystallogr Sect F Struct Biol Cryst Commun **63**(Pt 2): 69-73.

Tanji, K., T. Kamitani, F. Mori, A. Kakita, H. Takahashi and K. Wakabayashi (2010). "TRIM9, a novel brain-specific E3 ubiquitin ligase, is repressed in the brain of Parkinson's disease and dementia with Lewy bodies." Neurobiol Dis **38**(2): 210-218.

Thibeault, D., C. Bousquet, R. Gingras, L. Lagace, R. Maurice, P. W. White and D. Lamarre (2004). "Sensitivity of NS3 serine proteases from hepatitis C virus genotypes 2 and 3 to the inhibitor BILN 2061." J Virol **78**(14): 7352-7359.

Thomas, D. L., C. L. Thio, M. P. Martin, Y. Qi, D. Ge, C. O'Huigin, J. Kidd, K. Kidd, S. I. Khakoo, G. Alexander, J. J. Goedert, G. D. Kirk, S. M. Donfield, H. R. Rosen, L. H. Tobler, M. P. Busch, J. G. McHutchison, D. B. Goldstein and M. Carrington (2009). "Genetic variation in IL28B and spontaneous clearance of hepatitis C virus." Nature **461**(7265): 798-801.

Thompson, A. J. and S. A. Locarnini (2007). "Toll-like receptors, RIG-I-like RNA helicases and the antiviral innate immune response." Immunol Cell Biol **85**(6): 435-445.

Tillmann, H. L., K. Patel, A. J. Muir, C. D. Guy, J. H. Li, X. Q. Lao, A. Thompson, P. J. Clark, S. D. Gardner, J. G. McHutchison and J. J. McCarthy (2011). "Beneficial IL28B genotype associated with lower frequency of hepatic steatosis in patients with chronic hepatitis C." J Hepatol **55**(6): 1195-1200.

Tu, B., R. N. Ziemann, B. C. Tieman, D. J. Hawksworth, J. Tyner, J. Scheffel, M. S. Pinkus, S. E. Brophy, J. M. Werneke, R. Gutierrez and M. White (2010). "Generation and characterization of chimeric antibodies against NS3, NS4, NS5, and core antigens of hepatitis C virus." Clin Vaccine Immunol **17**(6): 1040-1047.

Uchil, P. D., A. Hinz, S. Siegel, A. Coenen-Stass, T. Pertel, J. Luban and W. Mothes (2013). "TRIM protein-mediated regulation of inflammatory and innate immune signaling and its association with antiretroviral activity." J Virol **87**(1): 257-272.

Verbinnen, T., T. Jacobs, L. Vijgen, H. Ceulemans, J. Neyts, G. Fanning and O. Lenz (2012). "Replication capacity of minority variants in viral populations can affect the assessment of resistance in HCV chimeric replicon phenotyping assays." J Antimicrob Chemother **67**(10): 2327-2337.

Versteeg, G. A., R. Rajsbaum, M. T. Sanchez-Aparicio, A. M. Maestre, J. Valdiviezo, M. Shi, K. S. Inn, A. Fernandez-Sesma, J. Jung and A. Garcia-Sastre (2013). "The E3-ligase TRIM family

of proteins regulates signaling pathways triggered by innate immune pattern-recognition receptors." Immunity **38**(2): 384-398.

Vigano, S., M. Perreau, G. Pantaleo and A. Harari (2012). "Positive and negative regulation of cellular immune responses in physiologic conditions and diseases." Clin Dev Immunol **2012**: 485781.

Wakayama, N. I., D. C. Yin, K. Harata, T. Kiyoshi, M. Fujiwara and Y. Tanimoto (2006). "Macromolecular crystallization in microgravity generated by a superconducting magnet." Ann N Y Acad Sci **1077**: 184-193.

Wakita, T. (2007). "HCV research and anti-HCV drug discovery: toward the next generation." Adv Drug Deliv Rev **59**(12): 1196-1199.

Wang, M., K. K. Ng, M. M. Cherney, L. Chan, C. G. Yannopoulos, J. Bedard, N. Morin, N. Nguyen-Ba, M. H. Alaoui-Ismaili, R. C. Bethell and M. N. James (2003). "Non-nucleoside analogue inhibitors bind to an allosteric site on HCV NS5B polymerase. Crystal structures and mechanism of inhibition." J Biol Chem **278**(11): 9489-9495.

Wang, Q. M., R. B. Johnson, D. Chen, V. J. Leveque, J. Ren, M. A. Hockman, K. Abe, T. Hachisu, Y. Kondo, Y. Isaka, A. Sato and T. Fujiwara (2004). "Expression and purification of untagged full-length HCV NS5B RNA-dependent RNA polymerase." Protein Expr Purif **35**(2): 304-312.

Wang, S., X. Wu, T. Pan, W. Song, Y. Wang, F. Zhang and Z. Yuan (2012). "Viperin inhibits hepatitis C virus replication by interfering with binding of NS5A to host protein hVAP-33." J Gen Virol **93**(Pt 1): 83-92.

Wartelle-Bladou, C., G. Le Folgoc, M. Bourliere and L. Lecomte (2012). "Hepatitis C therapy in non-genotype 1 patients: the near future." J Viral Hepat **19**(8): 525-536.

Welzel, T. M., G. Dultz and S. Zeuzem (2014). "Interferon-free antiviral combination therapies without nucleosidic polymerase inhibitors." J Hepatol **61**(1 Suppl): S98-S107.

Westbrook, R. H. and G. Dusheiko (2014). "Natural history of hepatitis C." J Hepatol **61**(1 Suppl): S58-68.

Williams, S. P., L. F. Kuyper and K. H. Pearce (2005). "Recent applications of protein crystallography and structure-guided drug design." Curr Opin Chem Biol **9**(4): 371-380.

Wilson, G. K. and Z. Stamataki (2012). "In vitro systems for the study of hepatitis C virus infection." Int J Hepatol **2012**: 292591.

Winkle, C. C., R. H. Olsen, H. Kim, S. S. Moy, J. Song and S. L. Gupton (2016). "Trim9 Deletion Alters the Morphogenesis of Developing and Adult-Born Hippocampal Neurons and Impairs Spatial Learning and Memory." J Neurosci **36**(18): 4940-4958.

Wlodawer, A., W. Minor, Z. Dauter and M. Jaskolski (2008). "Protein crystallography for non-crystallographers, or how to get the best (but not more) from published macromolecular structures." FEBS J **275**(1): 1-21.

Woerz, I., V. Lohmann and R. Bartenschlager (2009). "Hepatitis C virus replicons: dinosaurs still in business?" Journal of Viral Hepatitis **16**(1): 1-9.

Wu, F., A. Kirmaier, R. Goeken, I. Ourmanov, L. Hall, J. S. Morgan, K. Matsuda, A. Buckler-White, K. Tomioka, R. Plishka, S. Whitted, W. Johnson and V. M. Hirsch (2013). "TRIM5 alpha drives SIVsmm evolution in rhesus macaques." PLoS Pathog **9**(8): e1003577.

Xuan Su1, Jianning Wang2,*, Weichao Chen1, Zhaoqu Li1, Xiaoyan Fu1, Ankui Yang1 (2016). "Overexpression of TRIM14 promotes tongue squamous cell carcinoma aggressiveness by activating the NF-jB signaling pathway." Oncotarget **7**(9).

Xue, W., M. Wang, X. Jin, H. Liu and X. Yao (2012). "Understanding the structural and energetic basis of inhibitor and substrate bound to the full-length NS3/4A: insights from molecular dynamics simulation, binding free energy calculation and network analysis." Mol Biosyst **8**(10): 2753-2765.

Yang, L., R. Li, T. Kaneko, K. Takle, R. K. Morikawa, L. Essex, X. Wang, J. Zhou, K. Emoto, Y. Xiang and B. Ye (2014). "Trim9 regulates activity-dependent fine-scale topography in Drosophila." Curr Biol **24**(9): 1024-1030.

Ye, B., X. Liu, X. Li, H. Kong, L. Tian and Y. Chen (2015). "T-cell exhaustion in chronic hepatitis B infection: current knowledge and clinical significance." Cell Death Dis **6**: e1694.

Ye, Y. and M. Rape (2009). "Building ubiquitin chains: E2 enzymes at work." Nat Rev Mol Cell Biol **10**(11): 755-764.

Zeisel, M. B., I. Fofana, S. Fafi-Kremer and T. F. Baumert (2011). "Hepatitis C virus entry into hepatocytes: molecular mechanisms and targets for antiviral therapies." J Hepatol **54**(3): 566-576.

Zhang, P., S. Elabd, S. Hammer, V. Solozobova, H. Yan, F. Bartel, S. Inoue, T. Henrich, J. Wittbrodt, F. Loosli, G. Davidson and C. Blattner (2015). "TRIM25 has a dual function in the p53/Mdm2 circuit." Oncogene **34**(46): 5729-5738.

Zhou, S., R. Liu, B. M. Baroudy, B. A. Malcolm and G. R. Reyes (2003). "The effect of ribavirin and IMPDH inhibitors on hepatitis C virus subgenomic replicon RNA." Virology **310**(2): 333-342.

Zhou, X., J. J. Michal, L. Zhang, B. Ding, J. K. Lunney, B. Liu and Z. Jiang (2013). "Interferon induced IFIT family genes in host antiviral defense." Int J Biol Sci **9**(2): 200-208.

Zhou, Z., X. Jia, Q. Xue, Z. Dou, Y. Ma, Z. Zhao, Z. Jiang, B. He, Q. Jin and J. Wang (2014). "TRIM14 is a mitochondrial adaptor that facilitates retinoic acid-inducible gene-I-like receptor-mediated innate immune response." Proc Natl Acad Sci U S A **111**(2): E245-254.

Zhu, J. W., F. L. Liu, D. Mu, D. Y. Deng and Y. T. Zheng (2016). "Increased expression and dysregulated association of restriction factors and type I interferon in HIV, HCV mono- and co-infected patients." J Med Virol **88**(6): 987-995.

Zhu, Z., Y. Wang, C. Zhang, S. Yu, Q. Zhu, K. Hou and B. Yan (2016). "TRIM25 blockade by RNA interference inhibited migration and invasion of gastric cancer cells through TGF-beta signaling." Sci Rep **6**: 19070.

Zuniga, E. I., M. Macal, G. M. Lewis and J. A. Harker (2015). "Innate and Adaptive Immune Regulation During Chronic Viral Infections." Annu Rev Virol **2**(1): 573-597.